Geology of the Wadley South Quadrangle and geochronology of the Dadeville Complex, southernmost Appalachians of east Alabama

by

Dane Scott VanDervoort

A thesis submitted to the Graduate Faculty of
Auburn University
in partial fulfillment of the
requirements for the Degree of
Master of Science

Auburn, Alabama
August 6, 2016

Keywords: Wadley South, Dadeville Complex, Taconic orogeny, Inner Piedmont, southernmost Appalachians, east Alabama

Approved by

Mark G. Steltenpohl, Chair, Professor of Geoscience
Willis E. Hames, Professor of Geoscience
Haibo Zou, Associate Professor of Geoscience

ABSTRACT

Geologic mapping results from rocks in the area of the Wadley South Quadrangle are reported to address basic research questions concerning the Paleozoic tectonometamorphic evolution of the southernmost Appalachians. Key findings of this mapping investigation include the following. (1) The Jacksons Gap Group (Brevard zone lithologies) is subdivided into three main lithofacies: a structurally lower section of predominantly of fine-grained garnetiferous-graphitic-quartz-biotite schist and phyllite and interlayered micaceous quartzite; a middle section of interlayered graphitic phyllite; and an upper section of graphitic and sericitic phyllite. (2) First generation, D_1, structures accompanied Neoacadian lower-to middle-amphibolite-facies metamorphism of eastern Blue Ridge units, upper-greenschist to lower-amphibolite-facies metamorphism of the Jacksons Gap Group, and upper-amphibolite-facies metamorphism of rocks of the Dadeville Complex. (3) Early-syn D_1 fabrics and lithologic contacts are truncated along the Katy Creek fault, implying juxtaposition of the Dadeville Complex and Jacksons Gap Group during syn- to late-stages of metamorphism. An inverted metamorphic gradient may be associated with the Katy Creek fault, suggesting formation during down heating associated with thrust emplacement of the overlying Dadeville Complex. (4) Crystal-Plastic reactivation of the Brevard shear zone under middle-greenschist facies conditions during Alleghanian movement is recorded in retrograde mylonites associated with the Abanda fault. Oblique-normal and dextral-strike-slip displacement along the Abanda

fault apparently juxtaposed rocks of different metamorphic grade. (5) The presence of cataclasite along the northwest side of the Alexander City and Abanda faults marks the final translation of the eastern Blue Ridge and Jacksons Gap Group under supra-ductile-brittle conditions during the Mesozoic rifting of Pangea.

The precise age and tectonic affinity of rocks of the Dadeville Complex in Alabama and Georgia is not well defined, so a U-Pb geochronological investigation of magmatic and detrital zircons from the complex was performed. The Dadeville Complex comprises a thick (>6 km) klippe of amphibolite-facies sedimentary, volcanic, and plutonic tocks in the core of the shallow-northeast plunging Tallassee synform and cradled between Laurentian units of the eastern Blue Ridge and Pine Mountain window. Laser ablation sector field inductively coupled plasma mass spectrometry (LA-SF-ICP-MS) $^{206}Pb/^{238}U$ age dates indicate that this terrane is a Cambrian- to Early Ordovician-aged arc emplaced during the early Paleozoic Taconic orogeny. Detrital zircons from a metasiliciclastic unit (i.e., Agricola Schist) reveal populations at that are not typical of rocks found along the present-day southeastern Laurentian margin. Grenville-aged zircons are conspicuously sparse in the Dadeville Complex and suggest that the Inner Piedmont in Alabama and Georgia has an exotic tectonic affinity. A prominent zircon population in the detrital age spectrum at ~480 Ma contains a Th/U ratio of less than 0.1 that likely developed as result of Taconian emplacement of the Dadeville Complex arc atop the slope-rise facies of the eastern Blue Ridge. The ~480 Ma date overlaps with high-grade metamorphism reported in the eastern Blue Ridge (i.e., the Lick Ridge Eclogite and Winding Stair Gap granulite) in western North Carolina, and synorogenic clastic wedge deposition (Blount clastic wedge) reported in Alabama, Georgia, and

Tennessee, documenting significant Taconian orogenic effects in the southernmost Appalachians where it had previously been considered absent.

ACKNOWLEDGEMENTS

I am indebted to a number of people who have helped me throughout my academic career:

First, thanks to Dr. Mark G. Steltenpohl, who has provided me with numerous opportunities that I likely would not have received elsewhere or under the advisement of any other major professor. His conceptualizations of the many aspects of the geosciences are unmatched, and I hope that at least a small part of his intellect has rubbed off on me.

Additional thanks to Dr. Charles “Chuck” H. Trupe for sparking my interest in the Paleozoic tectonometamorphic evolution of the southern Appalachians. His exceptional skills in the field are unmatched, and I will forever be indebted to him for helping to lay the foundations of my geological education.

Many thanks to my professors and colleagues in the Department of Geosciences that have helped to shape me into the researcher that I have become. I have interacted with John P. Whitmore, Rylleigh P. Harstad, and John F. Hawkins the most and I hope to continue to work with these talented geologists throughout my professional career.

Finally, many thanks to my family and friends for their support in pushing me to pursue all of my educational and professional goals.

Style of manual used: Geological Society of America Bulletin

Computer software used: Adobe Illustrator CS, Microsoft Word 2010, ESRI ArcGIS 10.2, and Rick Allmendinger's Stereonet 9

TABLES OF CONTENTS

LIST OF FIGURES

Chapter II

LIST OF TABLES

LIST OF PLATES

INTRODUCTION

The format used herein is manuscript style, comprising two papers that have been prepared for journal submission. The first paper, Geology of the 1:24,000 Wadley South, Alabama, Quadrangle was prepared as a geologic report for submission to the Geological Survey of Alabama using their manuscript guidelines. The second paper, An early Paleozoic Taconic arc discovered in the southernmost Appalachians of Alabama and Georgia: Implications for the crustal growth of eastern North America has been prepared according to the manuscript guidelines for Geology, which is the same as the Bulletin of the Geological Society of America.

The 1:24,000 Wadley South, Alabama, Quadrangle is located in a geologically critical area, as it contains one of the largest faults in the southernmost Appalachians, the Brevard shear zone, which marks the boundary between the eastern Blue Ridge and Inner Piedmont lithotectonic terranes. The first paper provides a detailed lithologic description and structural analysis of the rocks underlying the Wadley South Quadrangle (Plate 1). The purpose of this manuscript is to document the polyphase kinematic history across the Brevard shear zone and its associated rheological changes through time and space. This manuscript is the result of a detailed (1:24,000 scale) field investigation of 90 km^2 within the quadrangle. Standard field mapping techniques (i.e., Brunton compass and hand sample collection) were employed during approximately ten weeks of mapping in summer of 2015. This mapping was augmented by numerous daylong visits throughout the 2014-2015 academic year. Mapping was performed along all primary and secondary roads with open access, and in private lands where permission could be obtained. Lithologic and structural data were compiled from 331 stations throughout the mapping area. Laboratory work included kinematic and petrographic analyses of nineteen thin sections in order to characterize the mineral assemblages, microstructures, fabrics, and lithologies. Structural analyses were performed using the Stereonet 9 software package available on Dr. Rick Allmendinger's personal webpage at the Cornell University Earth and Atmospheric Sciences Departmental website (http://www.geo.cornell.edu/geology/faculty/RWA/programs/stereonet.html).

The second paper is a geochronologic investigation of the Alabama Inner Piedmont Dadeville Complex. Since no igneous crystallization or metamorphic ages are reported for any rocks of the Dadeville Complex in Alabama, the purpose of this paper is to do so. Samples were collected from their type locality for five constituent units comprising the Dadeville Complex, and analyses were performed using the Laser Ablation Sector Field Inductively Coupled Plasma Mass Spectrometry Laboratory at the University of California, Northridge. U-Pb age dating of magmatic zircons from the Waresville Formation, Camp Hill Gneiss, Ropes Creek Amphibolite, and Waverly Gneiss yield late Cambrian to Early Ordovician igneous crystallization ages for the Dadeville Complex. U-Pb age dating of detrital zircons from the Agricola Schist document that the Dadeville Complex is an exotic (i.e., non-Laurnetian) terrane accreted during the Taconic orogeny. Paper two further describes the author's interpretation for the plate-tectonic significance of these findings.

I. GEOLOGY OF THE 1:24,000 WADLEY SOUTH, ALABAMA, QUADRANGLE

MS Candidate Dane S. VanDervoort and PI Mark G. Steltenpohl

ABSTRACT

The geology of the 1:24,000 Wadley South, Alabama, Quadrangle has the second highest mapping priority in the State of Alabama due to rapid development along the US-280 corridor and drainages emptying into a major reservoir and recreational feature (State of Alabama Geologic Mapping Advisory Committee, 2013). Detailed geologic mapping is needed for: (1) planning, development, environmental concerns, and for Source Water Protection studies as required by the Alabama Department of Environmental Management; (2) further characterization of precious metal and aggregate resources; and (3) addressing basic research questions concerning geologic evolution. Investigations of the study area are aimed at addressing several problems of Appalachian orogenic evolution. Objectives for this research are: (1) to map and characterize lithologies and clarify their distributions; (2) to analyze structures and fabrics; (3) to produce a vector ArcGIS® geologic map of the Wadley South Quadrangle, and; (4) to synthesize the geological history. Key findings are five-fold: (1) Brevard zone lithologies (i.e., Jacksons Gap Group) in the Wadley South Quadrangle are not easily separated into individual map

units as depicted on 1:24,000-scale maps to the southwest because of their gradational nature and subtle lithologic differences. The current authors subdivide the Jacksons Gap Group into three main lithofacies: a structurally lower section consisting predominantly of fine-grained garnetiferous-graphitic-quartz-biotite schist and phyllite and interlayered micaceous quartzite; a middle section of interlayered graphitic phyllite; and an upper section of graphitic and sericitic phyllite. (2) Formation of first generation D_1 structures accompanied Neoacadian lower-to middle-amphibolite-facies metamorphism of eastern Blue Ridge units, upper-greenschist to lower- amphibolite-facies metamorphism of the Jacksons Gap Group, and upper-amphibolite-facies metamorphism of rocks of the Inner Piedmont. (3) Early-syn D_1 fabrics and lithologic contacts are truncated along the Katy Creek fault, implying juxtaposition of the Dadeville Complex and Jacksons Gap Group during syn- to late-stages of metamorphism. An inverted metamorphic gradient may be associated with the Katy Creek fault, suggesting formation during down heating associated with thrust emplacement of the overlying Dadeville Complex. (4) Plastic reactivation of the Brevard shear zone under middle-greenschist facies conditions during Alleghanian movement is recorded in meso- and microstructures preserved in retrograde mylonites associated with the Abanda fault. Oblique-normal and dextral-strike-slip displacement along the Abanda fault apparently juxtaposed rocks of different metamorphic grade. (5) The presence of cataclasite along the northwest side of the Alexander City and Abanda faults marks the final translation of the Eastern Blue Ridge and Jacksons Gap Group under supra-ductile-brittle conditions during the Mesozoic rifting of Pangea. The cataclasite zone is a strong ridge former due to its high-silica content and interlocking nature of quartz-grain boundaries.

INTRODUCTION

The Wadley South Quadrangle is located in the Piedmont province of the southern Appalachians in east-central Alabama. The Piedmont province consists of an allochthonous sequence of metamorphosed rocks that formed in response to a complex series of Paleozoic deformational episodes related to the Taconic, Acadian, and Alleghanian orogenic events (Hatcher, 1989, 2005). Detailed geologic mapping of the Wadley South Quadrangle has never been performed. Previous investigations of the study area are primarily restricted to broad regional reconnaissance mapping studies and large-scale mineral exploration surveys that provide a limited amount of structural and metamorphic data (e.g., Tuomey, 1858; Phillips, 1892; Adams, 1926, 1930; Park, 1935; and Pardee and Park, 1948), hence their significance for Appalachian tectonic evolution is unknown. The Wadley South Quadrangle is located near the Interstate I-85 and U.S. Highway 280 corridor in eastern Alabama, approximately 28 miles northeast of Lake Martin. I-85 and U.S 280 serve as main transportation arteries for Birmingham, AL, the Auburn-Opelika metropolitan area, and Atlanta, GA. Due to its location, the Geological Survey of Alabama's Mapping Advisory Board determined that the Wadley South Quadrangle has the second highest mapping priority in the state (Steltenpohl, 2013). Reasons for this mapping include: (1) the need for detailed geologic maps for urban planning and development, and Source Water Protection studies, as required by the Alabama Department of Environmental Management; and, (2) the need for detailed geologic maps in order to identify and clarify precious mineral and industrial stone resources (Steltenpohl, 2013; Steltenpohl and Singleton, 2014).

Location and Physiographic Setting

The 1:24,000 Wadley South, Alabama, Quadrangle (Latitudes: 33°00'N and 33°07'30"N; Longitudes: 85°30'W and 85°37'30"W) lies in parts of Randolph, Chambers, and Tallapoosa Counties in the Piedmont province of the southern Appalachians in east-central Alabama (Figs. 1 and 2). The principal communities in the Wadley South Quadrangle are Blake and Wadley in southwest Randolph County; Abanda, Bosworth, Shiloh, Penton, and Union Hill in northwest Chambers County; and, Truett and Frog Eye in northeast Tallapoosa County. Alexander City, with an estimated population of 14,876 (2013, U.S. Census Bureau) lies approximately 19.5 miles (31.5 km) to the southwest. The topography is typical of the Alabama Piedmont, characterized by low rolling hills, with prominent topographic ridges forming due to the differential weathering of more silica-rich units (Bentley and Neathery, 1970). The elevation ranges from greater than 920 feet (280.4 meters) AMSL in the hills west of Truett, to less than 580 feet (176.8 meters) AMSL along the banks of the Tallapoosa River, in northeastern Tallapoosa County. The Tallapoosa River and its major tributaries provide the primary surface drainage, and the general direction of water flow is from the north to the southwest, towards the Lake Martin reservoir.

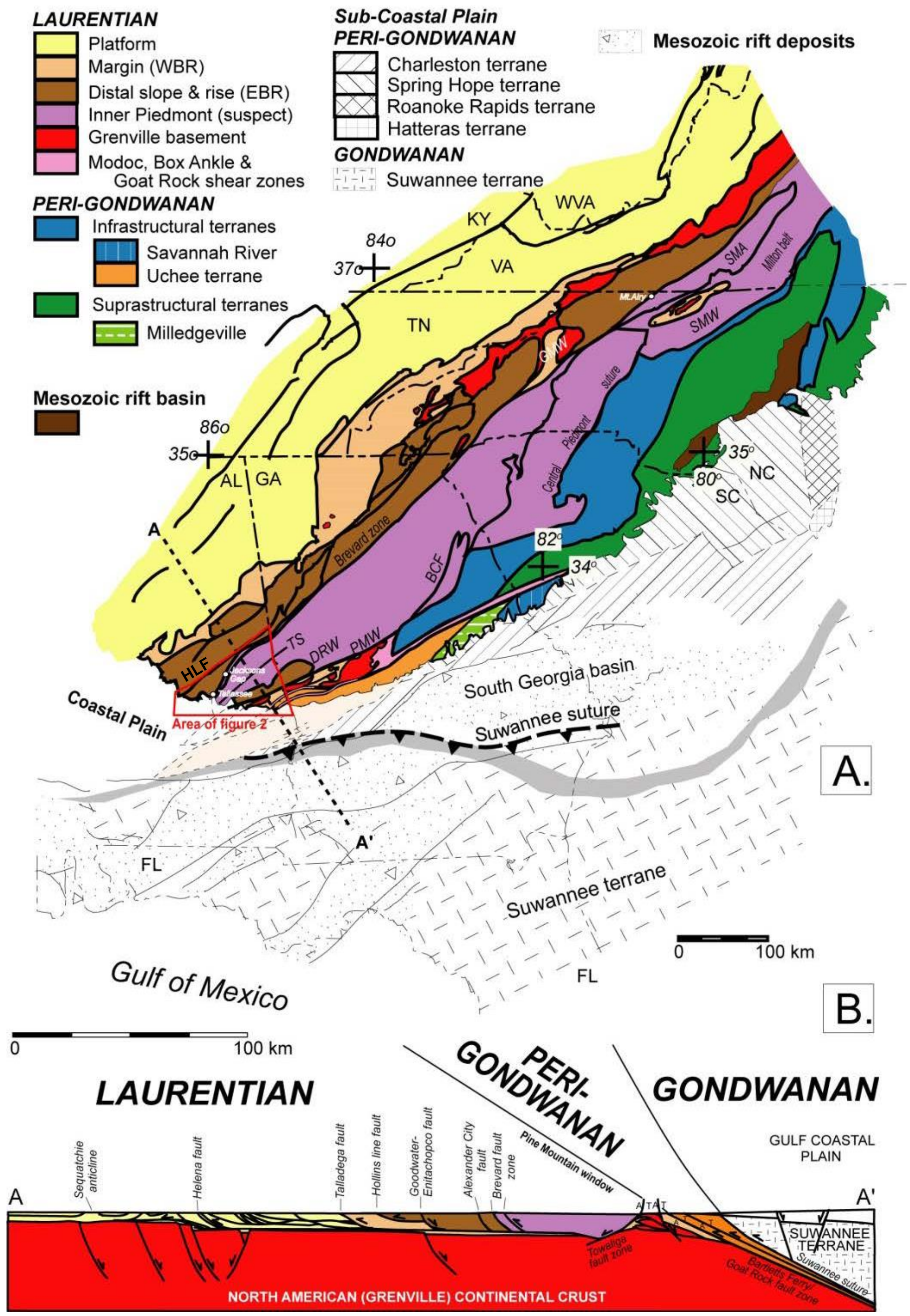

Figure 1: A. Tectonic map illustrating Alabama's position within the southern Appalachians with section line A-A' (from Steltenpohl et al., 2007, 2013; as modified from Hatcher, 2004, Horton et al., 1989; Hibbard et al., 2002, 2006; Steltenpohl, 2005). Red Polygon illustrates the area of Fig. 2. **B.** Simplified cross section A-A' (modified from W.A. Thomas and coworkers as depicted in Thomas et al. [1989], Hatcher et al. [1990], and Steltenpohl [2005]). Map abbreviations: BCF-Brindle Creek fault; CR-Cartersville reentrant; CST-Cat Square terrane; DRW-Dog River window; EBR-eastern Blue Ridge; GMW-Grandfather Mountain Window; HLF-Hollins Line fault; PMW-Pine Mountain window; SMW-Sauratown Mountain Window; SRA-Smith River allochthon; TS-Tallassee synform; WBR-western Blue Ridge. Cross-Section: A-away; T-toward; no vertical exaggeration.

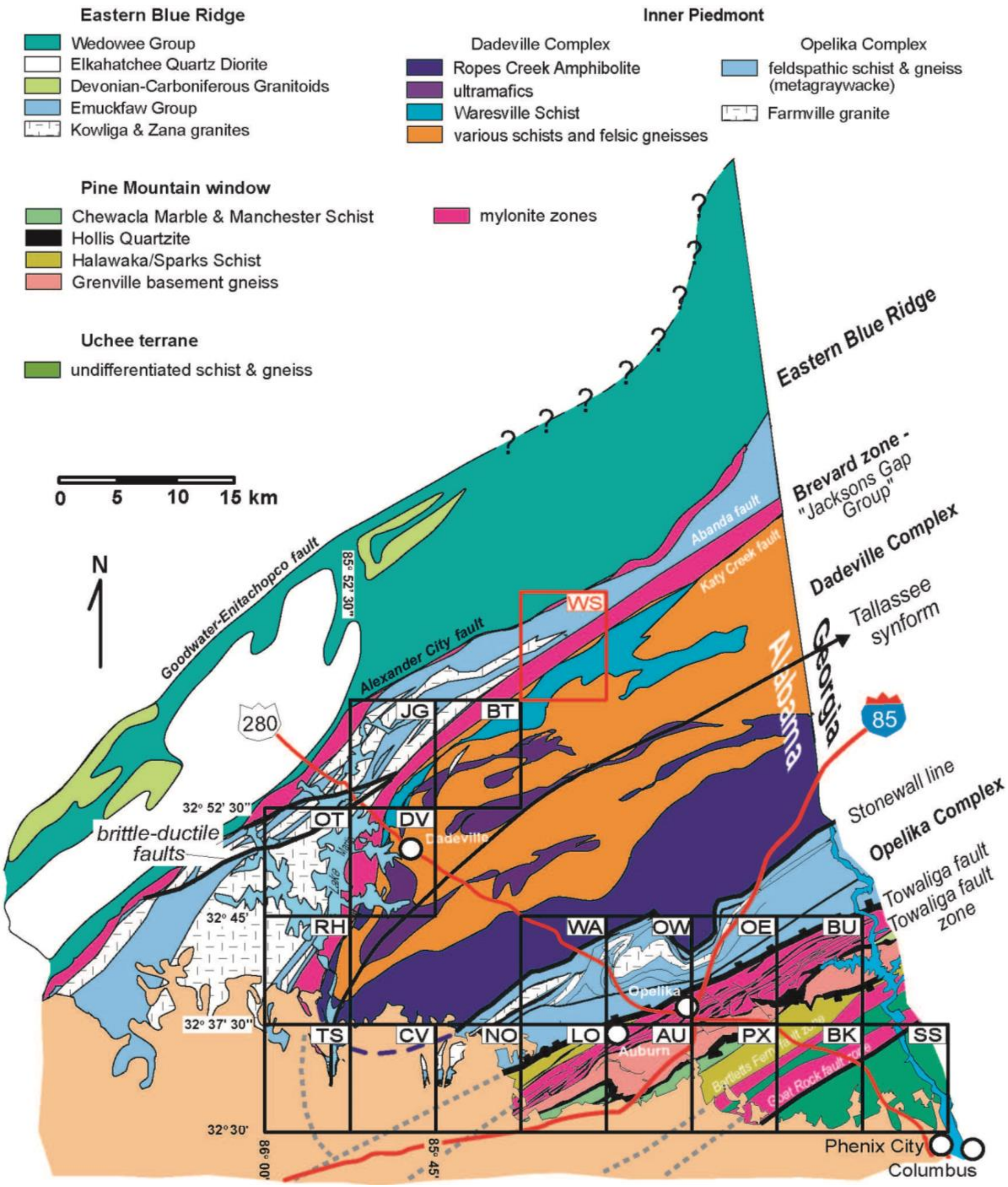

Figure 2: Geologic map of the Alabama Piedmont (from Osborne et al., 1988, Steltenpohl, 2005, and Steltenpohl et al., 2013) noting the location of the Wadley South (WS) Quadrangle (outlined in red). EDMAP Quad abbreviations: AU-Auburn; BT-Buttston; BU-Beulah; BK-Bleeker; CV-Carrville; DV-Dadeville; JG-Jacksons Gap; LO-Loachapoka; NO-Notasulga; OE-Opelika East; OW-Opelika West; OT-Our Town; OT-Our Town; PX-Parker's Crossroad; RH-Red Hill; SS-Smith's Station; TS-Tallassee; WA-Waverly. Dashed gray lines are geophysical lineaments from Horton et al. (1989). Dashed blue line represents the base of the Dadeville Complex from White (2007).

Geologic Setting

The structurally lowest terrane in the study area is the eastern Blue Ridge (Figs. 1 and 2). In Figure 2, the eastern Blue Ridge is composed of two different metasedimentary sequences structurally bounded by the Goodwater-Enitachopco fault and the Brevard shear zone, in the northwest and southeast respectively. The Wedowee Group, located structurally above the Goodwater-Enitachopco fault, is composed of interlayered graphitic and sericitic phyllite, mylonitic schist, sheared amphibolite, and Devonian- to Carboniferous-aged granitic intrusives (Bentley and Neathery, 1970; Neathery and Reynolds, 1975; Russell, 1978; Tull et al., 2012). The Emuckfaw Group, structurally below the Brevard shear zone, is a sequence of undifferentiated metagraywacke, graphitic and aluminous schist, quartzite, amphibolite, and Ordovician- to Silurian-aged Zana Granite and Kowaliga Gneiss plutons (Fig. 2) (Neathery and Reynolds, 1975; Steltenpohl et al., 2005; Hawkins, 2013). The dextral strike-slip Alexander City fault generally separates the Wedowee and Emuckfaw Groups (Fig. 2) (Neathery and Reynolds, 1975; Steltenpohl et al., 2013). Rocks of the eastern Blue Ridge contain peak upper-amphibolite facies metamorphic mineral assemblages and locally exhibit up to three different foliations, the nature and timing of which is not well-constrained (Neathery and Reynolds, 1975; Steltenpohl et al., 2005; Hawkins, 2013). Most workers interpret these rocks as being the outboard slope/rise facies of the Neoproterozoic eastern Laurentian margin, and recent work by Steltenpohl (2005) and Tull et al. (2014) indicates that at least some of them (i.e., the Emuckfaw Formation) may have evolved in a distal back-arc basin (Neathery and Reynolds, 1975; Steltenpohl, 1988).

The Brevard zone is an extensive retrograded shear zone juxtaposing high-grade metasedimentary and metaplutonic rocks of the eastern Blue Ridge with high-grade metavolcanic and metaplutonic rocks of the Inner Piedmont (Figs. 1 and 2) (Bentley and Neathery, 1970; Hatcher, 1978; Steltenpohl, 2005). The origin of the Brevard zone remains debatable, but most workers interpret it as being a polyphase fault zone that formed in response to Acadian-Neoacadian crystal-plastic thrusting and subsequent Alleghanian brittle-plastic dextral strike-slip shearing (Hatcher, 1972, 1987, 2005; Sterling, 2006; Steltenpohl et al., 2013). In Alabama, the Brevard zone is defined by an up to 2.0-mile (3.2 km) wide zone of strongly to weakly deformed metasiliciclastic and metapelitic rocks identified as the Jackson Gap Group (Fig. 2) (Bentley and Neathery, 1970). The Jacksons Gap Group comprises an allochthonous sequence of graphitic button-schist, phyllonite, blastomylonite, and mylonitic quartzite structurally bounded between the Abanda and Katy Creek faults, to the northwest and southeast respectively (Fig. 2) (Bentley and Neathery, 1970; Wielchowsky, 1986; Steltenpohl, 2005; Sterling, 2006).

The structurally highest terrane in the study area is the Inner Piedmont (Figs. 1 and 2). Recent work by Steltenpohl et al. (2005) and Abrahams (2014) has documented that some units previously correlated to the Inner Piedmont (i.e., the Opelika Complex) are in fact a part of the eastern Blue Ridge terrane and now only the Dadeville Complex (Bentley and Neathery, 1970) is considered to have a true Inner Piedmont affinity (Fig. 2). The Dadeville Complex consists of a package of interlayered schist, metaquartzite, and amphibolite (Waresville Formation), thinly-layered to massive amphibolite (Ropes Creek Amphibolite), tonalitic gneiss (Waverly Gneiss), aluminous schist (Agricola Schist), and two different felsic intrusives suites (the Camp Hill Gneiss and the Rock

Mills Granite Gneiss) (Fig. 2) (Bentley and Neathery, 1970; Neilson, 1988; Steltenpohl, 2005). The felsic intrusions occur as both slightly foliated coarse-grained granite-gneiss and as well-foliated biotite-granite gneiss (Bentley and Neathery, 1970). These rocks contain peak upper amphibolite-facies metamorphic mineral assemblages that were locally retrograded to upper-greenschist facies during ductile shearing associated with Alleghanian reactivation of the Brevard zone (Steltenpohl and Moore, 1988; Steltenpohl and Kunk, 1993; Steltenpohl, 2005). Geochemical analyses of amphibolites and ultramafic rocks in the Dadeville Complex by Neilson and Stow (1986), Hall (1991), and Sterling (2006) indicate that they developed in a back-arc basin setting. Neilson et al. (1996) reported geochemistry on the felsic metaplutonic rocks in the Dadeville Complex that suggest the Camp Hill Gneiss evolved in an island-arc setting. Despite these interpretations, the true tectonic affinity and accretionary history of the Dadeville Complex remains conjectural (Steltenpohl and Moore, 1988; Steltenpohl and Kunk; 1993; Hatcher, 2005; Steltenpohl, 2005). The only known reported age for the Dadeville Complex is a Rb-Sr whole-rock isochron crystallization age of ~460 Ma (Middle Ordovician) for the Franklin Gneiss in western Georgia (Seal and Kish, 1990); the Franklin Gneiss is correlative to the Rock Mills Granite Gneiss.

Previous Investigations

Early investigations of the Alabama Piedmont (Fig. 1) focused primarily on gold occurrences and included mine locations, descriptions, mineralogy and a brief account of the regional geology (e.g. Tuomey, 1858; Phillips 1892; Adams, 1930; Park, 1935; Pardee and Park, 1948). Adams (1926, 1933), describing the crystalline rocks of

Alabama, first defined the Wedowee formation and interpreted rocks of the Brevard zone as being correlative with altered Wedowee formation. Significant regional work by Bentley and Neathery (1970) delimited the geology of the Brevard shear zone and Inner Piedmont, setting the foundation for subsequent geological studies in the area. In their report Bentley and Neathery (1970) designated the Wedowee formation as the Wedowee Group. In addition, rocks between the Wedowee Group and the Brevard shear zone were designated as the Heard Group, with associated Kowaliga Gneiss and Zana Granite felsic intrusives. The same authors subdivided rocks of the Inner Piedmont into the Dadeville Complex and Opelika Complex and delineated several mappable units (e.g., the Waresville Formation, Agricola Schist, Camp Hill gneiss, Ropes Creek Amphibolite, and the Boyds Creek mafic Complex). Bentley and Neathery (1970) suggested that the southern Appalachian Piedmont is allochthonous along a west-directed thrust comprising the Brevard shear zone and faults framing the Pine Mountain basement window (i.e., Towaliga, Bartletts Ferry, and Goat Rock fault zones). The Consortium for Continental Reflection Profiling (COCORP) later independently developed a similar interpretation of the southern Appalachian master décollement based on their seismic-reflection profiling (Cook et al., 1979).

Following the work of Bentley and Neathery (1970), rocks in the eastern Blue Ridge were renamed the Heard Group (Neathery and Reynolds, 1973), the Emuckfaw formation (Neathery and Reynolds, 1973), and finally the Emuckfaw Group (Raymond et al., 1988). Subsequent mapping, geochemistry, and geochronology was aimed at better characterizing the magmagenesis and timing of emplacement of the Zana and Kowaliga intrusions into the Emuckfaw Group. Results indicated the Zana and the Kowaliga are genetically related (Muangonoicharoen, 1975; Stoddard, 1983; and Hawkins 2013). Russell (1987), using multi-grain U-Pb zircon analytical techniques constrained an age of 461+/-12 Ma for both the Kowaliga Gneiss and Zana Granite, as well as a Rb-Sr whole-rock age of 437 Ma and 395 Ma with analytical uncertainties on the order of +/- 100 Ma. More recently, Secondary Ionization Mass Spectrometry (SIMS) U/Pb isotopic analysis of zircons from the Kowaliga Gneiss indicates a crystallization age of 440 Ma (Hawkins, 2013; Hawkins et al., 2013).

Following Bentley and Neathery (1970), Wielchowsky (1983), mapping within and adjacent to the Brevard zone fault zone from the Alabama-Georgia state line southwest to Jacksons Gap, Alabama, described the rocks as a "lithologically distinctive" metasedimentary sequence within a shear zone that flattens with depth. This model was supported by the COCORP seismic profile that suggested the fault rooted at depth into the southern Appalachian master décollement (Cook et al., 1979). Further contributions to understanding the geology and gold/precious metal occurrences (see Saunders et al., 2013) within the Jacksons Gap Group in the vicinity of the Buttston Quadrangle were made through detailed 1:24,000 scale geologic mapping, structural analysis, and geochemical analysis conducted as part of multiple Auburn University student theses between 1988 and 2015 (Johnson, 1988; Keefer, 1992; Grimes, 1993; Reed, 1994; McCullars, 2001; Sterling, 2006; White, 2007; Hawkins, 2013; Abrahams, 2014; Steltenpohl and Singleton, 2014; Poole, 2015). Of particular importance, Johnson (1988) and Reed (1994), mapping in the Jacksons Gap Group within the western parts of the Dadeville and the eastern parts of the Jacksons Gap quadrangles (Fig. 2), delineated mappable units that have been modified during subsequent studies.

Acknowledgments

The National Cooperative Geologic Mapping Program (NCGMP) and the United States Geologic Survey (USGS) provided funding for this project through an EDMAP Grant (USGS-G14AC00325) awarded to Mark G. Steltenpohl in the Department of Geosciences at Auburn University. The authors are very appreciative of this support. Additional thanks to John P. Whitmore for providing field assistance throughout this mapping investigation.

GEOLOGY

Metasedimentary, metaplutonic, and metavolcanic rocks of the eastern Blue Ridge, the Brevard shear zone, and the Inner Piedmont underlie the Wadley South Quadrangle. The eastern Blue Ridge comprises the northwestern half of the quadrangle and encompasses the lower- to middle-amphibolite facies rocks of the Wedowee and Emuckfaw Groups and the sill-like plutons of the Zana Granite and Kowaliga Gneiss. The Brevard shear zone, structurally above the Abanda fault, encompasses the lower greenschist- to middle amphibolite-facies metasedimentary sequences of the Jacksons Gap Group and occupies an approximately 1.75-mile (2.8 km) wide swath through the middle part of the quadrangle. The Inner Piedmont, structurally above the Katy Creek fault, encompasses the middle- to upper-amphibolite facies rocks of the Dadeville Complex and occupies the southwestern third of the quadrangle. Below, units depicted on Plate 1 are described generally from northwest to southeast or from structurally lowest to highest order. Map unit names and their map symbols listed below correspond to those used on Plate 1.

Lithostratigraphic Units

Eastern Blue Ridge

The structurally lowest terrane in the Wadley South Quadrangle is the eastern Blue Ridge (Fig. 2). Units of the eastern Blue Ridge that relate to the current report are defined by the Wedowee and Emuckfaw Groups (Fig. 2), structurally bounded between the Goodwater-Enitachopco fault in the northwest and the Abanda fault in the southeast (Bentley and Neathery, 1970; Neathery and Reynolds, 1975; Tull, 1978; Steltenpohl et al., 2013). These rocks contain numerous distributed retrograde mylonitic/phyllonitic shears associated with movement along the dextral strike-slip Alexander City and Brevard shear zones.

Wedowee Group (Ewe)

The Wedowee Group, named for exposures near the community of Wedowee, in Randolph County, Alabama (Neathery and Reynolds, 1975), occupies a small portion of the eastern Blue Ridge in the northern portion of the Wadley South Quadrangle. The Wedowee Group consists of a sequence of multiply foliated and interbedded medium- to coarse-grained locally graphitic and garnetiferous muscovite-biotite-quartz-feldspar-chlorite phyllite and schist (Figs. 3 and 4), garnet-sericite phyllite and schist, graphite-quartz-sericite phyllite, thin muscovite-biotite quartzite (Fig. 5), rare thin beds of fine-grained feldspathic biotite gneiss, and banded to massive amphibolite (Beaverdam Amphibolite) (Eba) (Fig. 6). Each of these rocks locally record a relatively high-degree of dextral shear strain, as indicated by strongly-developed S-C fabrics, rotated garnet porphyroblasts with asymmetric pressure shadows, and phacoidal-shaped quartz and/or feldspar composites and veins. Color of the schists and phyllites varies in fresh outcrop depending on graphite content, but they generally are a bronzy- to silvery-gray, and in weathered outcrops, it is orange/reddish-orange saprolite or micaceous soil. Exposures of this unit are limited due to dense vegetation and deep weathering but are best observed in

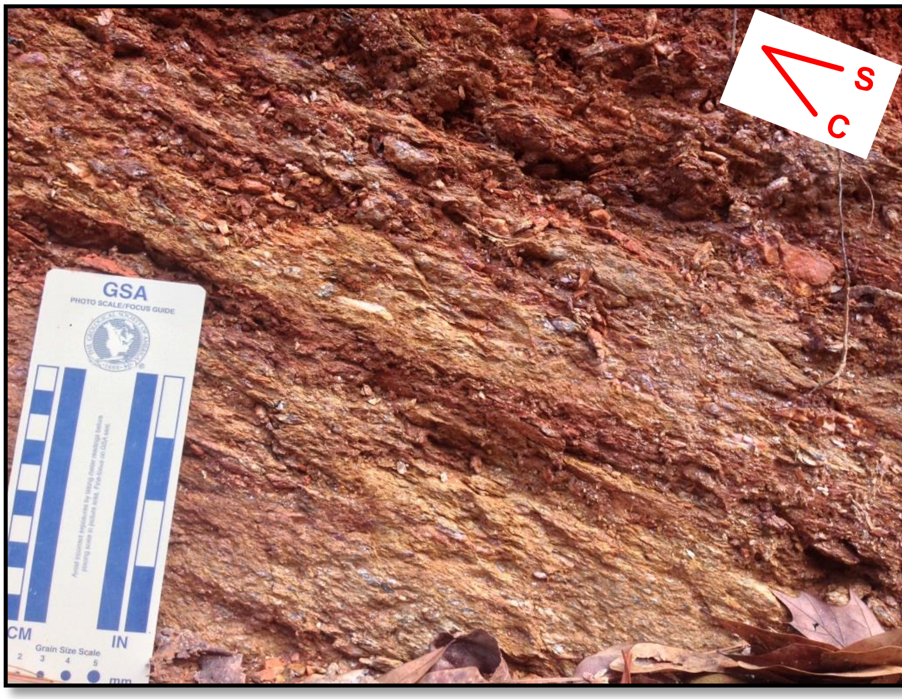

Figure 3: Photograph of a sheared, fine- to medium-grained muscovite-biotite-quartz-feldspar-chlorite button-schist from the Wedowee Group (33°07’25”N, 85°37’6”W). Note the strongly developed S-C fabric indicative of dextral motion during shearing.

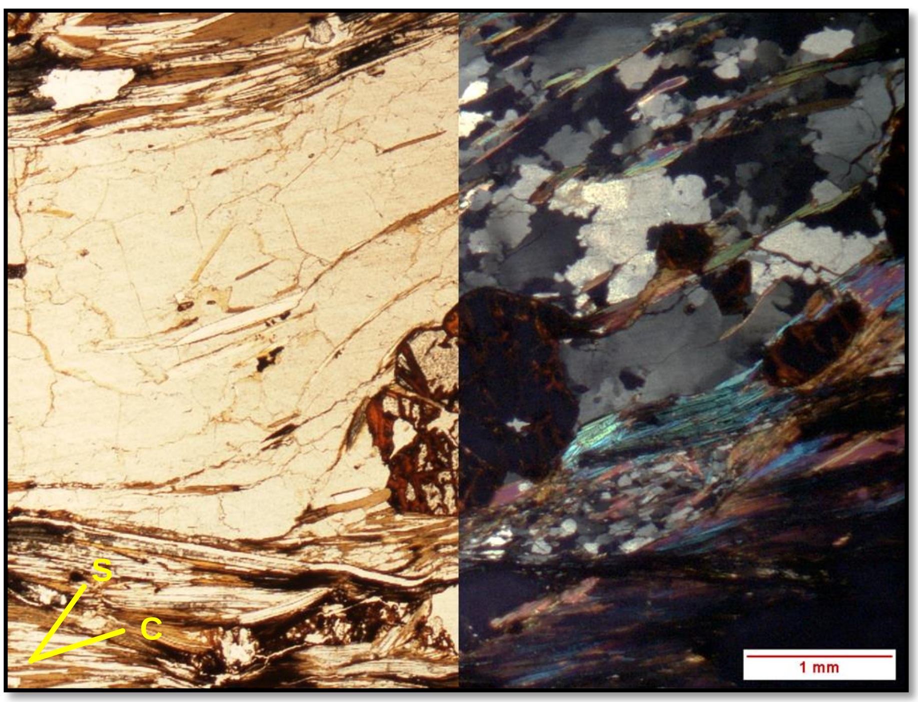

Figure 4: Upper greenschist- to lower amphibolite-facies phyllonite of the eastern Blue Ridge Wedowee Group (Ewe) containing retrograded sigma-type garnets and recrystallized quartz ribbons with interlobate grain boundaries. Quartz recrystallization due to subgrain rotation and grain boundary migration.

Figure 5: Photograph of an interlayered muscovite-biotite quartzite (standing at higher relief) and graphitic muscovite-biotite-quartz-feldspar-chlorite button-schist of in the Wedowee Group (33°05’46”N, 85°36’32”W).

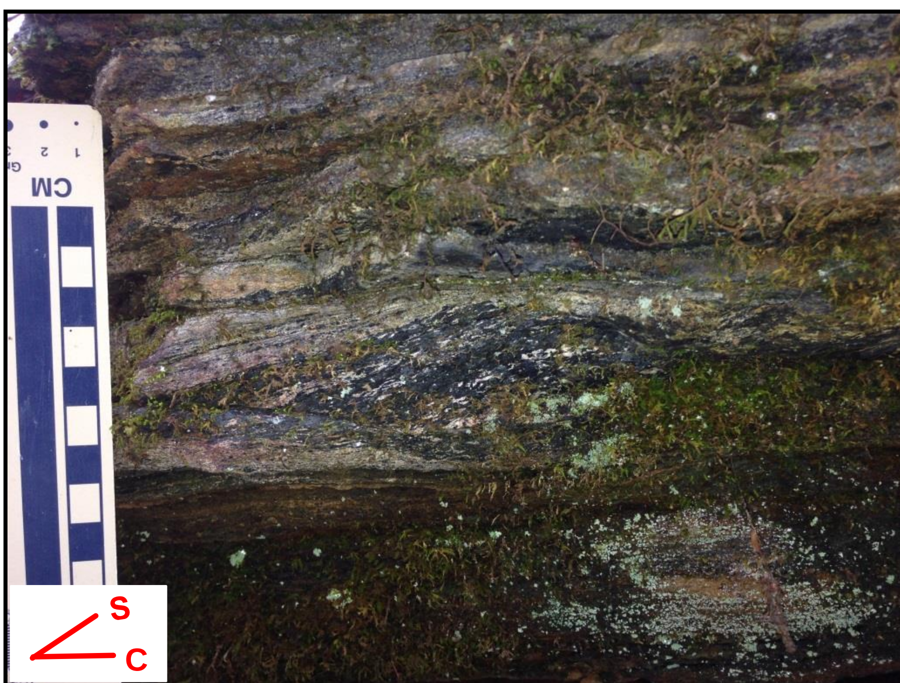

Figure 6: Photograph of a thinly layered, sheared amphibolite of the Beaverdam Amphibolite (33°06’58”N, 85°35’54”W). Thin quartzose and feldspathic layers define the banding. Note the more competent phacoidal-shaped amphibolite lense encapsulated by the shear foliation.

road cut exposures along CR-12, CR-839, CR-33, and CR-828 in the study area. The contact between the Wedowee Group and overlying Emuckfaw Group in the Wadley South Quadrangle is marked by a thin cataclastic zone associated with the Alexander City fault.

Beaverdam Amphibolite (Eba)

The Beaverdam Amphibolite is named for exposures along Beaverdam Creek, near the community of Wadley, in Randolph County, Alabama, and includes all amphibolite associated with the Wedowee Group (Bentley and Neathery, 1970; Neathery and Reynolds, 1975). In the Wadley South Quadrangle, the Beaverdam Amphibolite consists of a package of folded and extensively sheared very fine- to coarse-grained hornblende amphibolite containing thin (1-3 cm thick) alternating bands of light-colored quartz and feldspar and dark-green to black amphibole-rich material (Fig. 6). Near its contact with the Wedowee Group, the amphibolite is locally retrograded to actinolite-tremolite-chlorite schist containing minor albite, magnetite, and epidote. In outcrop, the amphibolite has a dark-green to dark-gray color and it weathers to a deep-red soil. Exposures of the Beaverdam Amphibolite in the Wadley South Quadrangle are best observed in road cut exposures along CR-24, CR-834, CR-33, and CR-828.

Emuckfaw Group (Eem)

The Emuckfaw Group, named for exposures along Emuckfaw Creek, near Horseshoe Bend, in Tallapoosa County, Alabama, occupies the remainder of the eastern Blue Ridge in the Wadley South Quadrangle (Neathery and Reynolds, 1975). The

Emuckfaw Group consists of an undifferentiated sequence of medium-grained, locally garnet- and graphite-bearing muscovite-biotite-quartz-feldspar schist (Figs. 7, 8 and 9), fine-grained muscovite-biotite-quartz-feldspar gneiss, thin micaceous quartzite, and rare fine-grained amphibolite that are intruded by Zana (Ezg) and Kowaliga (Ekg) granites. These rocks respectively record a relatively high-degree of dextral shear strain along locally distributed mylonitic/phyllonitic shear zones. Color in fresh outcrop varies with graphite content, but the Emuckfaw Group generally has a bronzy- to silvery-gray sheen and weathers to an orange/reddish-orange buff sandy, muscovite- and garnet-rich soil. Exposures of this are limited due to dense vegetation and deep weathering but are best observed in road cut exposures along Cotney Rd., CR-131, CR-133, and CR-140.

Zana Granite (Ezg) and Kowaliga Gneiss (Ekg)

The Zana Granite and Kowaliga Gneiss occur as strongly foliated interleaved granitic intrusives within the metasedimentary units of the Emuckfaw Group. The Zana Granite is named for exposures near the community of Zana, in Tallapoosa County, Alabama, and the Kowaliga Gneiss is named for exposures along Kowaliga Creek, in Elmore County, Alabama (Bentley and Neathery, 1970; Neathery and Reynolds, 1975). Bentley and Neathery (1970) and Hawkins (2013) concluded that the Zana Granite and Kowaliga Gneiss are mineralogically and geochemically similar, with the only differences being their textures and geographical occurrence. The Zana Granite is a medium- to coarse-grained granitic-gneiss containing quartz, potassium feldspar, plagioclase, biotite, and muscovite (Fig. 10). This unit exhibits a well-developed foliation defined by the alignment of biotite- and muscovite-grains. The Kowaliga Gneiss is

Figure 7: Photograph of a saprolitized medium-grained graphitic muscovite-biotite-quartz-feldspar button-schist from the Emuckfaw Group (33°04’18”N, 85°37’01”W). Exposure contains a well-developed S-C fabric recording dextral motion. View is looking parallel to strike.

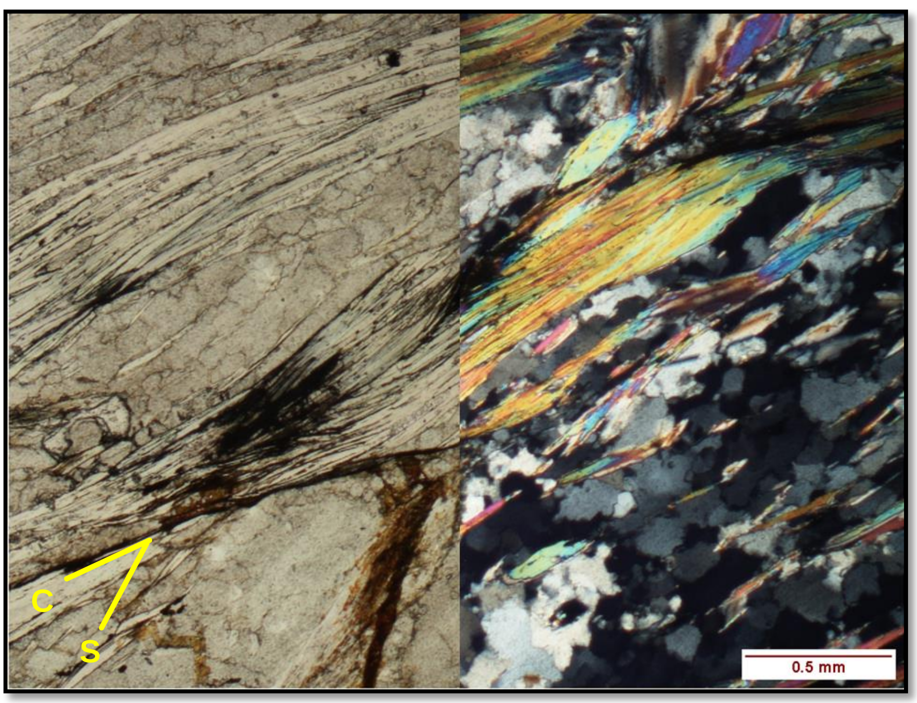

Figure 8: Upper greenschist- to lower amphibolite-facies phyllonite of the eastern Blue Ridge Emuckfaw Group (Eem) containing retrograde chlorite and recrystallized quartz ribbons with interlobate grain boundaries. Quartz recrystallization due to subgrain rotation and grain boundary migration.

Figure 9: Photograph of a sheared, medium-grained schist in the Emuckfaw Group, near the Alexander City fault shear zone (33°05’23”N, 85°35’55”W). The mylonitic foliation contains an obliquely plunging mineral elongation lineation.

Figure 10: Photograph of a granitic exposure of the Zana Granite from the Emuckfaw Group (33°05’25”N, 85°34’11”W). Foliation is defined by the alignment of medium-grained muscovite and biotite and coarse-grained feldspars.

medium- to coarse-grained augen gneiss containing quartz, potassium feldspar, plagioclase, biotite, muscovite, and retrograde chlorite and epidote. The dominant gneissosity is defined by the alignment of biotite- and muscovite-grains that drape larger, more competent subhedral potassic-feldspar augens. The Zana Granite and Kowaliga Gneiss commonly exhibit composite S-C fabrics and asymmetric porphyroblasts, and contain stretched biotite-, plagioclase-, and potassium feldspar-grains and elongate quartz ribbons. In fresh outcrops, the color varies from white to light gray, and saprolitized outcrops are light orange-buff and commonly retain the primary metamorphic foliation. Outcrops of these units in the Wadley South Quadrangle are best observed in road cut exposures along Cotney Rd., CR-62, Cr-140, and CR-141.

Jacksons Gap Group/Brevard Shear Zone

The Jacksons Gap Group separates the underlying rocks of the EBR from the structurally higher rocks of the (Inner Piedmont) Dadeville Complex, and defines the lithologies of the Brevard shear zone in eastern Alabama (Fig. 2). The Jacksons Gap Group is named for exposures near the community of Jacksons Gap, in Tallapoosa, Alabama (Bentley and Neathery, 1970). Within the study area, the Jacksons Gap Group occupies an approximately 2.8 km wide zone through the middle of the study area and on Plate 1 divided into at least five mappable units: garnetiferous phyllite, micaceous quartzite, garnetiferous graphitic phyllite, garnetiferous quartz schist, and sericite-chlorite phyllite. Outcrops through sections of these units in the study area are best observed in road cut exposures along CR-53, CR-138, CR-128, and CR- 62. The contact between the Jacksons Gap Group and overlying Emuckfaw Group in the Wadley South Quadrangle is marked by a thin cataclastic zone associated with the Abanda fault.

Garnetiferous Phyllite (JGgp)

The structurally lowest unit of the Jacksons Gap Group is the garnetiferous phyllite. The garnetiferous phyllite is a fine-grained garnet-quartz-biotite phyllite with interlayered micaceous quartzite and locally graphitic phyllite. Accessory minerals include chlorite, epidote, and unidentified opaque minerals. This unit exhibits a well-developed S-C composite-planar fabric containing shallowly southeastern-plunging mineral stretching lineations. These asymmetric fabrics clearly document oblique-dextral normal-slip movement along the Abanda fault. In fresh exposures, this unit is tan to dark brown in color and commonly possesses a gray, graphitic sheen. In the study area, the contact between the garnetiferous phyllite and the underlying units of the eastern Blue Ridge (Emuckfaw Group and Zana Granite/Kowaliga Gneiss) is marked by a thin cataclastic zone.

Garnetiferous Graphitic Phyllite (JGggp)

The garnetiferous graphitic phyllite is a medium- to coarse-grained graphitic muscovite-quartz-garnet phyllonite (Fig. 11). The phacoidal, phyllonitic texture, is a strongly planar S-C composite shear fabric. This unit is dextrally sheared, locally well lineated, with highly crenulated portions, and some portions are more of a button-schist. This unit is locally garnetiferous, well foliated, interlayered with sericitic quartzite, and generally has a silvery to light gray sheen and weathers to an orange/reddish-orange micaceous- and garnetiferous soil.

Figure 11: Photograph of a saprolitized exposure of fine-grained garnet-quartz-biotite phyllite (JGggp) from the Jackson Gap Group (33°04’47”N, 85°33’05”W). Exposure exhibits a well-developed S-C composite-planar fabric indicative of oblique-dextral normal-slip movement along the Abanda fault.

Micaceous Quartzite (JGmq)

Overlying the garnetiferous phyllite is a fine to medium-grained, well-foliated and highly sheared micaceous quartzite containing varying amounts of muscovite, sericite, chlorite, and accessory feldspar, epidote, biotite, graphite, and unidentified opaques (Fig. 12). This unit may be locally quite aluminous and contain porphyroblastic garnets and a continuous phyllitic cleavage defined by the alignment of muscovite, flattened quartz, and very fine-grained graphite. The micaceous quartzite is commonly interlayered with alternating quartz-rich and mica-rich layers (<5 cm and <10 cm thick, respectively). The layers show weak gradational boundaries over a <0.5 cm thick interval indicating deposition in waxing and waning (turbidity) currents. Their fining-upward geometry overwhelmingly indicates an upright sequence. The current authors were not able to split out separate mappable units, as depicted on the adjacent mapping of the Dadeville (Abrahams, 2014) or Jacksons Gap (Poole, 2015) quadrangles. In fresh exposures, this unit is light tan-buff in color and weathers to a white sandy and micaceous soil.

Garnetiferous Quartz Schist (JGgqs)

The garnetiferous quartz schist is a medium- to coarse-grained button-schist containing garnet, quartz, biotite, chloritoid, and sericite (Figs. 13 and 14). Kinematic indicators consist of asymmetric mica-fish, garnet porphyroblasts with asymmetric pressure shadows, sigmodal-shaped feldspar porphyroclasts (σ-clasts), and quartz ribbons (Fig. 14). Quartz ribbons contain strain-free grains, subgrains, and lobate grain boundaries. Garnetiferous quartz schists constitute a large volume of the interior of the Jacksons Gap Group and have the lowest graphite content in comparison to the other

Figure 12: Photograph of a fine-grained micaceous quartzite (JGmq) in the Brevard shear shear zone (33°05’54”N, 85°31’14”W). Outcrop has a well-developed S-C fabric indicative of dextral shearing. View is looking vertically downward, down-plunge of the S-C intersection.

Figure 13: Photograph of medium to coarse-grained button-schist (JGgqs) from the Jackson Gap Group (33°05’53”N, 85°31’17”W). Outcrop has a well-developed S-C fabric indicative of dextral motion during shearing. The red line represents the attitude of the C-plane and the blue line represents the attitude of the S-plane.

A

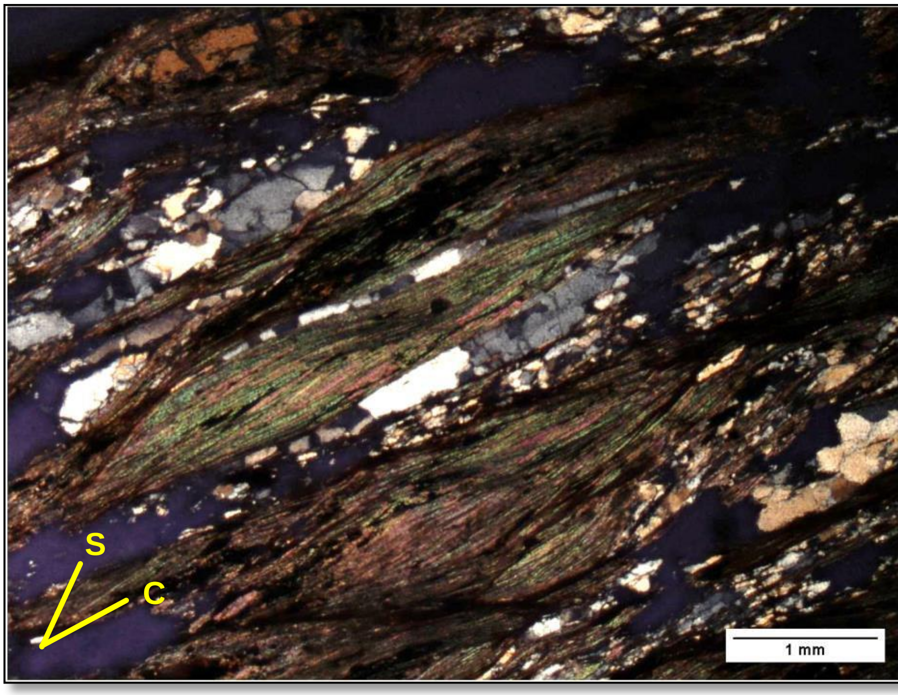

B

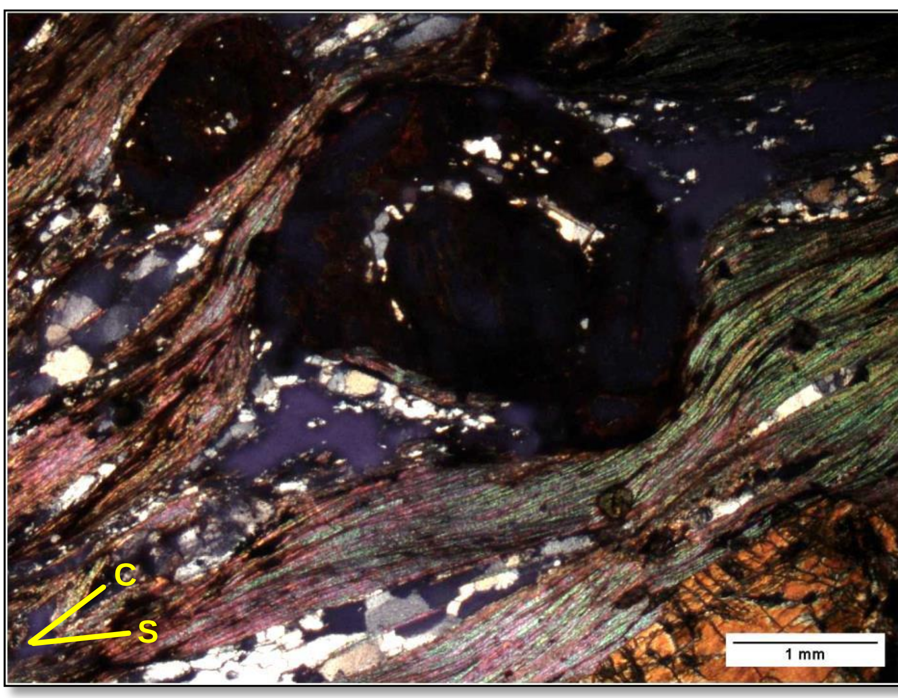

Figure 14: Photomicrographs of the Garnetiferous Quartz Schist (JGgqs) of the Jacksons Gap Group. This is the same rock depicted in Fig. 13. **A**. Photomicrograph of mica fish and quartz ribbons exhibiting a tops-to-the-right kinematics. **B**. Photomicrograph of poikiloblastic almandine garnet and chloritoid porphyroblasts Garnet contains discordant inclusion trails. Asymmetric quartz pressure shadows exhibits tops-to-the-right kinematics.

metapelitic rocks of the Jacksons Gap Group, and its high quartz content make it a prominent ridge former. In fresh exposures, the Garnetiferous Quartz Schist is typically gray-olive-brown to light-orange in color, and weathers to a light olive-orange sandy soil.

Sericite-Chlorite Phyllite (JGscp)

Structurally overlying and interlayered with the phyllites and quartzites of the Jacksons Gap Group is a sericite-chlorite phyllite. The sericite-chlorite graphitic phyllite is a fine- to medium-grained, well foliated, locally graphitic phyllite containing muscovite, sericite, chlorite, quartz, garnet, and chloritoid. This unit is locally interlayered with micaceous quartzite along gradational boundaries. In fresh outcrops, it is light olive-green to silvery-gray in color, and it weathers to a deep brick-red micaceous soil.

Inner Piedmont/Dadeville Complex

The structurally highest terrane in the Wadley South Quadrangle is the Dadeville Complex (Fig 2). The Dadeville Complex is separated from the Jacksons Gap Group along the Katy Creek fault. Within the study area, the Dadeville Complex consists of an interlayered package of metamorphosed mafic and felsic metavolcanics (Waresville Schist), and granitic metaplutonics (Rock Mills Granite Gneiss). The Dadeville Complex is named for exposures near the town of Dadeville, in Tallapoosa County, Alabama (Bentley and Neathery, 1970).

Waresville Schist (Idws)

The Waresville Schist, named for exposures near the community of Waresville, in Heard County, Georgia (Bentley and Neathery, 1970), is characterized by interlayered fine- to medium-grained mafic and felsic schist, and thinly banded to massive amphibolite exhibiting a distinctive fine-scale (1mm-2mm) cleavage that results in thin (~2.5mm thick) tabular microlithic elements. Mafic layers within the Waresville Schist (Fig. 15) consist of very fine- to medium-grained amphibole-bearing schist, banded amphibolite, chlorite schist, chlorite amphibolite, and chlorite-actinolite schist. The mafic layers are interpreted to be metamorphosed basaltic lava flows. Felsic layers within the Waresville Schist (Fig. 16) consist of medium-grained schist containing quartz, plagioclase, potassium feldspar, and sericite (Fig. 17). The felsic layers are interpreted to be metamorphosed felsic lava flows. In outcrop, the mafic layers have a dark gray color and the felsic layers have a white to light gray color. These units weather to a deep red and light tan to buff saprolite, respectively. Outcrops of this unit in the study area are best observed in road cut exposures along CR-64, CR-127, CR-53, and CR-147.

Rock Mills Granite Gneiss (Idrm)

The Rock Mills Granite Gneiss occurs interleaved in the Waresville Schist and is named for pavement exposures near the community of Rock Mills, in Randolph County, Alabama (Raymond et al, 1988). In the Wadley South Quadrangle, the Rock Mills Granite Gneiss occurs as a well-foliated, medium- to coarse-grained, granitic gneiss containing quartz, oligoclase, biotite, and muscovite, with minor amounts of microcline, epidote, and chlorite. Metamorphic foliation is defined by sheared oligoclase

Figure 15: Photograph of an exposure of a mafic unit of the Waresville Schist (33°01'12"N, 85°34'20"W). Rock is a very fine- to fine-grained, thinly banded hornblende amphibolite exhibiting a fine-scale (1mm-2mm) cleavage resulting in thin (~2.5mm) thick tabular microlithic elements.

Figure 16: Photograph of an outcrop of the felsic portion of the Waresville Schist (33°03'12"N, 85°32'23"W). The rock is a medium-grained quartz, potassium feldspar, plagioclase, and sericite schist with a strongly developed shear fabric.

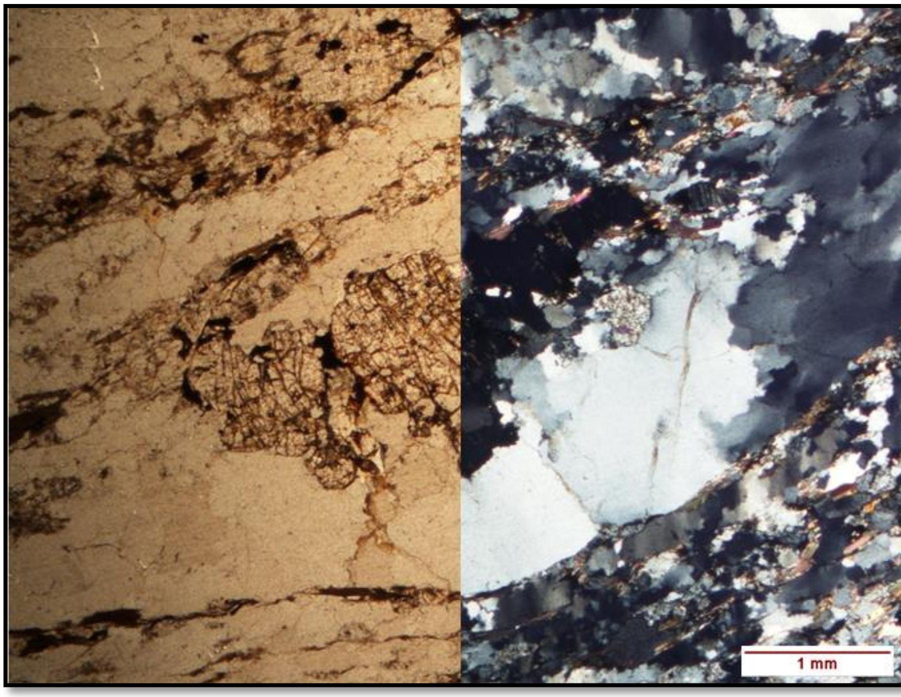

Figure 17: Retrograde upper greenschist- to lower amphibolite-facies felsic Waresville Schist (DCws) of the Dadeville Complex containing muscovite, biotite, plagioclase, quartz, potassium feldspar, chlorite, and sericite. Feldspars exhibits undulatory extinction and quartz ribbons interlobate grain boundaries. Quartz recrystallization is due to subgrain rotation and grain-boundary migration.

porphyroclasts, elongate biotite-grains, and quartz-ribbons. In exposures, the Rock Mills Granite Gneiss has a white to light-pink color, and produces to a pale-orange saprolitic soil that commonly retains its metamorphic foliation (Fig. 18). This unit is a ridge former and exhibits spheroidal weathering such that the topographic surface is covered with rounded boulders. The Rock Mills Granite Gneiss is Outcrops of this unit in the study area are best observed in road cut exposures along Cr-62, CR-121, and CR-123.

Figure 18: P hotograph of an exposure of the Rock Mills Granite Gneiss (33°00'53"N, 85°31'13"W). This unit rock commonly displays a spheroidal weathering pattern, as seen in this photograph.

METAMORPHISM

Rocks throughout the eastern Blue Ridge and Inner Piedmont of the southern Appalachians are interpreted to have undergone metamorphism during at least two separate events at ~350 Ma (Neoacadian) and at ~330 Ma (Early Alleghanian), with localized shearing between ~300 and 285 Ma (late Alleghanian) (Steltenpohl and Kunk, 1993). This is compatible with studies in the immediate vicinity of the Wadley South Quadrangle, in which the rocks of the eastern Blue Ridge, Jacksons Gap Group, and Inner Piedmont are documented as having experienced one period of lower greenschist- to upper amphibolite-facies, Barrovian-style prograde metamorphism, followed later by an extensive retrogressive middle to upper greenschist-facies metamorphic event (Muangnoicharoen, 1975; Wielchowsky, 1983; Johnson, 1988; Steltenpohl et al., 1990; Reed, 1994; Sterling, 2006; Hawkins, 2013; Abrahams, 2014; Steltenpohl and Singleton, 2014; Poole, 2015) (Fig. 19).

Within the Emuckfaw Group, Guthrie and Dean (1989) documented the prograde mineral assemblages of kyanite + staurolite + muscovite + biotite + garnet + plagioclase + quartz, indicating lower to middle amphibolite-facies peak metamorphism (Holdaway, 1971; Ernst, 1973). This is consistent with mineral assemblages of muscovite + biotite + garnet + quartz reported by Hawkins (2013), Abrahams (2014), and Poole (2015). Hawkins (2013) documented deformational microstructures in quartz and feldspar grains of the Kowaliga Gneiss that include subgrain rotation, bulging recrystallization, and grain

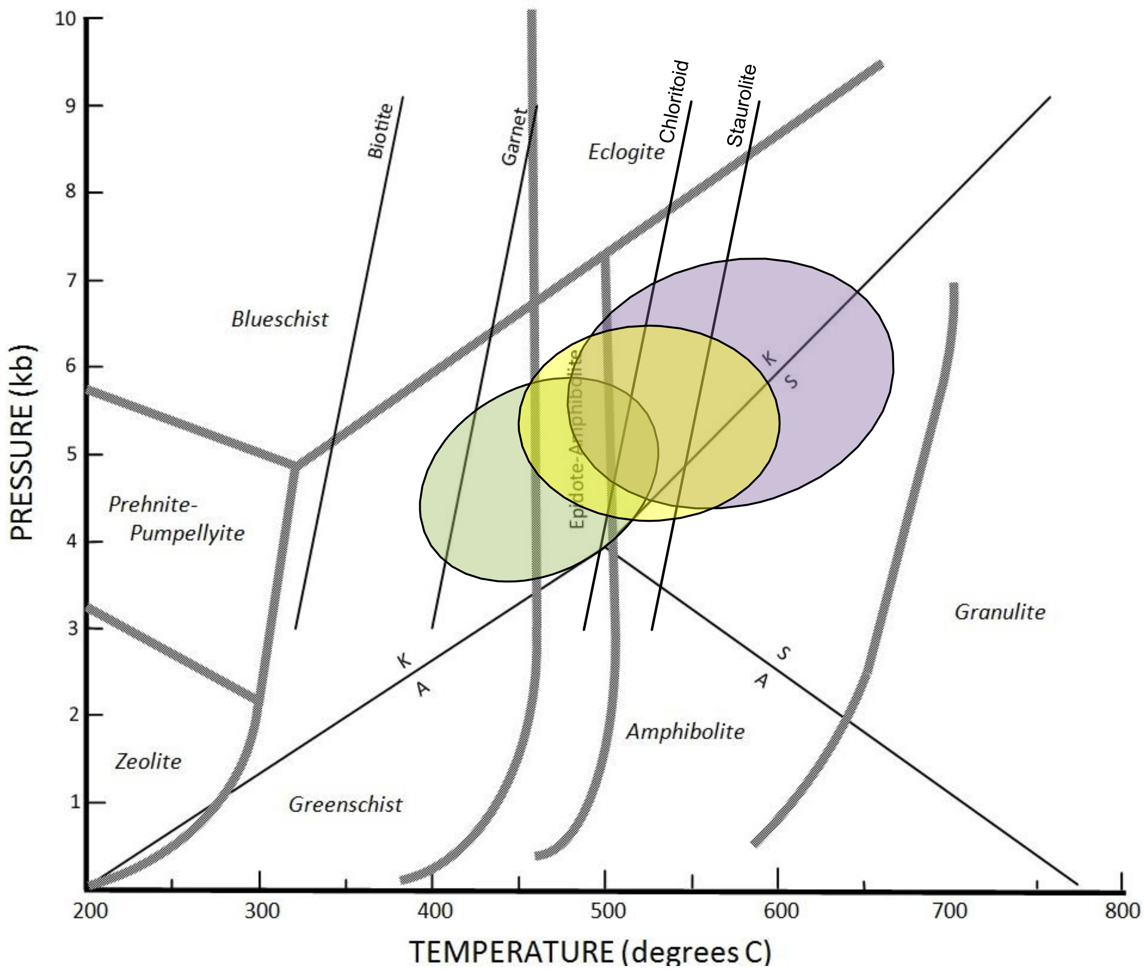

Figure 19: Metamorphic conditions suggested for the peak metamorphism within rocks of the eastern Blue Ridge (yellow circle), Jacksons Gap Group (green), and Inner Piedmont (purple) (modified from Hawkins, 2013). Grid univariant reaction curves and facies boundaries from Richardson (1968), Hoschek (1969), Holdaway (1971) and Ernst (1973).

boundary migration indicative of lower amphibolite-facies deformational conditions (Fig. 19). Additionally, Guthrie and Dean (1989) interpreted the replacement of hornblende by actinolite and chlorite in the Emuckfaw Group as having occurred under middle to upper greenschist-facies retrogressive metamorphism.

The prograde mineral assemblage of muscovite + biotite + garnet + quartz dominates the pelitic lithologies of the Jacksons Gap Group within the study area, but it is not diagnostic of metamorphic conditions. Mineral assemblages containing kyanite and garnet are documented locally along the structural top of the Jacksons Gap Group, in units adjacent to the overlying Dadeville Complex. Johnson (1988), working in a ~10 mi^2 area in the Buttston Quadrangle, documented coexisting quartz + muscovite + biotite + garnet + staurolite + chlorite in a button schist. Sterling (2006), working in the Red Hill Quadrangle, similarly reported mineral assemblages from rocks of the upper sections of the Jacksons Gap Group that contain chlorite + staurolite + kyanite + sillimanite. Staurolite ± kyanite assemblages are indicative of middle-amphibolite-facies peak metamorphic conditions, and the presence of chlorite suggests retrograde metamorphism at upper greenschist- to lower amphibolite-facies conditions. In addition, the Jacksons Gap Group contains preserved primary sedimentalogical structures such as cross stratification, graded bedding, and conglomerate pebbles, cobbles, and boulders, implying a low degree of metamorphism and strain (Bentley and Neathery, 1970; Sterling, 2006; Poole, 2015). The current investigation is consistent with peak metamorphic grade increasing from lower-greenschist facies assemblages in the base of the Jacksons Gap Group to lower to middle amphibolite-facies assemblages structurally below the Katy Creek fault (Fig. 19).

Prograde mineral assemblages in the Jacksons Gap Group have been retrograded to a lower to middle greenschist-facies mineral assemblage containing chlorite + chloritoid + sericite. M_1 minerals including biotite are replaced by chlorite, and muscovite is commonly replaced by sericite. M_2 chloritoid occur as randomly oriented, euhedral, and undeformed porphyroblasts containing helicitic inclusions trails (Fig. 14B).

The Waresville Schist and Rock Mills Granite Gneiss of the Dadeville Complex contain prograde assemblages of garnet + biotite + muscovite, compatible with middle amphibolite-facies metamorphic conditions (Fig. 19). Subhedral garnet porphyroblasts are rotated and include abundant inclusions of biotite, quartz, muscovite, and unidentified opaques. Retrogressive greenschist to lower amphibolite-facies mineral assemblages are not pervasive within the Dadeville Complex, but are observed as the alteration of hornblende to actinolite and chlorite, and biotite to chlorite within the Waresville schist. This is consistent with observations of Dadeville Complex rocks made by Johnson (1988), Steltenpohl and Moore (1988), Steltenpohl et al. (1990), Goldberg and Steltenpohl (1992), Reed (1994), Drummond et al. (1997), Sterling (2006), Abrahams (2014), Steltenpohl and Singleton (2014), and Poole (2015).

STRUCTURE

Structural observations in rocks of the Wadley South Quadrangle indicate that they have been multiply deformed and retain the evidence of at least four deformational events, D_1 through D_4 (Table 1; all structural measurements are imbedded as data files in the ArcGIS map). Upward fining sequences and cross-bedding (not observed in the Wadley South Quadrangle) in Jacksons' Gap siliciclastics define a rarely preserved primary bedding (S_0) that is otherwise subparallel to and likely transposed into the S_1 foliation, resulting in a composite S_0/S_1 fabric (Sterling, 2006; Poole, 2015). The dominant regional foliation (S_1) formed during peak metamorphic conditions (lower greenschist- to amphibolite-facies) is defined by the parallel alignment of phyllosilicate and inequant minerals. Tightly folded quartz and opaque minerals form helicitic inclusion (S_i) trails in M_1, Neoacadian (Devonian-Mississippian), garnet poikiloblasts that are discordant to the external foliation (S_e) (Fig. 14B). Whether these S_i fabrics reflect S_0 bedding or an earlier metamorphic event (Taconian?) is not known but should be investigated in the future. Mineral stretching lineations (L_1) are defined by a grain shape preferred orientation of inequant grains or elongated phyllosilicates and quartz rods. The Katy Creek fault is interpreted to be a cryptic D_1 structure with no through-going retrogressive fabric disruption, implying a pre- or syn-peak metamorphic origin. Figure 20 indicates that the primary S_0/S_1 foliation has an average strike and dip of 050°, 61° SE. L_1 mineral stretching lineations generally trend 215°and plunge 23° (Fig. 20).

Table 1. Summary of deformational events in the Wadley South, Alabama, Quadrangle.

Deformational Phases	Structural Elements	Description
	S_0	Bedding - Compositional layering
D_1	M_1	Regional prograde dynamothermal metamorphism of the EBR, JGG, and DC
	S_1	Regional foliation (schistosity and gneissosity)
		Early movement along the BFZ
		Syn- to late-peak metamorphic Katy Creek fault movement
	L_1	Inequant mineral elongation lineation
D_2	M_2	Retrogressive reactivation of the Katy Creek fault
		Early movement along the Abanda and Alexander City faults
	F_2	Isoclinal, intrafolial folding of S_0/S_1
		Late-F_2 folding of the Tallassee synform
	S_2	Local transposition of S_1 into S_2 in the JGG
		Composite S-C mylonitic fabric indicating oblique dextral-normal movement
D_3	M_3	Upper greenschist-facies reactivation of the Abanda and Alexander City faults
	F_3	Asymmetric folds associated with movement along the Abanda fault
	S_3	Composite S-C mylonitic fabric indicating oblique dextral-normal movement along the Abanda Alexander City faults
D_4		Brittle reactivation of the Alexander City fault and BFZ
		Characterized by siliceous cataclasite along the Alexander and Abanda faults

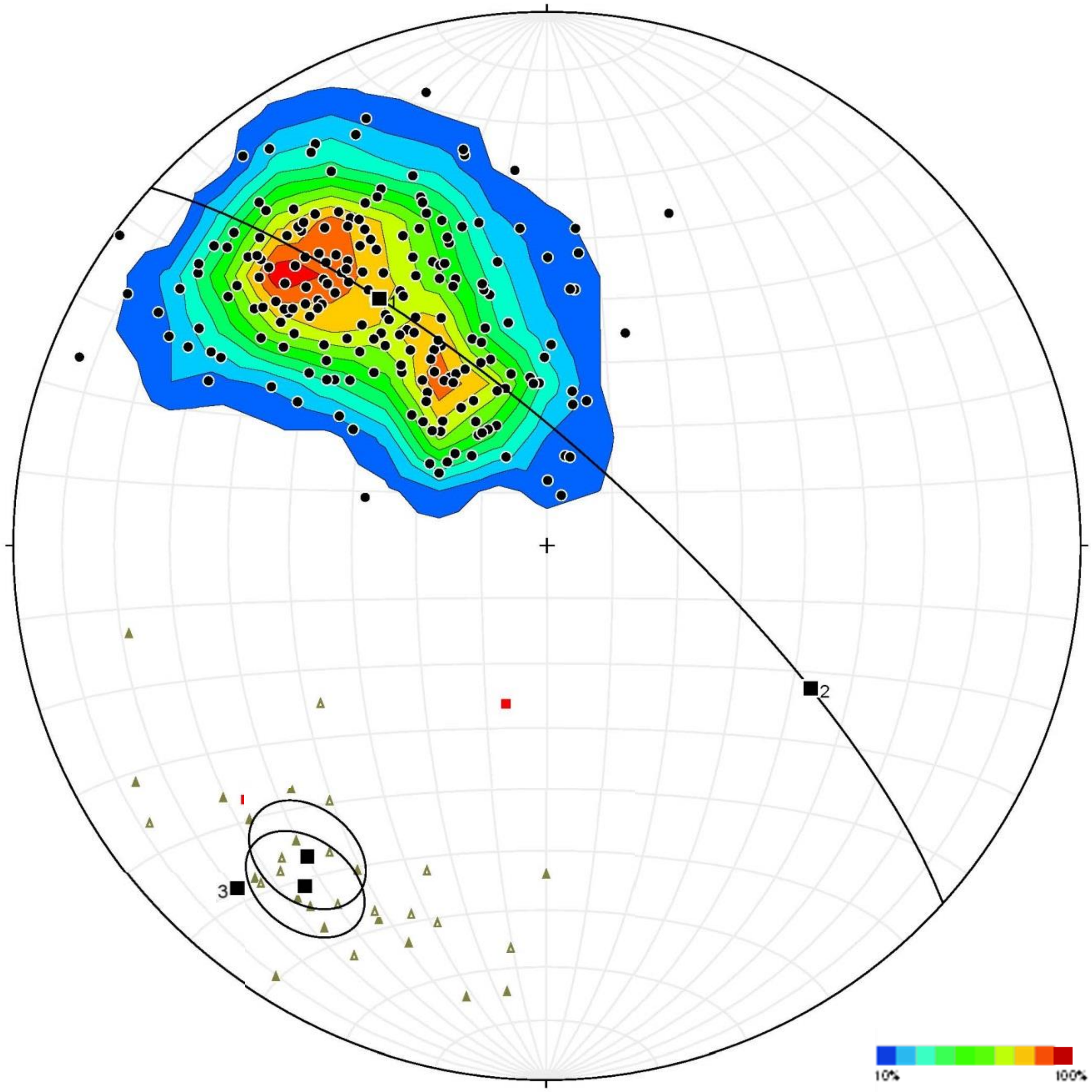

Figure 20: Lower hemisphere stereogram of structural elements measured in the Wadley South Quadrangle. Poles (contoured) to S_2/S_3 mylonitic foliations (C-planes, black dots, n=236), π-girdle: 133°, 77° SW, β-axis: 223°/14°. L_1 lineations: mineral stretchings, solid green triangles, 215°/23 ° (n=19); crenulation folds, hollow green triangles, 218°/27° (n=18); fold-axes, red squares, 213°/36° (n=4).

Compositional layering (S_0/S_1) was deformed into mesoscopic- to microscopic-scale intrafolial tight to isoclinal folds (F_1) (Fig. 21) in which the hinge surfaces of F_1 are coplanar with S_1, and fold hinges are collinear with L_1. F_2 folds generally trend 213° and plunge 36° (Fig. 20).

A second deformational event (D_2) occurred at lower to upper greenschist-facies conditions, and deformed and retrograded the earlier-formed M_1 mineral assemblages, fabrics, and structures. The S_2 foliation is defined by the parallel alignment of retrogressive chlorite and sericite that is generally associated with shear zones and fold axial surfaces. The associated mineral lineation (L_2) is generally collinear with L_1 and is defined by a grain shape preferred orientation of inequant retrogressive grains. F_2 folds are characterized by microscopic to mesoscopic, tight to open folds of S_1 that are coaxial with F_1 folds and collinear with L_1, and are coincident with regional, long-wavelength macroscale antiforms and synforms (Steltenpohl et al., 1990). The partial girdle pattern observed is S_1 measurements in Figure 20 has a β-axis oriented at 14°, 223° that is roughly coaxial with the Tallassee Synform. Minor reactivation of the Katy Creek fault is recognized locally in a weak composite S-C fabric defined by dynamically recrystallized tectosilicates and phyllosilicates.

The third deformational event (D_3) represents a prominent retrograde composite S-C fabric indicative of oblique dextral-normal movement along the Alexander City (Figs. 3, 4, 5, 6, 7, 8, 9, and 22) and Abanda (Figs. 11, 12, 13, and 23) faults. Measurements of S-C fabrics taken from within and immediately adjacent to the Alexander City fault indicate normal dextral strike-slip movement, with slip-lines trending 250° and plunging 36° (Fig. 22). Measurements of S-C fabrics taken from within

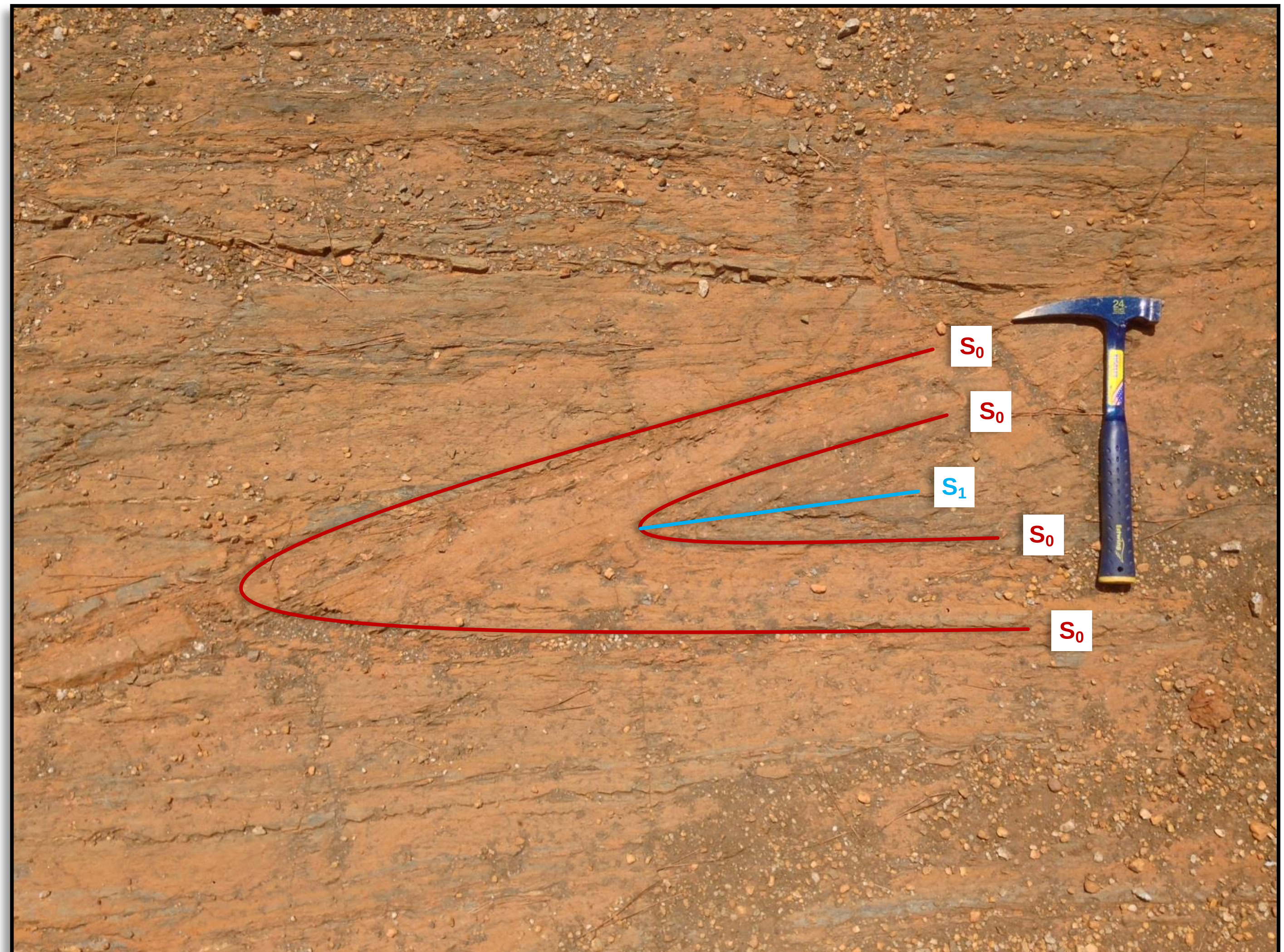

Figure 21: Photograph of isoclinal F_1 fold observed in a saprolitized mafic unit of the Waresville Schist (33°01'59"N, 85°31'06"W). S_0 is folded around the hinge and S_1 is axial planar to the F_1 fold.

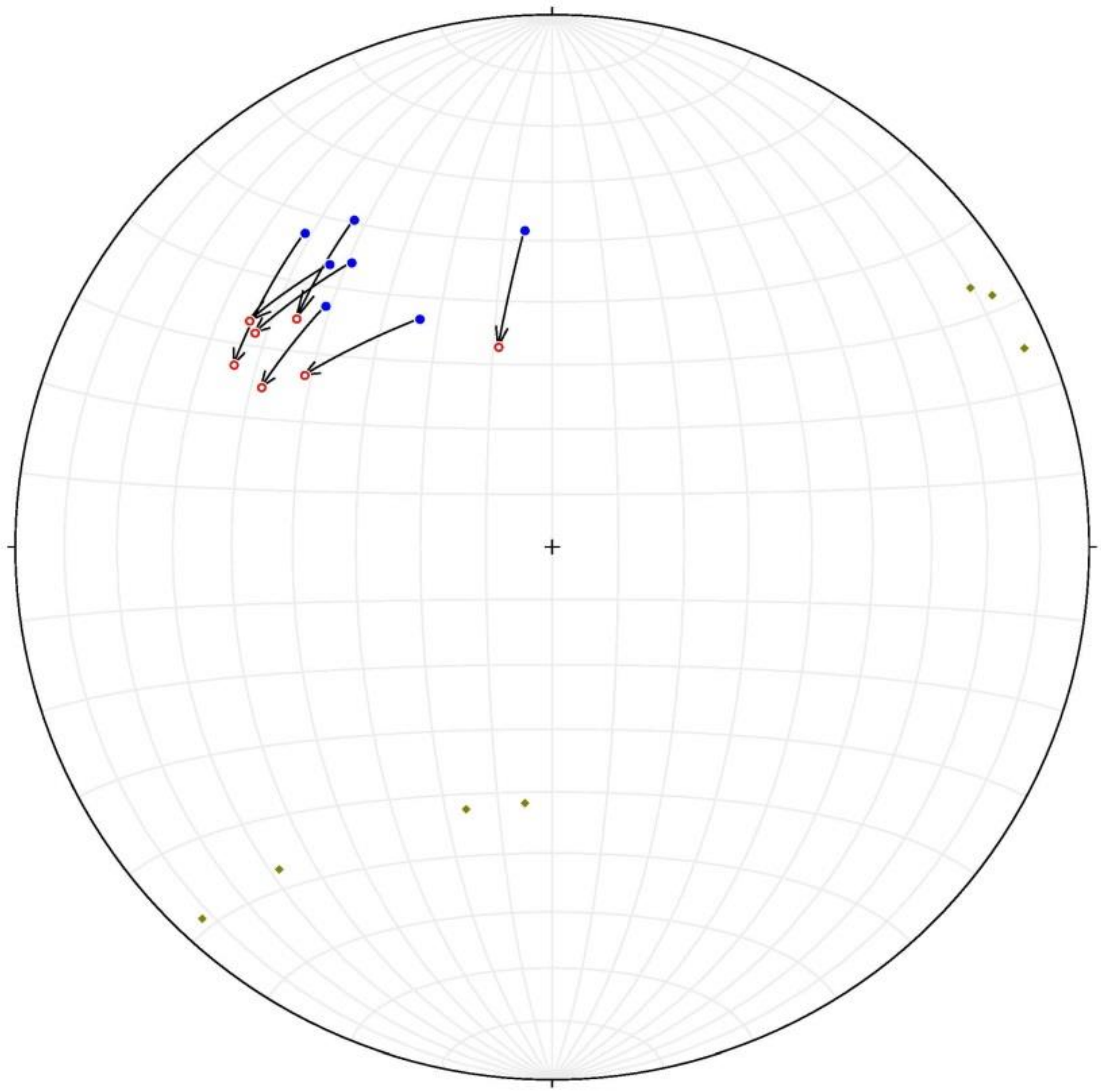

Figure 22: Lower hemisphere stereograms of S-C pairs (black arrows) and slip-lines (green diamonds) associated with the Alexander City shear zone (n=7). Poles to C-planes are unornamented end of arrows (blue dots) and poles to S-planes are the tip of the arrows (red circles).

and immediately adjacent to the Brevard shear zone indicate normal dextral strike-slip movement, with slip-lines trending 223° and plunging 40° (Fig. 23). Slip lines were geometrically constrained as being within the C-plane 90° from its intersection with the S-plane. The D_3 deformational event is interpreted to correspond to the array of Alleghanian dextral strike-slip shear zones that extend throughout the hinterland to the Goodwater-Enitachopco fault (Steltenpohl et al., 2013). Locally developed, mesoscopic and microscopic F_3 crenulation folds are coaxial to cleavage (S_3) and generally trend 218° and plunge 27° (Fig. 20). Microscopic analysis of phyllonites from the Abanda fault reveals microstructures including mica fish (Fig. 14), raveled muscovite, and crystal-plastic deformation of quartz via grain-boundary migration and bulging recrystallization (Fig. 14) and are indicative of middle-greenschist facies, sub-ductile-brittle-transition conditions for mylonitization (Passchier and Trouw, 1996). Muscovite $^{40}Ar/^{39}Ar$ ages determined for the Jacksons Gap Group (i.e., Abrahams, 2014; Poole, 2015) have been interpreted to record cooling following metamorphism and deformation, and thus do not provide constraints to decipher the possible differences in fabric age development.

Cataclasite along the northwestern side of the Alexander City and Abanda faults has overprinted earlier-formed fabrics and structures, and records a fourth (D_4) deformational event. The cataclastic zones along the northwestern-side of the Alexander City and Abanda faults in the Wadley South Quadrangle are characterized by the presence of a non-foliated, very fine- to fine-grained siliceous cataclasite containing thin (<3 mm thick) cross-cutting quartz veins with well-equilibrated triple-point grain boundaries. These zones are strong ridge formers due to their high-silica content and the interlocking nature of the quartz-grain boundaries, and likely represent supra-ductile-

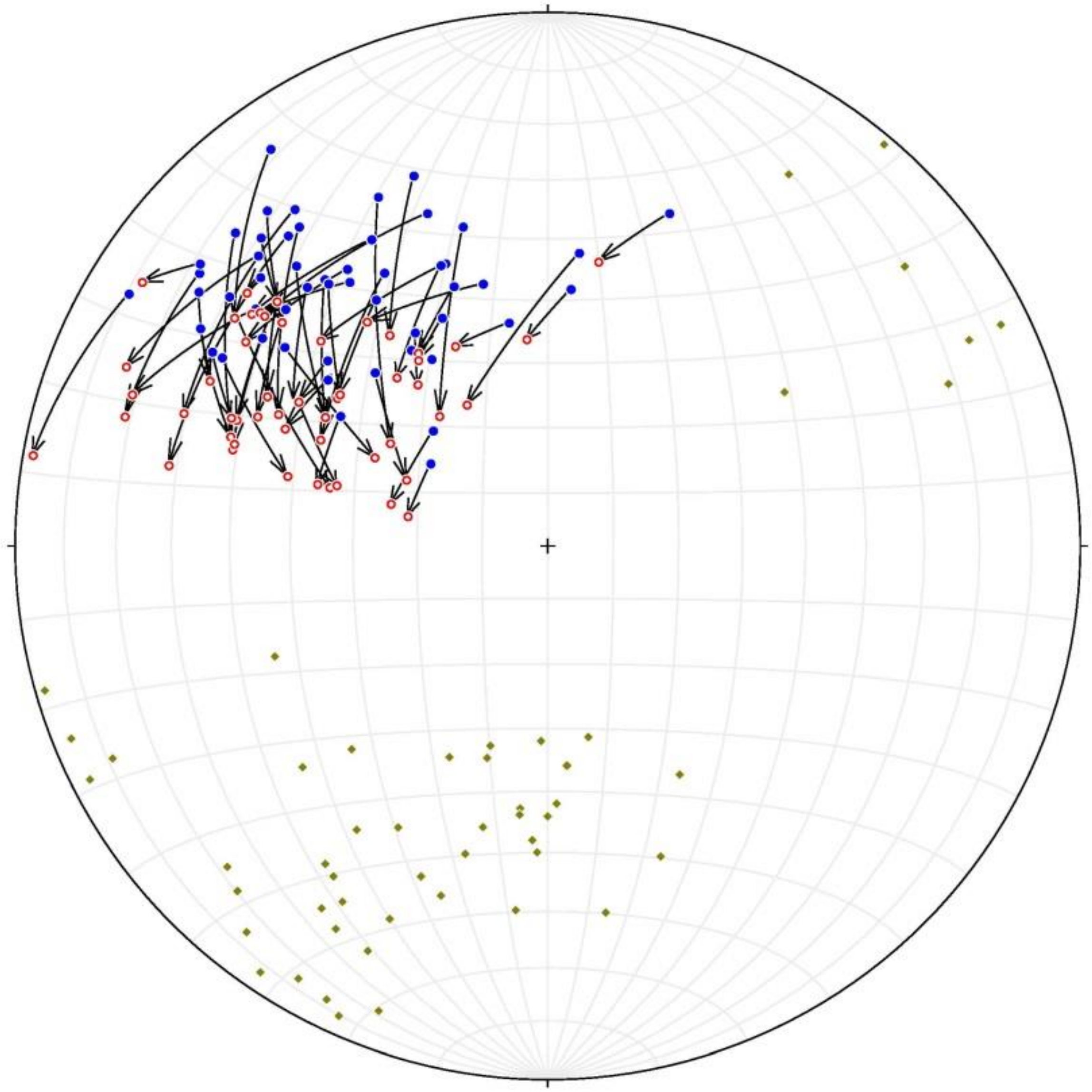

Figure 23: Lower hemisphere stereograms of S-C pairs (black arrows) and slip-lines (green diamonds) associated with the Brevard shear zone (n=52). Poles to C-planes are unornamented end of arrows (blue dots) and poles to S-planes are the tip of the arrows (red circles).

brittle-transition reactivation of the Alexander City and Abanda faults (Steltenpohl et al., 2013). Similar structures occur throughout the southern Appalachian orogen (Garihan and Ranson, 1992; Garihan et al., 1993) and are interpreted as being related to Mesozoic rifting of Pangea.

CONCLUSIONS

1. The lithologies of the Brevard zone (i.e., Jacksons Gap Group) are not easily separable into individual map units in the Wadley South Quadrangle due to their gradational nature and only display slight lithologic differences. Along-strike structural and/or stratigraphic variations have caused some units to pinch and swell or to be completely excised. The general lack of distinct marker units within the Jackson Gap Group in the study area appears to contrast with that reported in areas to the southwest (e.g., Sterling, 2006; Hawkins, 2013; Abrahams, 2014; Poole 2015). Therefore, the Jacksons Gap is subdivided into three main lithofacies types: a structurally lower section consisting predominantly of fine-grained garnetiferous-graphitic-quartz-biotite schists and phyllites and interlayered micaceous quartzites; a middle section of interlayered graphitic phyllites; and an upper section of graphitic and sericitic phyllites containing significantly less quartzite.

2. Formation of first generation, D_1, structures coincide with Neoacadian lower-to-middle-amphibolite-facies metamorphism in the eastern Blue Ridge, upper-greenschist to lower- amphibolite-facies metamorphism in the Jacksons Gap Group, and upper-amphibolite-facies metamorphism in the Inner Piedmont.

3. Helicitic S_i inclusion trails in M_1 garnet poikiloblasts are detached from S_e, the dominant S_1 foliation in rocks of the area. It is not known whether this internal foliation reflects bedding or an earlier (Taconian?) metamorphic event. Further studies should address this problem.

4. Early-syn D_1 fabrics and lithologic contacts are truncated along the Katy Creek fault, implying juxtaposition of the Dadeville Complex and Jacksons Gap Group during a syn- to late-metamorphism. An inverted metamorphic gradient may be associated with the Katy Creek fault, suggesting formation during down heating associated with thrust emplacement of the overlying Dadeville Complex.

5. Crystal-plastic reactivation of the Brevard shear zone under middle-greenschist facies conditions during the Alleghanian event is recorded in microstructures preserved in retrograde mylonites adjacent to the Abanda fault. Oblique-normal and dextral-strike-slip displacement along the Abanda fault apparently juxtaposed rocks of different metamorphic grade. Alternatively, the differences in metamorphic grade across the Abanda fault might reflect an unconformity with diachronous metamorphism of the footwall (earlier) and the later metamorphism of both packages of rocks.

6. Distributed D_3 shear zones throughout rocks of the Wedowee and Emuckfaw Groups in the Wadley South Quadrangle have identical orientations, rheologies, and kinematics as the Alexander City and Abanda faults. It appears that dextral

shearing in this area was distributed between these two fundamental southern Appalachian fault zones. Our current idea is that the Alexander City and Abanda faults are more commonly "shear zones" rather than faults, since it is not clear that any substantial displacement of units occurs across them.

7. The presence of cataclasite along the northwest side of the Alexander City and Abanda faults marks the final fault movement affecting rocks of the Eastern Blue Ridge and Brevard shear zone under supra-ductile-brittle conditions likely during the Mesozoic rifting of Pangea. The tabular zones of cataclasite are good ridge formers due to the high quartz content. Areas where the ridges have gaps are interpreted to correspond to places where the zone has been excised by high-angle normal faulting (e.g., Steltenpohl et al., 2013a).

REFERENCES

Abrahams, J.B., 2014, Geology of the Dadeville Quadrangle and the Tallassee synform in characterizing the Dog River window: Unpublished M.S. thesis, Auburn University, Auburn, Alabama, 126 p.

Adams, G.I., 1926, the crystalline rocks in Adams, G.I., Butts, D., Stephenson, L.W., and Cooke, C.W., eds., Geology of Alabama: Alabama Geological Survey Special Report 14, p. 40-223.

Adams, G.I., 1930, Gold deposits of Alabama, and occurrences of copper, pyrite, arsenic and tin: Alabama Geological Survey Bulletin 40, p. 91.

Adams, G.I., 1933, General geology of the crystalline rocks of Alabama: The Journal of Geology, v. 41, p. 159-173.

Bentley, R.D., and Neathery, T.L, 1970, Geology of the Brevard fault zone and related rocks of the Inner Piedmont of Alabama: Alabama Geological Society Field Trip Guidebook, n. 8, 119 p.

Carrigan, C.W., Bream, B., Miller, C.F., and Hatcher, R.D., Jr., 2001, Ion microprobe analyses of zircon rims from the eastern Blue Ridge and Inner Piedmont, NCSC-GA: Implications for the timing of Paleozoic metamorphism in the southern Appalachians: Geological Society of America Abstracts with Programs, v. 33, p. 7.

Cook, F.A., Albuagh, D.S., Brown, L.D., Kaufman, S., Oliver, J.E., and Hatcher, R.D., Jr., 1979, Thin-skinned tectonics in the crystalline southern Appalachians; COCORP seismic-reflection profiling of the Blue Ridge and Piedmont: Geology, v. 7, p. 563-567.

Ernst, W.G., 1973, Interpretative synthesis of metamorphism in the Alps: Geological Society of America Bulletin, v. 84, p. 2053-2078.

Garihan, J.M., and Ranson, W.A., 1992, Structure of the Mesozoic Marietta-Tryon graben, South Carolina and adjacent North Carolina, *in* Bartholomew, M.J., et al., eds., Basement tectonics 8: Characterization of ancient and Mesozoic continental margins—Proceedings of the 8th International Conference on Basement Tectonics, Butte, Montana, 1988: Dordrecht, Netherlands, Kluwer Academic Publishers, p. 539–555.

Garihan, J.M., Preddy, M.S., and Ranson, W.A., 1993, Summary of mid-Mesozoic brittle faulting in the Inner Piedmont and nearby Charlotte belt of the Carolinas, *in* Hatcher, R.D., Jr., and Davis, T., eds., Studies of Inner Piedmont geology with a focus on the Columbus Promontory: Carolina Geological Society Field Trip Guidebook, p. 55–66.

Grimes, J.E., 1993, Geology of the Piedmont rocks between the Dadeville Complex and the Pine Mountain Window in parts of Lee, Macon, and Tallapoosa Counties, Alabama: Unpublished M.S. Thesis, Auburn, Alabama, Auburn University, 129 p.

Guthrie, G.M., and Dean, L.S., 1989, Geology of the New site 7.5-Minute Quadrangle, Tallapoosa and Clay Counties, Alabama: Alabama Geological Survey Quadrangle Map 9, 41 p.

Hall, G.D., 1991, A comparative geochemical study of differing amphibolite types within the Ropes Creek Amphibolite, western Lee County, Alabama: Unpublished M.S. thesis, Auburn University, 131 p.

Hatcher, R.D., Jr., 1972, Developmental model for the southern Appalachians: Geological Society of America Bulletin, v. 83, p. 2735-2760.

Hatcher, R.D., Jr., 1978, Tectonics of the western Piedmont and Blue Ridge: Review and speculation: American Journal of Science, v. 278, p. 276-304.

Hatcher, R.D., Jr., 1987, Tectonics of the southern and central Appalachians Internides: Annual Review of Earth and Planetary Sciences, v. 15, p. 337-362.

Hatcher, R.D., Jr., 1989, Tectonic synthesis of the U.S. Appalachians, Chapter 14, *in* Hatcher R.D., Jr., Thomas, W.A., and Viele, G.W., eds., The Appalachian-Ouachita Orogen in the United States: Geology of North America, Geological Society of America, v. F-2, p. 511-535.

Hatcher, R.D., Jr, 2005, Southern and central Appalachians, *in* Selley R.C., Cocks, L.R.M., and Plimer, I.R. eds., Encyclopedia of Geology, Elsevier Academic Press, Amsterdam, p. 72-81.

Hawkins, J.F., 2013, Geology, petrology, and geochronology of rocks in the Our Town, Alabama Quadrangle: Unpublished M.S. thesis, Auburn University, Auburn, Alabama, p. 118.

Hawkins, J.F., Steltenpohl, M.G., Zou, H., Mueller, P.A., and Schwartz, J.J., 2013, New constraints on Ordovician magmatism in the southernmost exposures of the eastern Blue Ridge in Alabama: Geological Society of America Abstracts with Program, v. 45, n. 2, p. 62.

Holdaway, M.J., 1971, Stability of andalusite and the aluminosilicate phase diagram: American Journal of Science, v. 271, p. 97-131.

Hoschek, G., 1969, The Stability of Staurolite and Chloritoid and their Significance in Metamorphism of Pelitic Rocks: Contributions to Mineralogy and Petrology, v. 22, n. 3, p. 208-232.

Johnson, M.J., 1988, Geology of the gold occurrences near Jacksons Gap, Tallapoosa County, Alabama: Unpublished M.S. Thesis, Auburn, Alabama, Auburn University, p. 156.

Keefer, W.D., 1992, Geology of the Tallassee synform hinge zone and its relationship to the Brevard fault zone, Tallapoosa and Elmore Counties, Alabama: Unpublished M.S. thesis Auburn, Alabama, Auburn University, p. 195.

McCullars, J.M., 2001, Geology and trace-element geochemistry of the Brevard zone near Martin Lake, Tallapoosa County, Alabama: Unpublished M.S. thesis, Auburn, Alabama, Auburn University, p. 74.

McDonald, W.M., Hames, W.E., Marzen, L.J., and Steltenpohl, M.G., 2007, A GIS database for 40Ar/39Ar data of the southwestern Blue Ridge province: Geological Society of America Abstracts with Programs, v. 39, no. 2, p. 81.

Merschat, A.H., Hatcher, R.D., Jr., and Davis, T.L., 2005, The northern Inner Piedmont, southern Appalachians, USA: Kinematics of transpression and SW-directed mid-crustal flow: Journal of Structural Geology, v. 27, p. 1252–1281.

Merschat, A.J., and Hatcher, R.D., Jr., 2007, The Cat Square terrane: Possible Siluro-Devonian remnant ocean basin in the Inner Piedmont, southern Appalachians, USA, *in* Hatcher, R.D., Jr., Carlson, M.P., McBride, J.H., and Martínez Catalán, J.R., eds., 4-D Framework of Continental Crust: Geological Society of America Memoir 200, p. 553-565.

Muangnoicharoen, N., 1975, The geology and structure of a portion of the northern piedmont, east-central Alabama: Unpublished M.S. thesis, Tuscaloosa, University of Alabama, p. 72.

Neathery, T.L., and Reynolds, J.W., 1975, Geology of the Lineville East, Ofelia, Wadley North and Mellow Valley Quadrangles, Alabama: Geological Survey of Alabama Bulletin, v. 109, 120 p.

Neilson, M. J., 1987, The felsic gneisses of the Inner Piedmont, *in* Drummond, M.S., and Green, N.L., eds., Granites of Alabama: Tuscaloosa, Alabama, Geological Survey of Alabama, Special Publication, p. 9-16.

Neilson, M.J., 1988, The structure and stratigraphy of the Tallassee synform, Dadeville, Alabama: Southeastern Geology, v. 29, n. 1, p. 41-50.

Neilson, M.J. and Stow, S.H., 1986, Geology and geochemistry of the mafic and ultramafic intrusive rocks from the Dadeville Belt, Alabama: Geological Society of America Bulletin, v. 97, p. 296-304.

Neilson, M.J., Seal, T.L., and Kish, S.A., 1996, Two high-silica gneisses from the Dadeville Complex of Alabama's Inner Piedmont: Southeastern Geology, v. 36, n. 3, p. 123-132.

Pardee, J.T., and Park, C.F., Jr., 1948, Gold deposits of the southern Piedmont: U.S. Geological Survey Professional Paper 213, p. 156.

Park, C.F., Jr., 1935 Hog mountain gold district, Alabama: American Institute of Mining and Metallurgical Engineers Transactions, Mining Geology, v. 115, p. 209-228.

Passchier, C.W., and Trouw, R.A., 2005, Microtectonics: Springer-Verlag, Berlin, Germany, 289 p.

Phillips, W. B., 1892, a preliminary report on a part of the lower gold belt of Alabama in the counties of Chilton, Coosa, and Tallapoosa: Alabama Geological Survey Bulletin 3, p. 97.

Poole, J.D., 2015, Geology of the Jacksons Gap, Alabama, Quadrangle and structural implications for the Brevard fault zone: Unpublished M.S. thesis, Auburn University, Auburn, Alabama, 174 p.

Raymond, D.E., Osborne, W.E., Copeland, C.W., and Neathery, T.L., 1988, Alabama Stratigraphy: Geological Survey of Alabama, Tuscaloosa, 97 p.

Reed, A.S., 1994, Geology of the western portion of the Dadeville 7.5' Quadrangle, Tallapoosa County, Alabama: Unpublished M.S. thesis, Auburn, Alabama, Auburn University, p.108.

Richardson, S.W., 1968, Staurolite stability in a part of the system Fe-Al-Si-O-H: Journal of Petrology, v. 9, n. 3, p. 467-489.

Russell, G.S., 1978, U-Pb, Rb-Sr., and K-Ar geochronology of the Alabama Piedmont [Ph.D. dissertation]: Florida State University, Tallahassee, Florida, 198 p.

Saunders, J.A., Steltenpohl, M.G., and Cook, R.B., 2013, Gold Exploration and Potential of the Appalachian Piedmont of Eastern Alabama: Society of Economic Geologists Newsletter, July 2013, no. 94, v. 1, p. 12-17.

Seal, T.L., and Kish, S.A., 1990, The geology of the Dadeville Complex of the western Georgia and eastern Alabama Inner Piedmont; initial petrographic, geochemical, and geochronological results, *in* Steltenpohl, M.G., and others, eds., Geology of the southern Inner Piedmont, Alabama and southwest Georgia, Southeastern Section of the Geological Society of America Field Trip Guidebook, v. 39, p. 65-77.

Steltenpohl, M.G., 2005, An introduction to the terranes of the southernmost Appalachians of Alabama and Georgia, in Steltenpohl, M.G., Southernmost Appalachian terranes, Alabama and Georgia: Southeastern Section of the Geological Society of America Field Trip Guidebook, p. 1-18

Steltenpohl, M.G., 2013, Geology of the 1:24,000 Wadley South, Alabama, Quadrangle: Unpublished USGS-NCGMP-EDMAP proposal summary sheet, 15 p.

Steltenpohl, M.G., and Kunk, M.J., 1993, $^{40}Ar/^{39}Ar$ thermochronology and Alleghanian development of the southernmost Appalachian Piedmont, Alabama and southwest Georgia: Geological Society of America Bulletin, v. 105, p. 819-833.

Steltenpohl, M.G., and Moore, W.B., 1988, Metamorphism in the Alabama Piedmont: Alabama Geological Survey Circular, v. 138, 27 p.

Steltenpohl, M.G., and Singleton, R.T., 2014, Geology of the Buttston 7.5-minute quadrangle, Tallapoosa County, Alabama: Geological Survey of Alabama Open File-Report, 30 p.

Steltenpohl, M.G., Neilson, M.J., and Kish, S.A., 1990, Tectonometamorphic development in the southernmost Inner Piedmont terrane, Alabama, *in* Steltenpohl, M.G., Neilson, M.J., and Kish, S.A., eds., Geology of the southern Inner Piedmont, Alabama and southwest Georgia: Southeastern Section of the Geological Society of America Field Trip Guidebook, v. p. 1-16.

Steltenpohl, M.G., Heatherington, A., Mueller, P., and Miller, B.V., 2005, Tectonic implications of new isotopic dates on crystalline rocks from Alabama and Georgia, *in* Steltenpohl, M.G., ed., Southernmost Appalachian terranes, Alabama and Georgia: Southeastern Section of the Geological Society of America Field Trip Guidebook, p. 51-67.

Steltenpohl, M.G., Schwartz, J.J., and Miller, B.V., 2013, Late to post-Appalachian strain partitioning and extension in the Blue Ridge of Alabama and Georgia: Geosphere, v. 9, n. 3, p. 647-666.

Sterling, J.W., 2006, Geology of the southernmost exposures of the Brevard zone in the Red Hill Quadrangle, Alabama: Unpublished M.S. thesis, Auburn University, Auburn, Alabama, 118 p.

Stoddard, P.V., 1983, A petrographic and geochemical analysis of the Zana Granite and Kowaliga Augen Gneiss: Northern Piedmont, Alabama: Unpublished M.S. thesis, Memphis, Memphis State University, p. 74.

Stow, S.H., Neilson, M.J., and Neathery, T.L., 1984, Petrography, geochemistry and tectonic significance of the amphibolites o the Alabama Piedmont: American Journal of Science, v. 284, nos. 4 and 5, p. 416-436.

Tull, J.F, 1978, Structural development of the Alabama Piedmont northwest of the Brevard zone: American Journal of Science, v. 278, n. 4, 442-460.

Tull, J.F., Barineau, C.I., and Holm-Denoma, C.S., 2012, Characteristics, Extent, and Tectonic Significance of the Middle Ordovician Back-Arc Basin in the Southern Appalachian Blue Ridge, *in* Barineau, C.I., and Tull, J.F., The Talladega Slate Belt and the eastern Blue Ridge: Laurentian plate passive margin to back-arc basin tectonics in the southern Appalachian orogen: Field Trip Guidebook for the Alabama Geological Society, p. 12-26.

Tull, J.F., Holm-Denoma, C.H., and Barineau, C.I., 2014, Early to Middle Ordovician back-arc basin in the southern Appalachian Blue Ridge: Geological Society of America Bulletin, v. 126, n. 7/8, p. 990-1015.

Tuomey, M., 1858, Second biennial report on the geology of Alabama: Alabama Geological Survey Biennial report 2, p. 292.

White, T.W., 2007, Geology of the 1:24,000 Tallassee, Alabama, Quadrangle, and its implications for southern Appalachian tectonics: Unpublished M.S. thesis, Auburn University, Auburn, Alabama, 74 p.

Wielchowsky, C.C., 1983, The geology of the Brevard zone and adjacent terranes in Alabama [Ph.D. dissertation]: Rice University, Houston, Texas, 237 p.

II. AN EARLY PALEOZOIC TACONIC ARC DISCOVERED IN THE SOUTHERNMOST APPALACHIANS OF ALABAMA AND GEORGIA: IMPLICATIONS FOR THE CRUSTAL GROWTH OF EASTERN NORTH AMERICA

Dane S. VanDervoort[1], Chong Ma[1], Mark G. Steltenpohl[1], and Joshua J. Schwartz[2]

[1]Department of Geosciences, Auburn University, Auburn, Alabama 36849, USA

[2]Department of Geological Sciences, California State University Northridge, Northridge, California 91330, USA

ABSTRACT

The Inner Piedmont comprises a suspect terrane of high-grade (amphibolite-facies) metamorphic rocks that extends throughout much of the southern Appalachians and the precise age and tectonic affinity of these rocks is not well defined. In the southernmost Appalachian of Alabama and Georgia, the Dadeville Complex of the Inner Piedmont comprises a thick (>6 km) klippe of allochthonous metasedimentary, metavolcanic, and metaplutonic rocks. LA-SF-ICP-MS $^{206}Pb/^{238}U$ age dating of magmatic and detrital zircons from the Dadeville Complex, in conjunction with

previously reported geochemical, lithotectonic, and structural data, indicates that this terrane is a Cambrian- to Early Ordovician-aged Taconic arc located within the core of the shallow-northeast plunging Tallassee synform. Magmatic crystallization ages determined for each major plutonic or volcanic unit are 493.4 ± 6.0 Ma (Waresville Formation), 476.6 ± 6.8 Ma (Ropes Creek Amphibolite), 477.1 ± 4.8 Ma (Waverly Gneiss), and 499.8 ± 6.9 Ma (Camp Hill Gneiss). Age dating of detrital zircons from the structurally highest unit of the Dadeville Complex (Agricola Schist) reveal populations at ~883, ~755, and ~656 Ma, which are not typical of rocks developed along the southeastern Laurentian margin, and Grenville zircons are conspicuously sparse, suggesting an exotic affinity for this terrane. One zircon age-population in the detrital data set at ~480 Ma contain a Th/U ratio of less than 0.1, which appears to be the first reported record of Taconic metamorphism in the southernmost Appalachians. This date for high-grade metamorphism overlaps with eclogite- and granulite-facies metamorphism in rocks of the North Carolina Blue Ridge and synorogenic clastic wedge deposition (Blountian) reported in the foreland. The Taconic suture is exposed around the flanks of the Tallassee synform, and the Dadeville arc is a klippe cradled between Laurentian units of the eastern Blue Ridge and Pine Mountain window. This position is tectonostratigraphically equivalent to that of the Taconic suture throughout the orogen but it is peculiarly internal and structurally high, making it a unique setting in which to examine Taconian evolution of the southeastern U.S.A.

INTRODUCTION

The Taconic orogeny is classically known as the first of a series of plate tectonic collisional events that created the Appalachian Mountain chain that today underlies a large part of eastern North America. In the type area in New England, U.S.A., it is preserved as a system of island arcs that had beached upon the Iapetus-ocean-facing margin of the ancient Laurentian protocontinent during the Early-to-Middle Ordovician Period (Fig. 1A, Plate 2). The Taconic orogen has a foreland-fold-and-thrust belt that is known to extend from Newfoundland southwestward to Vermont. The continuation of the orogen into the central and southern Appalachians, however, remains debated. Hatcher (2010) reports that no Taconic allochthons occur south of New York State but that several nappes further south, within the central Appalachians, were emplaced during the Middle-to-Late Ordovician. Tull and coworkers (e.g., Tull, 1978, 1998, 2002; Tull et al., 1988, 2007; Das, 2006; Holm-Denoma, 2006; Barineau, 2009), working in the western Blue Ridge of Alabama and Georgia (Fig. 1B, Plate 2), cite a paucity of Early-to-Middle Ordovician-aged (480-460 Ma) deformation within the Talladega Slate belt and Hillabee Greenstone as evidence that the ca. ~480 Ma collisional Taconic event is absent in the southernmost exposures of the Appalachians. The apparent southward petering out of the system of Taconic arcs has played an important role in interpretations for why Laurentian crust is missing beneath the Coastal Plain to the south and west of Alabama (Fig. 1B,

Plate 2). For example, earlier workers argued that the Famatinian orogen, today exposed in western South America, was the rifted-and-orphaned southern continuation of the Taconic orogen formed by continent-continent collision between Laurentia and western Gondwana (see Dalla Salda et al., 1992). Others argue that this missing Laurentian crust had rifted-out of this area in the Cambrian and drifted across the Iapetus ocean as a microcontinent that was accreted to Gondwana (i.e., the Argentine Precordillera: Thomas and Astini, 1996). Despite the apparent lack of Taconic arc terranes south of New York, a system of terrane-boundary faults (i.e., Burnsville, Goodwater-Enitachopco, Hayesville-Fries, Hollins Line, and Holland Mountain faults) generally separates Ordovician (Taconic) metamorphic rocks and structures on the east from Laurentian units that do not contain them on the west – the so-called "Taconic suture" (see Hatcher, 2010). In addition, extensive, easterly-derived Middle-to-Late Ordovician synorogenic clastic wedges (i.e., the Sevier-Blount clastic wedge) occur in the Valley and Ridge of AL, GA, and TN, and record the Taconic collision (Keller, 1977; Shanmugam and Walker, 1978; Hatcher, 1989; Diecchio, 1993; Finney et al., 1996; Hibbard et al., 2007). Herein we report U-Pb isotopic age dates from rocks of the Dadeville Complex confirming, for the first time, the presence of a Taconic arc complex in the Inner Piedmont of Alabama and Georgia that fills a crucial void in our understanding of the plate tectonic evolution of the southeastern U.S.A.

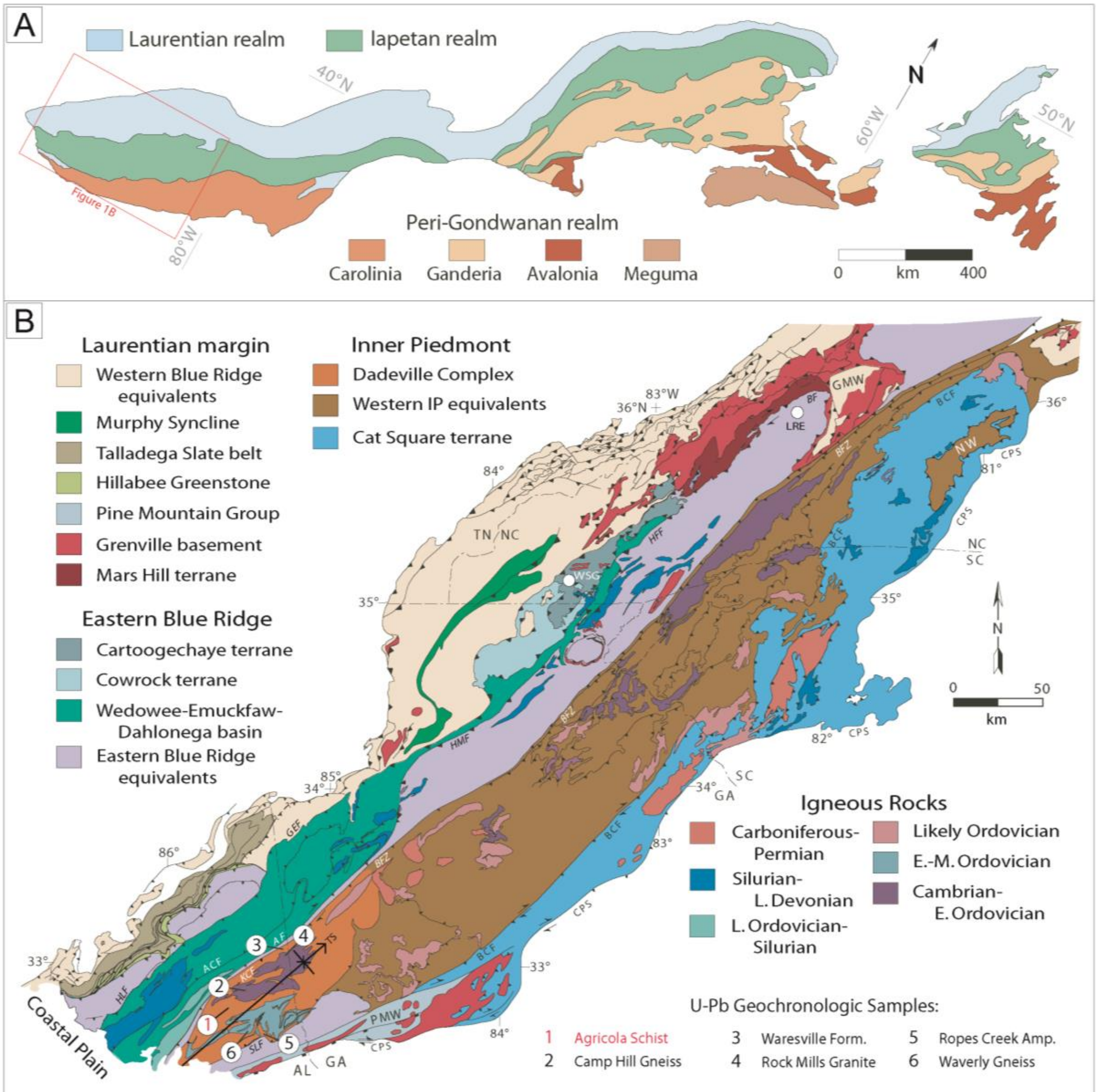

Figure 1A: First-order lithotectonic map of the Appalachian orogen (modified after Hibbard and Waldron, 2009). Red box outlines the area of 1B. **Figure 1B**: Geologic map of the southernmost Appalachians showing the location of U-Pb dating samples (modified after Merschat et al., 2010). *AF = Abanda fault*; ACF = Alexander City fault; BCF = Brindle Creek fault; *BF = Burnsville fault*; *BFZ = Brevard fault zone*; CPS = Central Piedmont shear zone; *GEF = Goodwater-Enitachopco fault*; GFW = Grandfather Mountain Window; *HFF = Hayesville-Fries fault*; *HLF = Hollins Line fault*; *HMF = Holland Mountain fault*; *KCF = Katy Creek fault*; LRE = Lick Ridge Eclogite; NW = Newton Window; PMW = Pine Mountain Window; *SLF = Stonewall Line*; TS = Tallassee Synform (plunge = 0-20°); WSG = Winding Stair Gap

TECTONOSTRATIGRAPHY OF THE SOUTHERNMOST APPALACHIANS

In the southernmost Appalachians, west of the Grenville basement massif of the Pine Mountain window (see Steltenpohl et al, 2010), late Neoproterozoic to early Paleozoic Laurentian margin rift-drift successions of the western Blue Ridge (i.e., Talladega Slate belt) are overthrust by late Precambrian to early Paleozoic distal slope-rise and arc units of the eastern Blue Ridge and Inner Piedmont terranes (Fig. 1B, Plate 2).

The Talladega Slate belt comprises a lower greenschist-facies sequence of lower Cambrian to middle Carboniferous carbonate and clastic rocks interpreted as the most outboard preserved portions of the southeastern Laurentian margin (Fig. 1B, Plate 2) (Tull 1982, 2002; Tull et al., 1988). The tectonostratigraphic base of the Talladega belt consists of Lower Cambrian Chilhowee Group equivalent siliciclastics (i.e., Kahatchee Mountain Group) conformably overlain by Cambrian to Early Ordovician Shady Dolomite and Knox Group equivalent carbonates (i.e., Sylacauga Marble Group) (Tull et al., 1988; Johnson and Tull, 2002). These sequences are in turn unconformably overlain by Early Devonian to Lower Carboniferous metaclastic rocks of the Talladega Group (i.e., Lay Day Formation, Butting Ram/Cheaha Quartzite Erin Slate, Jemison Chert) along the low-angle sub-Lay Dam Unconformity (Shaw, 1970; Cook, 1982; Tull et al., 1988; Gastaldo et al., 1993; Tull, 1998, 2002; Tull and Barineau, 2012). The Talladega Group is structurally overlain by allochthonous bimodal volcanic-plutonic rocks of the

Middle Ordovician (~470 Ma) Hillabee Greenstone along a Late Devonian- to middle Carboniferous-aged (~360-320 Ma) thrust fault (i.e., the Hillabee thrust) recording only one Paleozoic dynamothermal metamorphic event (i.e., Acadian to early Alleghanian?) (Fig. 1B, Plate 2) (McClellan et al., 2007; Tull et al., 2007; Barineau, 2009). The Hillabee Greenstone is interpreted to have formed within an extensional backarc basin during ca. ~480-460 Ma attenuation of the southeastern Laurnetian margin (Tull et al., 2007; Barineau, 2009; Tull and Barineau, 2012).

The eastern Blue Ridge consists of an allochthonous sequence of upper greenschist- to lower amphibolite-facies aluminous schist, micaceous quartzite, orthoamphibolite, and intercalated Middle to Late Ordovician bimodal volcanics. Barineau and Tull (2012) and Tull et al. (2014) use the term Wedowee-Emuckfaw-Dahlonega basin (Fig. 1B, Plate 2) and suggest a generally upright stratigraphic succession although internal faults and shear zones have disrupted this package of rocks (Bentley and Neathery, 1970; Neathery and Reynolds, 1975; Higgins et al., 1988; Osborne et al., 1988; McClellan et al., 2007; Hatcher, 2010; Steltenpohl et al., 2013). Detrital zircons from two different units of the Wedowee-Emuckfaw-Dahlonega basin reported by Tull et al. (2014) are plotted together in Figure 2. Individually, both contain ~480-460 Ma peaks; however, the sample from the Wedowee Group (Bentley and Neathery, 1970) has a prominent Grenville peak while the sample from the Emuckfaw Group (Neathery and Reynolds, 1975) has no Grenvillian signature. Tull et al. (2014) interpret geochemical analyses of the rocks to reflect a mixed Laurentian and arc/back-arc source, and argue that the occurrence of multiple intercalated Middle Ordovician- to Silurian-aged (~460-430 Ma) granitoid bodies within the Wedowee-Emuckfaw-

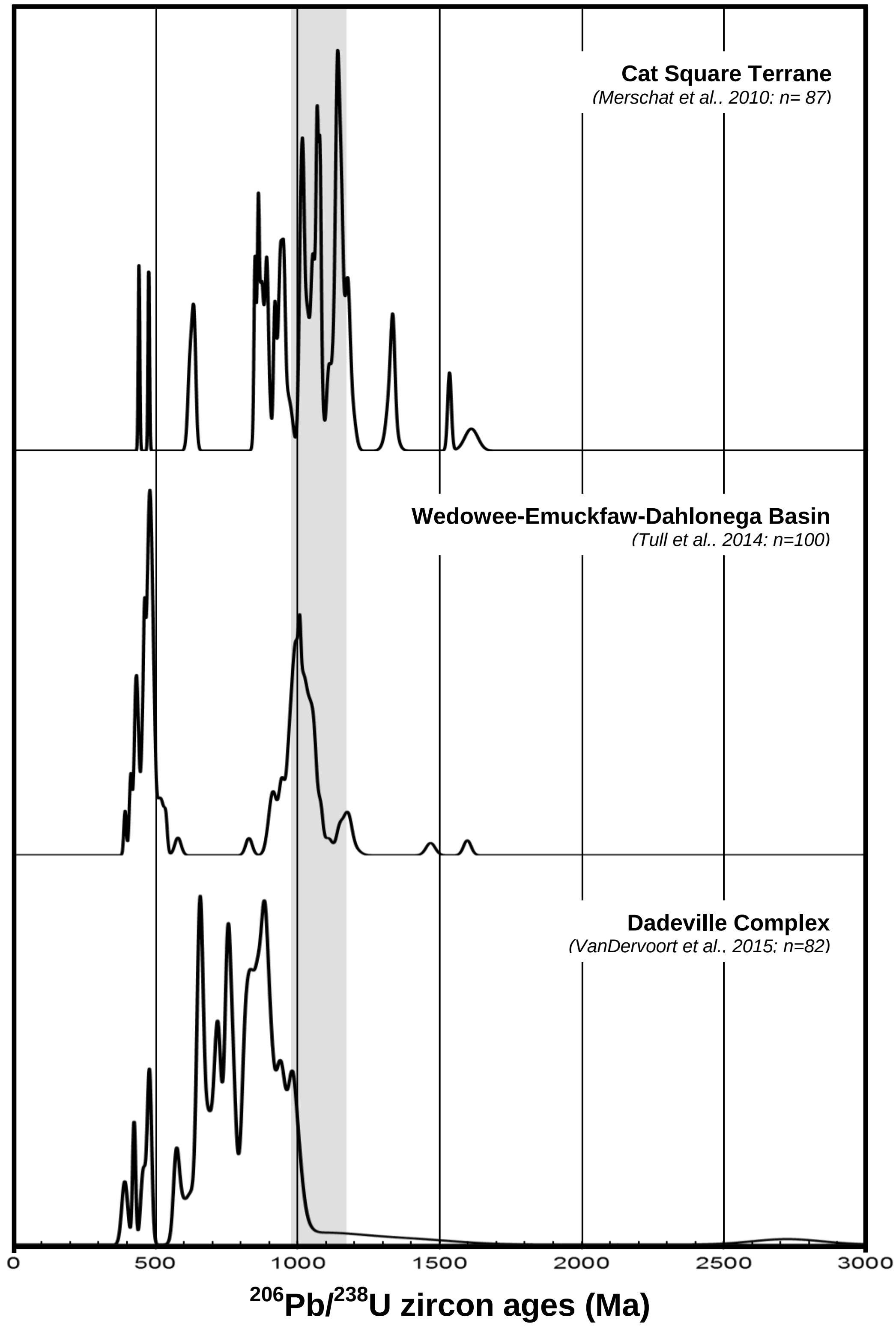

Figure 2: Detrital zircon probability density plots from the Dadeville Complex, compared to previously reported data for the Cat Square and Wedowee-Emuckfaw-Dahlonega basins. Grey box represents timing of the Grenville orogeny.

Dahlonega basin formed during ca. ~480-460 Ma Taconic-related B-type subduction. Workers in western North Carolina (Hatcher, 1978, 1987, 1989; Abbott and Raymond, 1984; Horton et al., 1989; Raymond et al., 1989; Willard and Adams, 1994; Stewart et al., 1997; Abbott and Greenwood, 2001), however, interpret a similar association of eastern Blue Ridge rocks, which include the ~480 Ma Lick Ridge Eclogite and Winding Stair Gap granulite, as an obducted Taconic accretionary assemblage formed during A-type subduction of the eastern Laurentian margin beneath an exotic Iapetan arc complex (Fig. 1B, Plate 2).

The Inner Piedmont, structurally above the eastern Blue Ridge, comprises a suspect terrane of upper amphibolite-facies volcanic, plutonic, and minor sedimentary rocks that extend throughout much of the southern and central Appalachians. In Alabama and Georgia, the Inner Piedmont consists of the allochthonous Dadeville Complex, a thick (>6 km) klippe of metasedimentary, metavolcanic, and metaplutonic rocks that lie within the core of the shallow northeast plunging Tallassee synform (Fig. 1B, Plate 2) (Bentley and Neathery, 1970; Steltenpohl et al, 1990; Steltenpohl and Kunk, 1993; Steltenpohl et al., 2005). This complex comprises interlayered amphibolite and felsic schist (Waresville Formation), interlayered amphibolite and tonalitic gneiss (Ropes Creek Amphibolite), tonalitic gneiss (Waverly Gneiss), two felsic intrusive suites (Camp Hill Gneiss and Rock Mills Granite Gneiss), migmatitic aluminous schist (Agricola Schist, which represents the structurally highest level preserved), and various unnamed mafic and ultramafic intrusive rocks (Fig. 1B, Plate 2) (Bentley and Neathery, 1970; Steltenpohl et al., 1990; Steltenpohl and Kunk, 1993; Steltenpohl et al., 2005). The relationship between the Camp Hill and Rock Mills is unclear (Bentley and Neathery, 1970). The only previously reported age for any Dadeville Complex units is a Rb-Sr whole-rock isochron crystallization age of 462 ± 4 Ma (MSWD = 1.9) for the Franklin Gneiss in western Georgia (i.e., the Rock Mills Granite gneiss in eastern Alabama) (Seal and Kish, 1990). The timing of assembly and accretion of the Dadeville Complex is not well-understood (Steltenpohl and Moore, 1988; Steltenpohl et al., 1990; Steltenpohl and Kunk, 1993), but is the topic of the current report.

Southeast of the Dadeville Complex, structurally below the Stonewall Line, are the rocks of the Opelika Complex, an interlayered sequence of upper amphibolite-facies aluminous and graphitic schist, quartzite, feldspathic and biotite-rich metagraywacke, and metagranite interpreted as being a continuation of the eastern Blue Ridge lithologies around the hinge of the Tallassee synform (Fig. 1B, Plate 2) (Bentley and Neathery, 1970; Steltenpohl et al., 1990; Steltenpohl and Kunk, 1993; Steltenpohl et al., 2005). The Opelika Complex is bounded to the east by the Pine Mountain window, which is a Grenville basement complex with its attached primary cover sequence called the Pine Mountain Group (see Steltenpohl et al., 2010).

Along strike to the northeast, western Inner Piedmont equivalents lie structurally below the eastern Inner Piedmont Cat Square terrane that was emplaced along the Brindle Creek fault. The Cat Square contains middle to upper amphibolite-facies Siluro-Devonian aluminous schist and paragneiss, calc-silicate, minor amphibolite, ultramafic rocks and Late Devonian- to Mississippian-aged anatecic granites (Fig. 1B, Plate 2) (Merschat et al., 2005; Hatcher and Merschat, 2006; Merschat and Hatcher, 2007; Merschat et al., 2010). Detrital zircons from the Cat Square terrane are dominated by 1.1 Ga and older Grenville-aged zircons, with additional population peaks at ~854, ~623, ~470, and ~430

Ma interpreted to be a mixture of both Laurentian and peri-Gondwanan sources (Fig. 2) (Bream et al. 2004; Merschat et al., 2010).

GEOCHRONOLOGY

We report laser ablation-sector field-inductively coupled plasma-mass spectrometry (LA-SF-ICP-MS) U-Pb ages on zircons from five constituent units in the Dadeville Complex of eastern Alabama and western Georgia (Fig. 1B, Plate 2). Sample locations are shown in Figure 1B and Plate 2, the Appendix contains data tables and plots, and catholuminescence images of magmatic and detrital zircon are provided in Plates 3 and 4, respectively. Data that were greater than 10% discordant were excluded from the plots.

Magmatic and detrital zircons were separated from samples weighing~5-10 kg, and U-Pb isotopes were measured using the laboratory at the California State University, Northridge. Samples were collected from their respective type locality within the Dadeville Complex in order to ensure that the correct lithologies were analyzed in the area that is not particularly well exposed due to deep weathering and abundant vegetative cover. Zircons were extracted using standard mineral separation techniques, including crushing and sieving. A Frantz magnetic separator was used to obtain a nonmagnetic fraction, and heavy liquids (methylene iodide) were used to concentrate the zircons. The zircons, standards, and unknown grains were then placed onto their mounts, mounted in epoxy, ground down to approximately half the width of the grains to expose the cores, and polished to a fine finish. The mounts were then imaged by scanning electron microscope (SEM) catholuminescence. U-Pb dating of zircons followed the methodology of Jackson et al. (2004). A primary beam of 100-μm diameter at 4-5 nA excavated a pit of ~40-μm. Measured $^{206}Pb/^{238}U$ ratios were normalized using zircon standards 91500 (Wiedenbeck et al., 2004) and Plešovice (Sláma et al., 2008). Data were reduced using SQUID-2 (Ludwig, 2009) and plotted using Isoplot v. 3.75 (Ludwig, 2012).

Magmatic zircons yielded peak $^{206}Pb/^{238}U$ age populations of 499.8 ± 6.9 Ma for the Camp Hill Gneiss (CH-1-14), 493.4 ± 6.0 Ma for the Waresville Formation (WS-1-14), 477.1 ± 4.8 Ma for the Waverly Gneiss (WA-1-14), and 476.6 ± 6.8 Ma for the Ropes Creek Amphibolite (RCA-FL6) (VanDervoort et al., 2015). The Waverly Gneiss and Ropes Creek Amphibolite contain secondary peaks at 433.1 ± 4.3 Ma and 430.0 ± 4.6 Ma, respectively. Observations based on CL images of zircons from the Rock Mills Granite Gneiss indicated that they were highly altered due to metasomatism and thus were not analyzed; if this unit correlates to the Franklin Gneiss in Georgia, as was previously thought, then the previously reported age for the latter unit likely represents the age of metamorphic closure rather than the true age of igneous crystallization. These zircon populations indicate that the Dadeville is a late Cambrian to Early Ordovician volcanic-plutonic complex.

Detrital zircons from the structurally highest unit, the Agricola Schist (AG-1-14), yielded $^{206}Pb/^{238}U$ age dates spanning from ~2.7 Ga to ~390 Ma, with prominent population peaks at ~883, ~755, ~656, and ~480 Ma (Fig. 2) (VanDervoort et al., 2015). Grenville-aged zircons are conspicuously sparse and could reflect only the very latest stages of orogenesis (7.3% of the total population; n = 6 ranging from 1070 to 980 Ma). This detrital spectrum, in fact, more closely resembles sediment derived from an Amazonian or peri-Gondwanan source rather than a Laurentian one (e.g., Keppie et al., 1998; Keppie and Ramos, 1999; Murphy and Hamilton, 2000; Saalman et al., 2007; Fyffe et al., 2009) (Fig. 2). The majority (8.5% of the total population; n = 7 ranging from 500 to 430 Ma) of the zircon population defining the ~480 Ma peak contain Th/U values less than 0.1 that most likely reflect metamorphic overgrowth (Hartman et al., 2000) related to Taconic accretion of the Dadeville Complex.

DISSCUSSION

Key discoveries from our investigation are that (1) the Dadeville Complex is an early Paleozoic arc preserved in the Alabama and Georgia Inner Piedmont, (2) the Dadeville arc records high-grade Taconian metamorphism at ca. ~480 Ma, (3) the paucity of Grenvillian detrital zircons combined with a plethora between 880 and 480 Ma implies an exotic orogen with respect to Laurentia, and (4) the Taconian suture occurs at the base of the Dadeville Complex.

The Dadeville Complex has long been recognized to contain arc affinity rocks (see Bentley and Neathery, 1970). The bulk of the complex (>50%) is composed of tholeiitic basalts, intermediate tuffs, and their differentiates (Bentley and Neathery, 1970; Sears et al., 1981; Neilson and Stow, 1986). These units are intercalated with intermediate (andesitic, dacitic, and/or tonalitic) gneisses and local mafic and ultramafic bodies that are potentially representative of an ophiolitic mélange (Neathery, 1968; Brown and Cook, 1981; Sears et al., 1981; Higgins et al., 1988; Steltenpohl et al., 1990). Geochemical analyses of the bimodal lithologies of the complex indicate enriched (E)-MORB signatures indicative of formation within an intra-oceanic island arc setting (Sears et al., 1981; Stow et al., 1984; Neilson and Stow, 1986; Spell and Norrell, 1990; Neilson et al., 1996). Similar geochemical signatures are found in rocks of the eastern Blue Ridge in Alabama and Georgia and are interpreted to indicate that the Wedowee-Emuckfaw-Dahlonega basin has a mixed provenance consistent with derivation from Laurentian

(Grenvillian) basement and its passive-margin cover, and an adjacent active volcanic arc (Higgins et al., 1988; Tull et al., 2007, 2014; Barineau, 2009). In combination with the U-Pb dates herein, the Dadeville Complex now clearly must be considered a tectonically emplaced early Paleozoic Taconic arc terrane.

The ~480 Ma zircon age-population in the Agricola Schist spectrum is the first documentation of peak Taconic metamorphism in rocks of the Alabama and Georgia Appalachians. The peak of Taconian metamorphism is well established in the eastern Blue Ridge of western North Carolina within the ~480 Ma Lick Ridge eclogite and Winding Stair Gap granulite (Fig. 1B, Plate 2) (Abbott and Raymond, 1984, 1997; Absher and McSween, 1986; Raymond et al., 1989; Adams et al., 1995; Stewart et al., 1997). $^{40}Ar/^{39}Ar$ mineral cooling data and other geochronologic means indicate that the principal amphibolite-facies metamorphic event in rocks of the Alabama-Georgia Blue Ridge and Inner Piedmont resulted from the Neoacadian event, which now appears to have overprinted and largely obliterated evidence for earlier Taconian metamorphism (see Steltenpohl and Kunk, 1993, and Hatcher and Merschat, 2006). This is compatible with petrologic and petrographic work and $^{40}Ar/^{39}Ar$ cooling dates from the Dadeville Complex (hornblende are ~347 Ma and muscovite ~325 Ma: Goldberg and Steltenpohl, 1990; Steltenpohl et al., 1990; Steltenpohl and Kunk, 1993).

Figure 2 compares the Dadeville Complex detrital zircon age populations to those of other southern Appalachian Blue Ridge (Wedowee-Emuckfaw-Dahlonega basin) and Inner Piedmont (Cat Square) terranes aiding in interpreting the tectonic evolution and emplacement of the arc. The Dadeville Complex is clearly discriminated by its paucity of Grenville zircons. Apparent Grenvillian zircons present in the spectrum are mostly younger than 980 Ma, which if from a Laurentian source could only reflect detritus from the Ottawan (~1090 to 1020 Ma) or Rigolet phases (~1010 to 980 Ma) (see Rivers, 2008), for which no basement found is exposed today in the southern Appalachians. Furthermore, in contrast, the Dadeville Complex lacks secondary peaks between ~1600 and ~1300 Ma, which workers generally attribute to Laurentian sources (Merschat et al., 2010; Tull et al., 2014). No currently known southeastern Laurentian sources exist to explain the Archean and Neoproterozoic zircons populations. Geochronologic investigations in Mexico and South America, however, document a Mesoproterozoic-link between Amazonia and Laurentia, and report that ~2700 and ~880 Ma zircons are common in rocks having an Amazonian or peri-Gondwanan tectonic affinity (Sadowski and Bettencourt, 1996; Dalziel et al, 2000; Nance et al., 2007; Saalmann et al., 2007). If the Dadeville arc was derived from the eastern edge of Laurentia (i.e., west-directed B-type subduction) then the middle-Neoproterozoic to Cambrian age populations might reflect pulses of extension between ~760-500 Ma along the post-Rodinian rifted margin (Bartholomew, 1992; Aleinikoff et al., 1995; Thomas et al., 2004; Thomas, 2006, 2011; Tull et al., 2014). On the other hand, in their analysis of the Cat Square terrane, Merschat et al. (2010) note that populations between ~750 and ~530 Ma serve as good indicators of an exotic (i.e., Amazonian or peri-Gondwanan) rather than Laurentian source area. It is noteworthy that both the Cat Square and Wedowee-Emuckfaw-Dahlonega basins lack detrital ages between ~800 and 680 Ma, whereas the Dadeville has prominent peaks in this age range. These ages likely serve as further documentation of the Proterozoic link between the Laurentian and Amazonian cratons (see Cordani and Teixeira, 2007; Li et al., 2008). The early to middle Paleozoic ages likely correspond to the ca. ~480 Taconic and ca. ~390 Acadian orogenies (Hatcher, 1978, 2005; Hibbard et al., 2007; Hibbard and Waldron, 2009; Thomas, 2011; Hibbard and Karabinos, 2013).

The base of the Dadeville Complex and the top of the eastern Blue Ridge Laurentian-margin units marks the Taconic suture in the study area. As such, the suture is exposed around the hinge and on both flanks of the Tallassee synform, affording a new opportunity to examine it. Faults mapped at this position are the Katy Creek fault along the northwest limb and its apparent counterpart, the Stonewall line fault, along the southeast limb (Fig. 1B, Plate 2). Neither fault is well understood owing to the spotty exposures, heavy vegetation, and deep weathering in near-subtropical Alabama. Fault rocks observed along both faults locally show evidence for retrograde right-slip shearing but in other localities, the structures are cryptic and parallel the metamorphic foliation, implying syn-metamorphic development (Steltenpohl et al., 1990; Grimes, 1993; Sterling, 2006; Abrahams, 2014; Poole, 2015). Clear truncations of major units within the Dadeville Complex are observed at map-scales along the Katy Creek fault but are not clear along the Stonewall line in Alabama. Sears et al. (1981) suggested that the Stonewall line is a stratigraphic boundary such that Laurentian units beneath it give way upward into a volcanic apron signaling the approach of the arc, which if verified by future geochronological work would push the actual suture to a higher structural level. The system of terrane-boundary faults that workers associate with the “Taconic suture” throughout the southern Appalachians (Fig. 1B, Plate 2) similarly have overprinted, reactivated, or excised the original suture. Regardless, the boundary still is a suture since it separates Taconian from non-Taconian rocks and structures, and in the case of the Dadeville Complex, has emplaced exotic arc rocks directly upon rocks of the Laurentian slope-rise facies. The Hayesville-Fries and Holland Mountain faults are interpreted as the suture in North Carolina and Georgia and they are considered counterparts to the Hollins-Line and Goodwater-Enitachopco faults in Alabama. Each of these are generally east-dipping boundaries marking either the eastern margin of the western Blue Ridge or an internal fault within the eastern Blue Ridge. The new occurrences where we have documented the suture are at a peculiarly internal and high-structural/erosional level surrounding the Dadeville klippe within the Tallassee synform. It is noteworthy that the east-limb of the synform, dipping westwardly, occurs in the same tectonostratigraphic position between Taconian and non-Taconian Laurentian margin units, but here lies against the orogen's most internal Grenville basement-cover massif, the Pine Mountain window.

Precisely how and where the Dadeville arc extends northeastward into Georgia and beyond remains to be fully understood (see Grimes, 1993, for a discussion). The extent of the complex depicted in Figure 1B is favored by the authors but future work will be needed to either refute or document it. The synformal geometry of the arc appears to imply that it has been excised along the most eastern/upper fault of the Brevard fault zone (i.e., Katy Creek fault). In their analysis of rock fabrics and other geological data from the Inner Piedmont, Hatcher and Merschat (2006) suggested that the Dadeville Complex was extruded toward the southwest along strike-parallel orogenic channel formed during Late Devonian to early Carboniferous (390-350 Ma) oblique subduction. The same authors interpreted ~200 km of tectonically-forced dextral displacement of the Dadeville Complex southeast of the Brevard shear zone. Given that the ~480 Ma Winding Stair Gap granulite in western North Carolina (Fig. 1B, Plate 2) is the nearest documented outcrop containing peak-Taconian metamorphic rocks northeastward from those we report in the Dadeville Complex, this would, hypothetically, indicate a minimum of ~220 km of right-slip displacement along the Brevard zone.

CONCLUSIONS

LA-SF-ICPMS U-Pb age dating of zircons combine with reported geochemical, lithotectonic, and structural data to document that the Dadeville Complex is the "missing" Taconic arc preserved in the southernmost Appalachians. A metasiliciclastic unit from the arc complex has detrital zircon age-population peaks at ~883, ~755, and ~656 Ma, none of which is typical of rocks developed along the early Paleozoic eastern Laurentian margin. Combined with a notable paucity of Grenville grains, we favor the interpretation that the arc has either an Amazonian or peri-Gondwanan affinity. Such an interpretation is compatible with east-directed subduction that is seemingly required by Taconian eclogites in the eastern Blue Ridge and the lack of a Taconic calc-alkaline plutonic belt in basement windows exposed throughout the southern Appalachians, especially the most internal one, the Pine Mountain basement-cover massif that lies directly east and structurally beneath the arc. Cambrian to Early Ordovician volcanic and plutonic rocks documented within the arc are older than Middle-to-Late Ordovician counterparts preserved in the eastern Blue Ridge beneath the arc. Early Taconian metamorphism of the arc complex is dated at ~480 Ma, overlapping in time with eclogite- and granulite-facies metamorphism documented in the Blue Ridge in western North Carolina and synorogenic deposition of the Blountian clastic wedge preserved in the foreland. Taken together, these relations seemingly favor the interpretation for east-dipping subduction polarity rather than subduction beneath Laurentia. The Taconic suture is exposed around the flanks of the Tallassee synform, and the Dadeville Complex is a klippe cradled between Laurentian units of the eastern Blue Ridge and Pine Mountain window. This position is tectonostratigraphically equivalent to that of the Taconic suture throughout the orogen but it is peculiarly internal and structurally high, making it a unique setting in which to examine Taconian evolution of the southeastern U.S.A. Future work should employ U-Pb dating of refractory minerals to read-through younger overprints and determine the true extent and nature of Taconian arc fragments and metamorphism that are left to be discovered in the southern Appalachians.

ACKNOWLEDGMENTS

We thank Meghann F.I. Decker at California State University, Northridge for mineral separation, sample preparation, and for assistance with the laser ablation-sector field-inductively coupled plasma-mass spectrometry; the Southeastern Section of the Geological Society of America for providing a Research Grant to help support this project; the Auburn University College of Sciences and Mathematics, the Auburn University Geosciences Advisory Board, and the Southeastern Section of the Geological Society of America for providing Travel Grants. Steltenpohl thanks the USGS-NCGMP-EDMAP for providing funding that supported this work.

REFERERENCES

Abbott, R.N., and Greenwood, J.P., 2001, Retrograde metamorphism of eclogite in the Southern Appalachian Mountains, USA-A case involving seamount subduction?: Journal of Metamorphic Geology, v. 19, no. 4, p. 433-443, doi: 10.1046/j.0263-4929.2001.00321.x.

Abbott, R.N., and Raymond, L.A., 1984, The Ashe Metamorphic Suite, northwest North Carolina: Metamorphism and observations of geologic history: American Journal of Science, v. 284, p. 350-375, doi: 10.2475/ajs.284.4-5.350.

Abbott, R.N., and Raymond, L.A., 1997, Petrology of pelitic and mafic rocks in the Ashe and Alligator Back metamorphic suites, northeast of the Grandfather Mountain Window, *in* Stewart, K.G., Adams, M.G., and Trupe, C.H., eds., Paleozoic Structure, Metamorphism, and Tectonics of the Blue Ridge of Western North Carolina: Durham, Carolina Geological Society, v. 1997, p. 87-101.

Absher, B.S., and McSween, H.Y., 1986, Winding Stair Gap granulites: The thermal peak of Paleozoic metamorphism: Geological Society of America Centennial Field Guide – Southeastern Section, p. 257-260.

Abrahams, J.B., 2014, Geology of the Dadeville Quadrangle and the Tallassee synform in characterizing the Dog River window, Unpublished M.S. thesis, Auburn University, Auburn, Alabama, 126 p.

Adams, M.G., Stewart, K.G., Trupe, C.H., and Willard, R.A., 1995, Tectonic significance of high-pressure metamorphic rocks and dextral strike slip faulting in the southern Appalachians, *in* Hibbard, J.P., van Staal, C.R., and Cawood, P., eds., Current Perspectives in the Appalachian-Caledonian Orogen: Geological Association of Canada Special Paper 41, p. 21-42.

Aleinikoff, J.N., Zartman, R.E., Walter, M., Rankin, D.W., Lyttle, P.T., and Burton, W.C., 1995, U-Pb age of metarhyolites of the Catoctin and Mount Rogers Formations, central and southern Appalachians: Evidence for two pulses of Iapetan rifting: American Journal of Science, v. 295, p. 428-454, doi: 10.2475/ajs.295.4.428.

Barineau, C.I., 2009, Superposed fault systems of the southernmost Appalachian Talladega belt: implications for Paleozoic orogenesis in the southern Appalachians [Ph.D. dissertation]: Tallahassee, Florida, Florida State University, 136 p.

Barineau, C.I., and Tull, J.F., 2012, The Talladega and Ashland-Wedowee-Emuckfaw belts of Alabama: Geological overview, *in* Barineau, C.I., and Tull, J.F., eds., The Talladega Slate Belt and Eastern Blue Ridge: Laurentian Plate Passive Margin to Back-Arc Basin Tectonics in the Southern Appalachian Orogen: Tuscaloosa, Alabama, Alabama Geological Society, 49th Annual Field Trip Guidebook, p. 27-37.

Bartholomew, M.J., 1992, Structural characteristics of the Late Proterozoic (post-Grenville) continental margin of the Laurentian crust, *in* Bartholomew, M.J., Hyndman, D.W., Mogk, D.W., and Mason, R., eds., Basement Tectonics 8: Characterization and Comparison of Ancient and Mesozoic Continental Margins: Proceeding of the Eighth International Conference on Basement Tectonics: Dordrecht, Netherlands, Kluwer Academic Publishers, p. 443-467.

Bentley, R.D., and Neathery, T.L, 1970, Geology of the Brevard fault zone and related rocks of the Inner Piedmont of Alabama: Alabama Geological Society Field Trip Guidebook, n. 8, 119 p.

Bream, B.R., Hatcher, R.D., Jr., Miller, C.F., and Fullagar, P.D., 2004, Detrital zircon ages and Nd isotopic data from the southern Appalachian crystalline core, GA-SC-NC-TN: New provenance constraints for Laurentian margin paragneisses, *in* Tollo, R.P., Corriveau, L., McLelland, J., and Bartholomew, M.J., eds., Proterozoic Evolution of the Grenville Orogen in North America: Geological Society of America Memoir 197, p. 459-475.

Brown, D.E., and Cook, R.B., 1981, Petrography of major Dadeville complex rock units in the Boyds Creek area, Chambers and Lee Counties, Alabama, *in* Sears, J.W., ed., Contrasts in Tectonic Style between the Inner Piedmont Terrane and the Pine Mountain Window: Tuscaloosa, Alabama Geological Society, 18th Annual Field Trip Guidebook, p. 15-40.

Cordani, U.G., and Teixeira, W., 2007, Proterozoic accretionary belts in the Amazonian Craton *in* Hatcher, R.D., Jr., Carlson, M.P., McBride, J.H., and Martínez Catalán, J.R., eds., 4-D Framework of Continental Crust: Geological Society of America Memoir 200, p. 297-320.

Cook, F.A., 1982, Stratigraphy and structure of the central Talladega slate belt, Alabama Appalachians; Tectonic studies in the Talladega and Carolina slate belts, southern Appalachian Orogen: Geological Society of America Special Paper 191, p. 47-59.

Dalla Salda, L.H., Cingolani, C.A., Varela, R., 1992, The Early Paleozoic orogenic belt of the Andes in southwestern South America: Result of Laurentia-Gondwana collision?: Geology, v. 20, p. 617-620.

Dalziel, I.W.D., Mosher, S., and Gahagan, L., 2000, Laurentia-Kalahari collision and the assembly of Rodinia: Journal of Geology, v. 108, p. 499-513.

Das, R., 2006, Geochemical and geochronological investigations in the southern Appalachians, southern Rocky Mountains and Deccan Traps [Ph.D. dissertation]: Tallahassee, Florida, Florida State University, 149 p.

Diecchio, R.J., 1993, Stratigraphic interpretation of the Ordovician of the Appalachian basin and implications for Taconian flexural modeling: Tectonics, v. 12, no. 6, p. 1410-1419.

Finney, S.C., Grubb, B.J., and Hatcher, R.D., Jr., 1996, Graphic correlation of Middle Ordovician graptolite shale, southern Appalachians: An approach for examining the subsidence and migration of a Taconic foreland basin: Geological Society of America Bulletin, v. 108, no. 3, p. 355-371,

Fyffe, L.R., Barr, S.M., Johnson, S.C., McLeod, M.J., McNicoll, V., Valverde-Vaquero, P., van Staal, C.R., and White, C.E., 2009, Detrital zircon ages from Neoproterozoic and early Paleozoic conglomerate and sandstone units of New Brunswick and coastal Maine: Implications for the tectonic evolution of Ganderia: Atlantic Geology, v. 45, p. 110-144.

Gastaldo, R.A., Guthrie, G.M., and Steltenpohl, M.G., 1993, Mississippian Fossils from Southern Appalachian Metamorphic Rocks and Their Implications for Late Paleozoic Tectonic Evolution: Science, v. 262, p. 732-734.

Goldberg, S.A., and Steltenpohl, M.G., 1990, Timing and characteristics of Paleozoic deformation and metamorphism in the Alabama Inner Piedmont: American Journal of Science v. 290, p. 1169-1200.

Grimes, J.E., 1993, Geology of the Piedmont rocks between the Dadeville Complex and the Pine Mountain window in parts of Lee, Macon, and Tallapoosa Counties, Alabama: Auburn University, M.S. thesis, Auburn, Alabama, 129 p.

Grimes, J.E., and Steltenpohl, M.G., 1993, Geology of the crystalline rocks along the fall line on the Carville, Notasulga, and Loachapoka quadrangles, Alabama, *in* Steltenpohl, M.G., and Salpas, P.A., eds., Geology of the southernmost exposed Appalachian Piedmont rocks along the Alabama fall line: Southeastern Section of the Geological Society of America Field Trip Guidebook, p. 66-94.

Hartmann, L.A., Leite, J.A.D., Silva, L.C., Remus, M.V.D., McNaughton, N.J., Groves, D.I., Fletcher, I.R., Santos, J.O.S., and Vasconcellos, M.A.Z., 2000, Advances in SHRIMP geochronology and their impact on understanding the tectonic and metallogenic evolution of southern Brazil: Australian Journal of Earth Sciences, v. 47, p. 829-844.

Hatcher, R.D., Jr., 1978, Tectonics of the western Piedmont and Blue Ridge, southern Appalachians: Review and speculation: American Journal of Science, v. 278, p. 267-304.

Hatcher, R.D., Jr., 1987, Tectonics of the southern and central Appalachian internides: Annual Review of Earth and Planetary Sciences, v. 15, p. 337-362,

Hatcher, R.D., Jr., 1989, Tectonic synthesis of the U.S. Appalachians, *in* Hatcher, R.D., Jr., Thomas, W.A., and Viele, G.W., eds., The Appalachian-Ouachita Orogen in the United States: Boulder, Colorado, Geological Society of America, Geology of North America, v. F-2, p. 511-535.

Hatcher, R.D., Jr., 2005, Southern and central Appalachians, *in* Selley R.C., Cocks, L.R.M., and Plimer, I.R., eds., Encyclopedia of Geology, Elsevier Academic Press, Amsterdam, p. 72-81.

Hatcher, R.D., Jr., 2010, The Appalachian orogen: A brief summary, *in* Tollo, R.P., Bartholomew, M.J., Hibbard, J.P., and Karabinos, P.M., eds., From Rodinia to Pangea: The Lithotectonic Record of the Appalachian Region: Geological Society of America Memoir 206, p. 1-19.

Hatcher, R.D., Jr., and Merschat, A.J., 2006, The Appalachian Inner Piedmont: An exhumed strike-parallel, tectonically forced orogenic channel, *in* Law, R.D., Searle, M., and Godin, L., eds., Channel flow, ductile extrusion and exhumation of lower-mid crust in continental collision zones: Geological Society of London Special Publication 268, p. 517-540.

Hatcher, R.D., Jr., Bream, B.R., and Merschat, A.J., 2007, Tectonic map of the southern and central Appalachians: A tale of three orogens and a complete Wilson cycle, *in* Hatcher, R.D., Jr., Carlson, M.P., McBride, J.H., and Martínez Catalán, J.R., eds., 4-D Framework of Continental Crust: Geological Society of America Memoir 200, p. 595-632.

Hibbard, J.P., and Karabinos, P., 2013, Disparate Paths in the Geologic Evolution of the Northern and Southern Appalachians: A Case for Inherited Contrasting Crustal/Lithospheric Substrates: Geoscience Canada, v. 40, n. 4, p. 303-317.

Hibbard, J.P., and Waldron, J.W.F., 2009, Truncation and translation of Appalachian promontories: Mid-Paleozoic strike-slip tectonics and basin initiation: Geology, v. 37, p. 487-490.

Hibbard, J.P., van Staal, C.R., and Rankin, D.W., 2007, A comparative analysis of pre-Silurian crustal building blocks of the northern and southern Appalachian orogen: American Journal of Science, v. 307, p. 23-45.

Higgins, M.W., Atkins, R.L., Crawford, T.J., Crawford, R.F., Brooks, R., and Cook, R.B., 1988, The structure, stratigraphy, tectonostratigraphy and evolution of the southernmost part of the Appalachian orogen: U.S. Geological Survey Professional Paper 1475, 173 p.

Holm-Denoma, C.S., 2006, Characterization of Paleozoic Terranes and Terrane Accretion at the Southeastern Margin of Laurentia: Georgia and Alabama Appalachians [Ph.D. thesis]: Tallahassee, Florida, Florida State University, 135 p.

Horton, J.W., Drake, A.A., Jr., and Rankin, D.W., 1989, Tectonostratigraphic terranes and their boundaries in the central and southern Appalachians, *in* Dallmeyer, R.D., ed., Terranes in the Circum-Atlantic Paleozoic orogens: Geological Society of America Special Paper 230, p. 213-245.

Jackson, S.E., Pearson, N.J., Griffin, W.L., and Belousova, E.A., 2004, The application of laser ablation-inductively coupled plasma-mass spectrometry to in situ U–Pb zircon geochronology: Chemical Geology, v. 211, p. 47-69.

Johnson, L.W., and Tull, J.F., 2002, Sylacauga Marble Group; distal fragment of the Southern Appalachian Cambrian-Ordovician carbonate platform: Southeastern Geology, v. 41.

Keller, F.B., 1977, Sandstone turbidites in the Tellico Formation, Indian Creek Embayment, Tennessee, *in* Ruppel, S.C., and Walker, K.R., eds., The ecostratigraphy of the Middle Ordovician of the Southern Appalachians (Kentucky, Tennessee, and Virginia) USA: Knoxville, University of Tennessee, Department of Geological Sciences, Studies in Geology 77-1, p. 117-121.

Keppie, J.D., and Ramos, V.A., 1999, Odyssey of terranes in the Iapetus and Rheic oceans during the Paleozoic, *in* Ramos, V.A., and Keppie, J.D., eds., Laurentia-Gondwana connections before Pangea: Boulder, Colorado, Geological Society of America Special Paper 336, p. 267-276.

Keppie, J.D., Davis, D.W., and Krogh, T.E., 1998, U-Pb geochronological constraints on Precambrian stratified units in the Avalon composite terrane of Nova Scotia, Canada: Tectonic implications: Canadian Journal of Earth Sciences, v. 35, p. 222-236.

Li, Z.X., et al., 2008, Assembly, configuration, and break-up history of Rodinia: A synthesis: Precambrian Research, v. 160, p. 179-210.

Ludwig, K.R., 2009, SQUID-2: A User's Manual, rev. 12 April 2009: Berkeley Geochronology Center Special Publication 5, 110 p.

Ludwig, K.R., 2012, Isoplot 3.75: A Geochronological Toolkit for Microsoft Excel: Berkeley Geochronology Center Special Publication 5, 75 p.

McClellan, E.A., Steltenpohl, M.G., Thomas, C., and Miller, C.F., 2007, Isotopic age constraints and metamorphic history of the Talladega Belt: New evidence for timing of arc magmatism and terrane emplacement along the southern Laurentian margin: The Journal of Geology, v. 115.

Merschat, A.J., and Hatcher, R.D., Jr., 2007, The Cat Square terrane: Possible Siluro-Devonian remnant ocean basin in the Inner Piedmont, southern Appalachians, USA, *in* Hatcher, R.D., Jr., Carlson, M.P., McBride, J.H., and Martínez Catalán, J.R., eds., 4-D Framework of Continental Crust: Geological Society of America Memoir 200, p. 553-565.

Merschat, A.J., Hatcher, R.D., Jr., and Davis, T.L., 2005, The northern Inner Piedmont, southern Appalachians, USA: Kinematics of transpression and SW-directed mid-crustal flow: Journal of Structural Geology, v. 27, p. 1252-1281.

Merschat, A.J., Hatcher, R.D., Jr., Bream, B.R., Miller, C.F., Byars, H.E., Gatewood, M.P., and Wooden, J.L., 2010, Detrital zircon geochronology and provenance of southern Appalachian Blue Ridge and Inner Piedmont crystalline terranes, *in* Tollo, R.P., Bartholomew, M.J., Hibbard, J.P., and Karabinos, P.M., eds., From Rodinia to Pangea: The Lithotectonic Record of the Appalachian Region: Geological Society of America Memoir, v. 206, p. 661-699.

Murphy, J.B., and Hamilton, M.A., 2000, Orogenesis and basin development: U-Pb detrital zircon age constraints on evolution of the late Paleozoic St. Marys basin, central mainland Nova Scotia: Journal of Geology, v. 108, p. 53-71.

Nance, R.D., Miller, B.V., Keppie, J.D., Murphy, J.B., 2007, Vestige of the Rheic Ocean in North America: the Acatlán Complex of southern Mexico, *in* Linnemann, U., Nance, R.D., Zulauf, G., Kraft, P., eds., The evolution of the Rheic Ocean: From Avalonian-Cadomian active margin to Alleghenian-Variscan collision: Geological Society of America Special Paper 423, p. 437-452.

Neathery, T.L., 1968, Talc and Anthophyllite Deposits in Tallapoosa and Chambers Counties, Alabama: Geological Survey of Alabama Bulletin 90, 98 p.

Neathery, T.L., and Reynolds, J.W., 1975, Geology of the Lineville East, Ofelia, Wadley North and Mellow Valley Quadrangles, Alabama: Geological Survey of Alabama Bulletin, v. 109, 120 p.

Neilson, M.J. and Stow, S.H., 1986, Geology and geochemistry of the mafic and ultramafic intrusive rocks from the Dadeville Belt, Alabama: Geological Society of America Bulletin, v. 97, p. 296-304.

Neilson, M.J., Seal, T.L., and Kish, S.A., 1996, Two high-silica gneisses from the Dadeville Complex of Alabama’s Inner Piedmont: Southeastern Geology, v. 36, n. 3, p. 123-132.

Osborne, W.E., Szabo, M.W., Neathery, T.L., and Copeland, C.W., Jr., compilers, 1988, Geologic map of Alabama, northeast sheet: Alabama Geological Survey Special Map 220, scale 1:250,000.

Poole, J.D., 2015, Geology of the Jacksons Gap, Alabama, Quadrangle and structural implications for the Brevard fault zone [M.S. thesis]: Auburn University, Auburn, Alabama, 174 p.

Raymond, L.A., Yurkovich, S.P., and McKinney, M., 1989, Block-in-matrix structures in the North Carolina Blue Ridge belt and their significance for the tectonic history of the southern Appalachian orogen, *in* Horton, J.W., Jr., and Rast, N., eds., Mélanges and olistostromes of the U.S. Appalachians: Geological Society of America Special Paper 228, p. 195-215.

Rivers, T., 2008, Assembly and preservation of lower, mid, and upper orogenic crust in the Grenville Province–Implications for the evolution of large hot long-duration orogens; Precambrian Research, v. 167, p. 237-259.

Sadowski, G.R., and Bettencourt, J.S., 1996, Mesoproterozoic tectonic correlations between eastern Laurentia and the western border of the Amazon craton: Precambrian Research, v. 76, p. 213-227.

Saalmann, K., Hartmann, L.A., and Remus, M.V.D., 2007, The assembly of West Gondwana-The view from the Rio de la Plata craton, *in* Linnemann, U., Nance, R.D., Kraft, P., and Zulauf, G., eds., The evolution of the Rheic Ocean: From Avalonian-Cadomian active margin to Alleghenian-Variscan collision: Geological Society of America Special Paper 423, p. 1-26.

Seal, T.L., and Kish, S.A., 1990, The geology of the Dadeville Complex of the western Georgia and eastern Alabama Inner Piedmont: Initial petrographic, geochemical, and geochronological results, *in* Steltenpohl, M.G., Neilson, M.J., and Kish, S.A., eds., Geology of the southernmost Inner Piedmont Terrane, Alabama and southwest Georgia: Tuscaloosa, Alabama, Geological Society of America, Southeastern Section Meeting, Field Trip Guidebook, p. 65-77.

Sears, J.W., Cook, R.B., Jr., and Brown, D.E., 1981, Tectonic evolution of the Pine Mountain Window and adjacent Inner Piedmont province, *in* Sean, J.W., ed., Contrasts in Tectonic Style between the Inner Piedmont Terrane and the Pine Mountain Window: Alabama Geological Society Guidebook 18, p. 1-13.

Shanmugam, G., and Walker, K.R., 1978, Tectonic significance of distal turbidites in the Middle Ordovician Blockhouse and lower Sevier Formations in east Tennessee: American Journal of Science, v. 278, p. 551-578.

Shaw, C.E., Jr, 1970, Age and stratigraphic relations of the Talladega slate, evidence of pre-middle Ordovician tectonism in central Alabama: Southeastern Geology, v. 11, p. 253-267.

Sláma, J., et al., 2008, Plešovice zircon-a new natural reference material for U-Pb and Hf isotopic microanalysis: Chemical Geology, v. 249, n. 1, p. 1-35.

Spell, T.L., and Norrell, G.T., 1990, The Ropes Creek assemblage; petrology, geochemistry, and tectonic setting of an ophiolitic thrust sheet in the southern Appalachians: American Journal of Science, v. 290, p. 811-842.

Steltenpohl, M.G., ed., 2005, Southernmost Appalachian terranes, Alabama and Georgia: Geological Society, Southeastern Section of the Geological Society of America Feld Trip guidebook, 162 p.

Steltenpohl, M.G., and Kunk, M.J., 1993, $^{40}Ar/^{39}Ar$ thermochronology and Alleghanian development of the southernmost Appalachian Piedmont, Alabama and southwest Georgia: Geological Society of America Bulletin, v. 105, p. 819-833.

Steltenpohl, M.G., and Moore, W.B., 1988, Metamorphism in the Alabama Piedmont: Alabama Geological Survey Circular, v. 138, 27 p.

Steltenpohl, M.G., Kish, S.A., and Neilson, M.J., eds., 1990, Geology of the southern Inner Piedmont terrane, Alabama and southwest Georgia: Southeastern Section of the Geological Society of America Field Trip Guidebook, 139 p.

Steltenpohl, M.G., Hatcher, R.D., Jr., Mueller, P.A., Heatherington, A.L., and Wooden, J.L., 2010, Geologic history of the Pine Mountain window, Alabama and Georgia: Insights from a new geologic map and U-Pb isotopic dates, *in* Tollo, R.P., Bartholomew, M.J., Hibbard, J.P., and Karabinos, P.M., eds., From Rodinia to Pangea: The Lithotectonic Record of the Appalachian Region: Geological Society of America Memoir 206. Boulder, Colorado, p. 837-858.

Steltenpohl, M.G., Schwartz, J.J, and Miller, B.V., 2013, Late to post-Appalachian strain partitioning and extension in the Blue Ridge of Alabama and Georgia: Geosphere, v. 9, n. 3, p. 647-666.

Sterling, J.W., 2006, Geology of the southernmost exposures of the Brevard zone in the Red Hill Quadrangle, Alabama: M.S. thesis, Auburn University, Auburn, Alabama, 118 p.

Stewart, K.G., Adams, M.G., and Trupe, C.H., 1997, eds., Paleozoic structure, metamorphism, and tectonics of the Blue Ridge of western North Carolina: Carolina Geological Society 1997 Field Trip Guidebook, 101 p.

Stow, S.H., Neilson, M.J., and Neathery, T.L., 1984, Petrography, geochemistry, and tectonic significance of the amphibolites of the Alabama Piedmont; mafic and ultramafic rocks of the Appalachian orogen: American Journal of Science, v. 284, p. 414-436.

Thomas, W.A., 2006, Tectonic inheritance at a continental margin: GSA Today, v. 16, no. 2, p. 4-11.

Thomas, W.A., 2011, Detrital-zircon geochronology and sedimentary provenance: Lithosphere, v. 3, n. 4, p. 304-308.

Thomas, W.A., and Astini, R.A., 1996, The Argentine Precordillera: A traveler from the Ouachita embayment of North American Laurentia: Science, v. 273, p. 752-757.

Thomas, W.A., Astini, R.A., Mueller, P.A., Gehrels, G.E., and Wooden, J.L., 2004, Transfer of the Argentine Precordillera terrane from Laurentia: Constraints from detrital-zircon geochronology: Geology, v. 32, no. 11, p. 965-968.

Tull, J.F., 1978, Structural development of the Alabama Piedmont northwest of the Brevard zone: American Journal of Science, v. 278, p. 442-460.

Tull, J.F., 1982, Polyphase late Paleozoic in the Appalachian thrust belt and Piedmont of Alabama; The Geological Society of America, 95th annual meeting: Geological Society of America Abstracts with Programs, v. 14, p. 634.

Tull, J.F., 1998, Analysis of a regional middle Paleozoic unconformity along the distal southeastern Laurentian margin, southernmost Appalachians: Implications for tectonic evolution: Geological Society of America Bulletin, v. 110, p. 1149-1162.

Tull, J.F., 2002, Southeastern margin of the middle Paleozoic shelf, southwesternmost Appalachians: Regional stability bracketed by Acadian and Alleghanian tectonism: Geological Society of America Bulletin, v. 114, p. 643-655.

Tull, J.F., and Barineau, C.I., 2012, Overview of the stratigraphic and structural evolution of the Talladega slate belt, Alabama Appalachians, *in* Eppes, M.C., and Bartholomew, M.J., eds., From the Blue Ridge to the Coastal Plain: Field Excursions in the Southeastern United States: Geological Society of America Field Guide 29, p. 263-302.

Tull, J.F., Harris, A.G., Repetzki, J.E., McKinney, F.K., Garrett, C.B., and Bearce, D.N., 1988, New paleontologic evidence constraining the age and paleotectonic setting of the Talladega slate belt, southern Appalachians: Geological Society of America Bulletin, v. 100, p. 1291-1299.

Tull, J.F., Barineau, C.I., Mueller, P.A., and Wooden, J.L., 2007, Volcanic arc emplacement onto the southernmost Appalachian Laurentian shelf; characteristics and constraints: Geological Society of America Bulletin, v. 119, p. 261-274.

Tull., J.F., Holm-Denoma, C.S., and Barineau, C.I., 2014, Early to Middle Ordovician back-arc basin in the southern Appalachian Blue Ridge: Characteristics, extent, and tectonic significance: Geological Society of America Bulletin, v. 126, n. 7/8, p. 990-1015.

VanDervoort, D.S., Steltenpohl, M.G., and Schwartz, J.J., 2015, U-Pb ages from the Dadeville Complex, southernmost Appalachians, eastern Alabama: an accreted Taconic arc: Geological Society of America Abstracts with Programs, v. 47, n. 7, p. 159.

Wiedenbeck, M., et al., 2004, Further Characterization of the 91500 Zircon Crystal: Geostandards and Geoanalytical Research, v. 28, n. 1, p. 9-39.

Willard, R.A., and Adams, M.G., 1994, Newly discovered eclogite in the southern Appalachian orogen, northwestern North Carolina: Earth and Planetary Science Letters, v. 123, p. 61-70.

CONCLUSIONS

The first manuscript focuses on structures and lithologies within the 1:24,000 Wadley South, Alabama, Quadrangle. Results from this paper indicate the following. (1) The metasedimentary and metaplutonic lithologies of the eastern Blue Ridge units in the study area likely reflect the evolution of the Laurentian margin from slope-rise facies to a back-arc basin. (2) The Jackson Gap Group may mark the shallowing of the eastern Blue Ridge passive margin into a flysch deposit as a result of the encroachment of the Dadeville Complex arc. (3) The Brevard shear zone contains metasedimentary lithologies with top-to-the-northeast, oblique right lateral and thrust kinematics that verify plastic reactivation of the Brevard shear zone under lower to middle greenschist-facies metamorphic conditions, (4) The Abanda and Katy Creek faults, which bound the Jackson Gap Group, are temporally, kinematically and rheologically different, whereas the Alexander City and Abanda faults are similar in each of these regards. And (5) cataclastic zones that parallel the Alexander City and Abanda faults mark the final movement of the Brevard shear zone under supra-ductile-brittle-transition zone conditions and likely record Mesozoic brittle reactivation of these shear zones.

The second manuscript reports geochronologic data from the suspect Dadeville Complex. U-Pb age dating of zircons for five constituent units comprising the Dadeville Complex in Alabama was performed using laser ablation sector field inductively coupled plasma mass spectrometry (LA-SF-ICP-MS). Results indicate igneous crystallization ages of 493.4 ± 6.0 Ma for the Waresville Formation, 499.8 ± 6.9 Ma for the Camp Hill Gneiss, 476.6 ± 6.8 Ma for the Ropes Creek Amphibolite, and 477.1 ± 4.8 Ma for the Waverly Gneiss. Observations of zircons extracted from the Rock Mills Granite Gneiss suggest that this unit has been subjected to a high-degree of metasomatism, and if it correlates to the Franklin Gneiss in Georgia, then the previously reported ~462 Ma Rb-Sr isochron age (MSWD 1.9) for the latter unit likely represent an age of metamorphic closure rather than the true age of igneous crystallization, as was previously thought.

The age dating of detrital zircons from the Agricola Schist yielded U-Pb ages spanning from ~2.7 Ga to ~400 Ma, with peaks at ~883, ~755, ~656, and ~480 Ma. This spectrum, with the exception of the ~480 Ma age population, is not typical for rocks that developed along the early Paleozoic eastern Laurentian margin. Additionally, the age population at ~480 Ma (8.5%) contains Th/U values of less than 0.1 and is interpreted as Taconian metamorphic overgrowth. Furthermore, Mesoproterozoic zircons are conspicuously sparse in the detrital spectrum (6.1%) and reflect only the very latest stages of the Grenville orogeny. The discrepancy in detrital age distributions between the eastern Blue Ridge, as documented in previous work, and the Dadeville Complex (Inner Piedmont), and an absence of a prominent Grenvillian signature indicates that the Dadeville Complex is an exotic (i.e., Amazonian or peri-Gondwanan) terrane that developed distal to the eastern Laurentian margin. These data, in conjunction with previously reported geochemical analyses, indicates that the Dadeville Complex likely is an early Paleozoic Taconic arc preserved within the Inner Piedmont of Alabama and Georgia. The Taconic suture, therefore, must lie at the base of the Dadeville Complex. The structural position of the Taconic suture in the study area, that is, along the flanks of the Tallassee synform cradled between Laurnetian units of the eastern Blue Ridge and Pine Mountain window, makes it a unique setting in which to examine Taconian evolution of the southeastern U.S.A.

COMBINED REFERENCES

Abbott, R.N., and Greenwood, J.P., 2001, Retrograde metamorphism of eclogite in the Southern Appalachian Mountains, USA-A case involving seamount subduction?: Journal of Metamorphic Geology, v. 19, no. 4, p. 433-443.

Abbott, R.N., and Raymond, L.A., 1984, The Ashe Metamorphic Suite, northwest North Carolina: Metamorphism and observations of geologic history: American Journal of Science, v. 284, p. 350-375.

Abbott, R.N., and Raymond, L.A., 1997, Petrology of pelitic and mafic rocks in the Ashe and Alligator Back metamorphic suites, northeast of the Grandfather Mountain Window, *in* Stewart, K.G., Adams, M.G., and Trupe, C.H., eds., Paleozoic Structure, Metamorphism, and Tectonics of the Blue Ridge of Western North Carolina: Durham, Carolina Geological Society, v. 1997, p. 87-101.

Absher, B.S., and McSween, H.Y., 1986, Winding Stair Gap granulites: The thermal peak of Paleozoic metamorphism: Geological Society of America Centennial Field Guide – Southeastern Section, p. 257-260.

Abrahams, J.B., 2014, Geology of the Dadeville Quadrangle and the Tallassee synform in characterizing the Dog River window: Unpublished M.S. thesis, Auburn University, Auburn, Alabama, 126 p.

Adams, G.I., 1926, the crystalline rocks in Adams, G.I., Butts, D., Stephenson, L.W., and Cooke, C.W., eds., Geology of Alabama: Alabama Geological Survey Special Report 14, p. 40-223.

Adams, G.I., 1930, Gold deposits of Alabama, and occurrences of copper, pyrite, arsenic and tin: Alabama Geological Survey Bulletin 40, p. 91.

Adams, G.I., 1933, General geology of the crystalline rocks of Alabama: The Journal of Geology, v. 41, p. 159-173.

Adams, M.G., Stewart, K.G., Trupe, C.H., and Willard, R.A., 1995, Tectonic significance of high-pressure metamorphic rocks and dextral strike slip faulting in the southern Appalachians, *in* Hibbard, J.P., van Staal, C.R., and Cawood, P., eds., Current Perspectives in the Appalachian-Caledonian Orogen: Geological Association of Canada Special Paper 41, p. 21-42.

Aleinikoff, J.N., Zartman, R.E., Walter, M., Rankin, D.W., Lyttle, P.T., and Burton, W.C., 1995, U-Pb age of metarhyolites of the Catoctin and Mount Rogers Formations, central and southern Appalachians: Evidence for two pulses of Iapetan rifting: American Journal of Science, v. 295, p. 428-454.

Barineau, C.I., 2009, Superposed fault systems of the southernmost Appalachian Talladega belt: implications for Paleozoic orogenesis in the southern Appalachians [Ph.D. dissertation]: Tallahassee, Florida, Florida State University, 136 p.

Barineau, C.I., and Tull, J.F., 2012, The Talladega and Ashland-Wedowee-Emuckfaw belts of Alabama: Geological overview, *in* Barineau, C.I., and Tull, J.F., eds., The Talladega Slate Belt and Eastern Blue Ridge: Laurentian Plate Passive Margin to Back-Arc Basin Tectonics in the Southern Appalachian Orogen: Tuscaloosa, Alabama, Alabama Geological Society, 49th Annual Field Trip Guidebook, p. 27-37.

Bartholomew, M.J., 1992, Structural characteristics of the Late Proterozoic (post-Grenville) continental margin of the Laurentian crust, *in* Bartholomew, M.J., Hyndman, D.W., Mogk, D.W., and Mason, R., eds., Basement Tectonics 8: Characterization and Comparison of Ancient and Mesozoic Continental Margins: Proceeding of the Eighth International Conference on Basement Tectonics: Dordrecht, Netherlands, Kluwer Academic Publishers, p. 443-467.

Bentley, R.D., and Neathery, T.L, 1970, Geology of the Brevard fault zone and related rocks of the Inner Piedmont of Alabama: Alabama Geological Society Field Trip Guidebook, n. 8, 119 p.

Bream, B.R., Hatcher, R.D., Jr., Miller, C.F., and Fullagar, P.D., 2004, Detrital zircon ages and Nd isotopic data from the southern Appalachian crystalline core, GA-SC-NC-TN: New provenance constraints for Laurentian margin paragneisses, *in* Tollo, R.P., Corriveau, L., McLelland, J., and Bartholomew, M.J., eds., Proterozoic Evolution of the Grenville Orogen in North America: Geological Society of America Memoir 197, p. 459-475.

Brown, D.E., and Cook, R.B., 1981, Petrography of major Dadeville complex rock units in the Boyds Creek area, Chambers and Lee Counties, Alabama, *in* Sears, J.W., ed., Contrasts in Tectonic Style between the Inner Piedmont Terrane and the Pine Mountain Window: Tuscaloosa, Alabama Geological Society, 18th Annual Field Trip Guidebook, p. 15-40.

Carrigan, C.W., Bream, B., Miller, C.F., and Hatcher, R.D., Jr., 2001, Ion microprobe analyses of zircon rims from the eastern Blue Ridge and Inner Piedmont, NCSC-GA: Implications for the timing of Paleozoic metamorphism in the southern Appalachians: Geological Society of America Abstracts with Programs, v. 33, p. 7.

Cook, F.A., 1982, Stratigraphy and structure of the central Talladega slate belt, Alabama Appalachians; Tectonic studies in the Talladega and Carolina slate belts, southern Appalachian Orogen: Geological Society of America Special Paper 191, p. 47-59.

Cook, F.A., Albuagh, D.S., Brown, L.D., Kaufman, S., Oliver, J.E., and Hatcher, R.D., Jr., 1979, Thin-skinned tectonics in the crystalline southern Appalachians; COCORP seismic-reflection profiling of the Blue Ridge and Piedmont: Geology, v. 7, p. 563-567.

Dalla Salda, L.H., Cingolani, C.A., Varela, R., 1992, The Early Paleozoic orogenic belt of the Andes in southwestern South America: Result of Laurentia-Gondwana collision?: Geology, v. 20, p. 617-620.

Dalziel, I.W.D., Mosher, S., and Gahagan, L., 2000, Laurentia-Kalahari collision and the assembly of Rodinia: Journal of Geology, v. 108, p. 499-513.

Das, R., 2006, Geochemical and geochronological investigations in the southern Appalachians, southern Rocky Mountains and Deccan Traps [Ph.D. dissertation]: Tallahassee, Florida, Florida State University, 149 p.

Diecchio, R.J., 1993, Stratigraphic interpretation of the Ordovician of the Appalachian basin and implications for Taconian flexural modeling: Tectonics, v. 12, no. 6, p. 1410-1419.

Ernst, W.G., 1973, Interpretative synthesis of metamorphism in the Alps: Geological Society of America Bulletin, v. 84, p. 2053-2078.

Finney, S.C., Grubb, B.J., and Hatcher, R.D., Jr., 1996, Graphic correlation of Middle Ordovician graptolite shale, southern Appalachians: An approach for examining the subsidence and migration of a Taconic foreland basin: Geological Society of America Bulletin, v. 108, no. 3, p. 355-371,

Fyffe, L.R., Barr, S.M., Johnson, S.C., McLeod, M.J., McNicoll, V., Valverde-Vaquero, P., van Staal, C.R., and White, C.E., 2009, Detrital zircon ages from Neoproterozoic and early Paleozoic conglomerate and sandstone units of New Brunswick and coastal Maine: Implications for the tectonic evolution of Ganderia: Atlantic Geology, v. 45, p. 110-144.

Garihan, J.M., and Ranson, W.A., 1992, Structure of the Mesozoic Marietta-Tryon graben, South Carolina and adjacent North Carolina, *in* Bartholomew, M.J., et al., eds., Basement tectonics 8: Characterization of ancient and Mesozoic continental margins—Proceedings of the 8th International Conference on Basement Tectonics, Butte, Montana, 1988: Dordrecht, Netherlands, Kluwer Academic Publishers, p. 539-555.

Garihan, J.M., Preddy, M.S., and Ranson, W.A., 1993, Summary of mid-Mesozoic brittle faulting in the Inner Piedmont and nearby Charlotte belt of the Carolinas, *in* Hatcher, R.D., Jr., and Davis, T., eds., Studies of Inner Piedmont geology with a focus on the Columbus Promontory: Carolina Geological Society Field Trip Guidebook, p. 55-66.

Gastaldo, R.A., Guthrie, G.M., and Steltenpohl, M.G., 1993, Mississippian Fossils from Southern Appalachian Metamorphic Rocks and Their Implications for Late Paleozoic Tectonic Evolution: Science, v. 262, p. 732-734.

Goldberg, S.A., and Steltenpohl, M.G., 1990, Timing and characteristics of Paleozoic deformation and metamorphism in the Alabama Inner Piedmont: American Journal of Science v. 290, p. 1169-1200.

Grimes, J.E., 1993, Geology of the Piedmont rocks between the Dadeville Complex and the Pine Mountain Window in parts of Lee, Macon, and Tallapoosa Counties, Alabama: Unpublished M.S. Thesis, Auburn, Alabama, Auburn University, 129 p.

Grimes, J.E., and Steltenpohl, M.G., 1993, Geology of the crystalline rocks along the fall line on the Carville, Notasulga, and Loachapoka quadrangles, Alabama, *in* Steltenpohl, M.G., and Salpas, P.A., eds., Geology of the southernmost exposed Appalachian Piedmont rocks along the Alabama fall line: Southeastern Section of the Geological Society of America Field Trip Guidebook, p. 66-94.

Guthrie, G.M., and Dean, L.S., 1989, Geology of the New site 7.5-Minute Quadrangle, Tallapoosa and Clay Counties, Alabama: Alabama Geological Survey Quadrangle Map 9, 41 p.

Hall, G.D., 1991, A comparative geochemical study of differing amphibolite types within the Ropes Creek Amphibolite, western Lee County, Alabama: Unpublished M.S. thesis, Auburn University, 131 p.

Hartmann, L.A., Leite, J.A.D., Silva, L.C., Remus, M.V.D., McNaughton, N.J., Groves, D.I., Fletcher, I.R., Santos, J.O.S., and Vasconcellos, M.A.Z., 2000, Advances in SHRIMP geochronology and their impact on understanding the tectonic and metallogenic evolution of southern Brazil: Australian Journal of Earth Sciences, v. 47, p. 829-844.

Hatcher, R.D., Jr., 1972, Developmental model for the southern Appalachians: Geological Society of America Bulletin, v. 83, p. 2735-2760.

Hatcher, R.D., Jr., 1978, Tectonics of the western Piedmont and Blue Ridge: Review and speculation: American Journal of Science, v. 278, p. 276-304.

Hatcher, R.D., Jr., 1987, Tectonics of the southern and central Appalachians Internides: Annual Review of Earth and Planetary Sciences, v. 15, p. 337-362.

Hatcher, R.D., Jr., 1989, Tectonic synthesis of the U.S. Appalachians, Chapter 14, *in* Hatcher R.D., Jr., Thomas, W.A., and Viele, G.W., eds., The Appalachian-Ouachita Orogen in the United States: Geology of North America, Geological Society of America, v. F-2, p. 511-535.

Hatcher, R.D., Jr, 2005, Southern and central Appalachians, *in* Selley R.C., Cocks, L.R.M., and Plimer, I.R. eds., Encyclopedia of Geology, Elsevier Academic Press, Amsterdam, p. 72-81.

Hatcher, R.D., Jr., 2010, The Appalachian orogen: A brief summary, *in* Tollo, R.P., Bartholomew, M.J., Hibbard, J.P., and Karabinos, P.M., eds., From Rodinia to Pangea: The Lithotectonic Record of the Appalachian Region: Geological Society of America Memoir 206, p. 1-19.

Hatcher, R.D., Jr., and Merschat, A.J., 2006, The Appalachian Inner Piedmont: An exhumed strike-parallel, tectonically forced orogenic channel, *in* Law, R.D., Searle, M., and Godin, L., eds., Channel flow, ductile extrusion and exhumation of lower-mid crust in continental collision zones: Geological Society of London Special Publication 268, p. 517-540.

Hatcher, R.D., Jr., Bream, B.R., and Merschat, A.J., 2007, Tectonic map of the southern and central Appalachians: A tale of three orogens and a complete Wilson cycle, *in* Hatcher, R.D., Jr., Carlson, M.P., McBride, J.H., and Martínez Catalán, J.R., eds., 4-D Framework of Continental Crust: Geological Society of America Memoir 200, p. 595-632.

Hawkins, J.F., 2013, Geology, petrology, and geochronology of rocks in the Our Town, Alabama Quadrangle: Unpublished M.S. thesis, Auburn University, Auburn, Alabama, p. 118.

Hawkins, J.F., Steltenpohl, M.G., Zou, H., Mueller, P.A., and Schwartz, J.J., 2013, New constraints on Ordovician magmatism in the southernmost exposures of the eastern Blue Ridge in Alabama: Geological Society of America Abstracts with Program, v. 45, n. 2, p. 62.

Hibbard, J.P., and Karabinos, P., 2013, Disparate Paths in the Geologic Evolution of the Northern and Southern Appalachians: A Case for Inherited Contrasting Crustal/Lithospheric Substrates: Geoscience Canada, v. 40, n. 4, p. 303-317.

Hibbard, J.P., and Waldron, J.W.F., 2009, Truncation and translation of Appalachian promontories: Mid-Paleozoic strike-slip tectonics and basin initiation: Geology, v. 37, p. 487-490.

Hibbard, J.P., van Staal, C.R., and Rankin, D.W., 2007, A comparative analysis of pre-Silurian crustal building blocks of the northern and southern Appalachian orogen: American Journal of Science, v. 307, p. 23-45.

Higgins, M.W., Atkins, R.L., Crawford, T.J., Crawford, R.F., Brooks, R., and Cook, R.B., 1988, The structure, stratigraphy, tectonostratigraphy and evolution of the southernmost part of the Appalachian orogen: U.S. Geological Survey Professional Paper 1475, 173 p.

Holdaway, M.J., 1971, Stability of andalusite and the aluminosilicate phase diagram: American Journal of Science, v. 271, p. 97-131.

Holm-Denoma, C.S., 2006, Characterization of Paleozoic Terranes and Terrane Accretion at the Southeastern Margin of Laurentia: Georgia and Alabama Appalachians [Ph.D. thesis]: Tallahassee, Florida, Florida State University, 135 p.

Hoschek, G., 1969, The Stability of Staurolite and Chloritoid and their Significance in Metamorphism of Pelitic Rocks: Contributions to Mineralogy and Petrology, v. 22, n. 3, p. 208-232.

Horton, J.W., Drake, A.A., Jr., and Rankin, D.W., 1989, Tectonostratigraphic terranes and their boundaries in the central and southern Appalachians, *in* Dallmeyer, R.D., ed., Terranes in the Circum-Atlantic Paleozoic orogens: Geological Society of America Special Paper 230, p. 213-245.

Jackson, S.E., Pearson, N.J., Griffin, W.L., and Belousova, E.A., 2004, The application of laser ablation-inductively coupled plasma-mass spectrometry to in situ U–Pb zircon geochronology: Chemical Geology, v. 211, p. 47-69.

Johnson, M.J., 1988, Geology of the gold occurrences near Jacksons Gap, Tallapoosa County, Alabama: Unpublished M.S. Thesis, Auburn, Alabama, Auburn University, p. 156.

Johnson, L.W., and Tull, J.F., 2002, Sylacauga Marble Group; distal fragment of the Southern Appalachian Cambrian-Ordovician carbonate platform: Southeastern Geology, v. 41, p. 75-102.

Keefer, W.D., 1992, Geology of the Tallassee synform hinge zone and its relationship to the Brevard fault zone, Tallapoosa and Elmore Counties, Alabama: Unpublished M.S. thesis Auburn, Alabama, Auburn University, p. 195.

Keller, F.B., 1977, Sandstone turbidites in the Tellico Formation, Indian Creek Embayment, Tennessee, *in* Ruppel, S.C., and Walker, K.R., eds., The ecostratigraphy of the Middle Ordovician of the Southern Appalachians (Kentucky, Tennessee, and Virginia) USA: Knoxville, University of Tennessee, Department of Geological Sciences, Studies in Geology 77-1, p. 117-121.

Keppie, J.D., and Ramos, V.A., 1999, Odyssey of terranes in the Iapetus and Rheic oceans during the Paleozoic, *in* Ramos, V.A., and Keppie, J.D., eds., Laurentia-Gondwana connections before Pangea: Boulder, Colorado, Geological Society of America Special Paper 336, p. 267-276.

Keppie, J.D., Davis, D.W., and Krogh, T.E., 1998, U-Pb geochronological constraints on Precambrian stratified units in the Avalon composite terrane of Nova Scotia, Canada: Tectonic implications: Canadian Journal of Earth Sciences, v. 35, p. 222-236.

Li, Z.X., et al., 2008, Assembly, configuration, and break-up history of Rodinia: A synthesis: Precambrian Research, v. 160, p. 179-210.

Ludwig, K.R., 2009, SQUID-2: A User's Manual, rev. 12 April 2009: Berkeley Geochronology Center Special Publication 5, 110 p.

Ludwig, K.R., 2012, Isoplot 3.75: A Geochronological Toolkit for Microsoft Excel: Berkeley Geochronology Center Special Publication 5, 75 p.

McClellan, E.A., Steltenpohl, M.G., Thomas, C., and Miller, C.F., 2007, Isotopic age constraints and metamorphic history of the Talladega Belt: New evidence for timing of arc magmatism and terrane emplacement along the southern Laurentian margin: The Journal of Geology, v. 115, p. 541-561.

McCullars, J.M., 2001, Geology and trace-element geochemistry of the Brevard zone near Martin Lake, Tallapoosa County, Alabama: Unpublished M.S. thesis, Auburn, Alabama, Auburn University, p. 74.

McDonald, W.M., Hames, W.E., Marzen, L.J., and Steltenpohl, M.G., 2007, A GIS database for 40Ar/39Ar data of the southwestern Blue Ridge province: Geological Society of America Abstracts with Programs, v. 39, no. 2, p. 81.

Merschat, A.J., and Hatcher, R.D., Jr., 2007, The Cat Square terrane: Possible Siluro-Devonian remnant ocean basin in the Inner Piedmont, southern Appalachians, USA, *in* Hatcher, R.D., Jr., Carlson, M.P., McBride, J.H., and Martínez Catalán, J.R., eds., 4-D Framework of Continental Crust: Geological Society of America Memoir 200, p. 553-565.

Merschat, A.H., Hatcher, R.D., Jr., and Davis, T.L., 2005, The northern Inner Piedmont, southern Appalachians, USA: Kinematics of transpression and SW-directed mid-crustal flow: Journal of Structural Geology, v. 27, p. 1252–1281.

Merschat, A.J., Hatcher, R.D., Jr., Bream, B.R., Miller, C.F., Byars, H.E., Gatewood, M.P., and Wooden, J.L., 2010, Detrital zircon geochronology and provenance of southern Appalachian Blue Ridge and Inner Piedmont crystalline terranes, *in* Tollo, R.P., Bartholomew, M.J., Hibbard, J.P., and Karabinos, P.M., eds., From Rodinia to Pangea: The Lithotectonic Record of the Appalachian Region: Geological Society of America Memoir, v. 206, p. 661-699.

Muangnoicharoen, N., 1975, The geology and structure of a portion of the northern piedmont, east-central Alabama: Unpublished M.S. thesis, Tuscaloosa, University of Alabama, p. 72.

Murphy, J.B., and Hamilton, M.A., 2000, Orogenesis and basin development: U-Pb detrital zircon age constraints on evolution of the late Paleozoic St. Marys basin, central mainland Nova Scotia: Journal of Geology, v. 108, p. 53-71.

Neathery, T.L., 1968, Talc and Anthophyllite Deposits in Tallapoosa and Chambers Counties, Alabama: Geological Survey of Alabama Bulletin 90, 98 p.

Neathery, T.L., and Reynolds, J.W., 1975, Geology of the Lineville East, Ofelia, Wadley North and Mellow Valley Quadrangles, Alabama: Geological Survey of Alabama Bulletin, v. 109, 120 p.

Neilson, M. J., 1987, The felsic gneisses of the Inner Piedmont, *in* Drummond, M.S., and Green, N.L., eds., Granites of Alabama: Tuscaloosa, Alabama, Geological Survey of Alabama, Special Publication, p. 9-16.

Neilson, M.J., 1988, The structure and stratigraphy of the Tallassee synform, Dadeville, Alabama: Southeastern Geology, v. 29, n. 1, p. 41-50.

Neilson, M.J. and Stow, S.H., 1986, Geology and geochemistry of the mafic and ultramafic intrusive rocks from the Dadeville Belt, Alabama: Geological Society of America Bulletin, v. 97, p. 296-304.

Neilson, M.J., Seal, T.L., and Kish, S.A., 1996, Two high-silica gneisses from the Dadeville Complex of Alabama’s Inner Piedmont: Southeastern Geology, v. 36, n. 3, p. 123-132.

Osborne, W.E., Szabo, M.W., Neathery, T.L., and Copeland, C.W., Jr., compilers, 1988, Geologic map of Alabama, northeast sheet: Alabama Geological Survey Special Map 220, scale 1:250,000.

Pardee, J.T., and Park, C.F., Jr., 1948, Gold deposits of the southern Piedmont: U.S. Geological Survey Professional Paper 213, p. 156.

Park, C.F., Jr., 1935 Hog mountain gold district, Alabama: American Institute of Mining and Metallurgical Engineers Transactions, Mining Geology, v. 115, p. 209-228.

Passchier, C.W., and Trouw, R.A., 2005, Microtectonics: Springer-Verlag, Berlin, Germany, 289 p.

Phillips, W. B., 1892, a preliminary report on a part of the lower gold belt of Alabama in the counties of Chilton, Coosa, and Tallapoosa: Alabama Geological Survey Bulletin 3, p. 97.

Poole, J.D., 2015, Geology of the Jacksons Gap, Alabama, Quadrangle and structural implications for the Brevard fault zone: Unpublished M.S. thesis, Auburn University, Auburn, Alabama, 174 p.

Raymond, D.E., Osborne, W.E., Copeland, C.W., and Neathery, T.L., 1988, Alabama Stratigraphy: Geological Survey of Alabama, Tuscaloosa, 97 p.

Raymond, L.A., Yurkovich, S.P., and McKinney, M., 1989, Block-in-matrix structures in the North Carolina Blue Ridge belt and their significance for the tectonic history of the southern Appalachian orogen, *in* Horton, J.W., Jr., and Rast, N., eds., Mélanges and olistostromes of the U.S. Appalachians: Geological Society of America Special Paper 228, p. 195-215.

Reed, A.S., 1994, Geology of the western portion of the Dadeville 7.5' Quadrangle, Tallapoosa County, Alabama: Unpublished M.S. thesis, Auburn, Alabama, Auburn University, p.108.

Richardson, S.W., 1968, Staurolite stability in a part of the system Fe-Al-Si-O-H: Journal of Petrology, v. 9, n. 3, p. 467-489.

Rivers, T., 2008, Assembly and preservation of lower, mid, and upper orogenic crust in the Grenville Province–Implications for the evolution of large hot long-duration orogens; Precambrian Research, v. 167, p. 237-259.

Russell, G.S., 1978, U-Pb, Rb-Sr., and K-Ar geochronology of the Alabama Piedmont [Ph.D. dissertation]: Florida State University, Tallahassee, Florida, 198 p.

Sadowski, G.R., and Bettencourt, J.S., 1996, Mesoproterozoic tectonic correlations between eastern Laurentia and the western border of the Amazon craton: Precambrian Research, v. 76, p. 213-227.

Saalmann, K., Hartmann, L.A., and Remus, M.V.D., 2007, The assembly of West Gondwana-The view from the Rio de la Plata craton, *in* Linnemann, U., Nance, R.D., Kraft, P., and Zulauf, G., eds., The evolution of the Rheic Ocean: From Avalonian-Cadomian active margin to Alleghenian-Variscan collision: Geological Society of America Special Paper 423, p. 1-26.

Saunders, J.A., Steltenpohl, M.G., and Cook, R.B., 2013, Gold Exploration and Potential of the Appalachian Piedmont of Eastern Alabama: Society of Economic Geologists Newsletter, July, 2013, no. 94, v. 1, p. 12-17.

Seal, T.L., and Kish, S.A., 1990, The geology of the Dadeville Complex of the western Georgia and eastern Alabama Inner Piedmont; initial petrographic, geochemical, and geochronological results, *in* Steltenpohl, M.G., and others, eds., Geology of the southern Inner Piedmont, Alabama and southwest Georgia, Southeastern Section of the Geological Society of America Field Trip Guidebook, v. 39, p. 65-77.

Sears, J.W., Cook, R.B., Jr., and Brown, D.E., 1981, Tectonic evolution of the Pine Mountain Window and adjacent Inner Piedmont province, *in* Sean, J.W., ed., Contrasts in Tectonic Style between the Inner Piedmont Terrane and the Pine Mountain Window: Alabama Geological Society Guidebook 18, p. 1-13.

Shanmugam, G., and Walker, K.R., 1978, Tectonic significance of distal turbidites in the Middle Ordovician Blockhouse and lower Sevier Formations in east Tennessee: American Journal of Science, v. 278, p. 551-578.

Sláma, J., et al., 2008, Plešovice zircon-a new natural reference material for U-Pb and Hf isotopic microanalysis: Chemical Geology, v. 249, n. 1, p. 1-35.

Steltenpohl, M.G., 2005, An introduction to the terranes of the southernmost Appalachians of Alabama and Georgia, in Steltenpohl, M.G., Southernmost Appalachian terranes, Alabama and Georgia: Southeastern Section of the Geological Society of America Field Trip Guidebook, p. 1-18

Steltenpohl, M.G., 2013, Geology of the 1:24,000 Wadley South, Alabama, Quadrangle: Unpublished USGS-NCGMP-EDMAP proposal summary sheet, 15 p.

Steltenpohl, M.G., and Kunk, M.J., 1993, $^{40}Ar/^{39}Ar$ thermochronology and Alleghanian development of the southernmost Appalachian Piedmont, Alabama and southwest Georgia: Geological Society of America Bulletin, v. 105, p. 819-833.

Steltenpohl, M.G., and Moore, W.B., 1988, Metamorphism in the Alabama Piedmont: Alabama Geological Survey Circular, v. 138, 27 p.

Steltenpohl, M.G., and Singleton, R.T., 2014, Geology of the Buttston 7.5-minute quadrangle, Tallapoosa County, Alabama: Geological Survey of Alabama Open File-Report, 30 p.

Steltenpohl, M.G., Neilson, M.J., and Kish, S.A., 1990, Tectonometamorphic development in the southernmost Inner Piedmont terrane, Alabama, *in* Steltenpohl, M.G., Neilson, M.J., and Kish, S.A., eds., Geology of the southern Inner Piedmont, Alabama and southwest Georgia: Southeastern Section of the Geological Society of America Field Trip Guidebook, v. p. 1-16.

Steltenpohl, M.G., Kish, S.A., and Neilson, M.J., eds., 1990, Geology of the southern Inner Piedmont terrane, Alabama and southwest Georgia: Southeastern Section of the Geological Society of America Field Trip Guidebook, 139 p.

Steltenpohl, M.G., Heatherington, A., Mueller, P., and Miller, B.V., 2005, Tectonic implications of new isotopic dates on crystalline rocks from Alabama and Georgia, *in* Steltenpohl, M.G., ed., Southernmost Appalachian terranes, Alabama and Georgia: Southeastern Section of the Geological Society of America Field Trip Guidebook, p. 51-67.

Steltenpohl, M.G., Hatcher, R.D., Jr., Mueller, P.A., Heatherington, A.L., and Wooden, J.L., 2010, Geologic history of the Pine Mountain window, Alabama and Georgia: Insights from a new geologic map and U-Pb isotopic dates, *in* Tollo, R.P., Bartholomew, M.J., Hibbard, J.P., and Karabinos, P.M., eds., From Rodinia to Pangea: The Lithotectonic Record of the Appalachian Region: Geological Society of America Memoir 206. Boulder, Colorado, p. 837-858.

Steltenpohl, M.G., Schwartz, J.J., and Miller, B.V., 2013, Late to post-Appalachian strain partitioning and extension in the Blue Ridge of Alabama and Georgia: Geosphere, v. 9; n. 3, p. 647-666.

Sterling, J.W., 2006, Geology of the southernmost exposures of the Brevard zone in the Red Hill Quadrangle, Alabama: Unpublished M.S. thesis, Auburn University, Auburn, Alabama, 118 p.

Stewart, K.G., Adams, M.G., and Trupe, C.H., 1997, eds., Paleozoic structure, metamorphism, and tectonics of the Blue Ridge of western North Carolina: Carolina Geological Society 1997 Field Trip Guidebook, 101 p.

Stoddard, P.V., 1983, A petrographic and geochemical analysis of the Zana Granite and Kowaliga Augen Gneiss: Northern Piedmont, Alabama: Unpublished M.S. thesis, Memphis, Memphis State University, p. 74.

Stow, S.H., Neilson, M.J., and Neathery, T.L., 1984, Petrography, geochemistry and tectonic significance of the amphibolites o the Alabama Piedmont: American Journal of Science, v. 284, nos. 4 and 5, p. 416-436.

Thomas, W.A., 2006, Tectonic inheritance at a continental margin: GSA Today, v. 16, no. 2, p. 4-11.

Thomas, W.A., 2011, Detrital-zircon geochronology and sedimentary provenance: Lithosphere, v. 3, n. 4, p. 304-308.

Thomas, W.A., and Astini, R.A., 1996, The Argentine Precordillera: A traveler from the Ouachita embayment of North American Laurentia: Science, v. 273, p. 752-757.

Thomas, W.A., Astini, R.A., Mueller, P.A., Gehrels, G.E., and Wooden, J.L., 2004, Transfer of the Argentine Precordillera terrane from Laurentia: Constraints from detrital-zircon geochronology: Geology, v. 32, no. 11, p. 965-968.

Tull, J.F, 1978, Structural development of the Alabama Piedmont northwest of the Brevard zone: American Journal of Science, v. 278, n. 4, 442-460.

Tull, J.F., 1982, Polyphase late Paleozoic in the Appalachian thrust belt and Piedmont of Alabama; The Geological Society of America, 95th annual meeting: Geological Society of America Abstracts with Programs, v. 14, p. 634.

Tull, J.F., 1998, Analysis of a regional middle Paleozoic unconformity along the distal southeastern Laurentian margin, southernmost Appalachians: Implications for tectonic evolution: Geological Society of America Bulletin, v. 110, p. 1149-1162.

Tull, J.F., 2002, Southeastern margin of the middle Paleozoic shelf, southwesternmost Appalachians: Regional stability bracketed by Acadian and Alleghanian tectonism: Geological Society of America Bulletin, v. 114, p. 643-655.

Tull, J.F., and Barineau, C.I., 2012, Overview of the stratigraphic and structural evolution of the Talladega slate belt, Alabama Appalachians, *in* Eppes, M.C., and Bartholomew, M.J., eds., From the Blue Ridge to the Coastal Plain: Field Excursions in the Southeastern United States: Geological Society of America Field Guide 29, p. 263-302.

Tull, J.F., Harris, A.G., Repetzki, J.E., McKinney, F.K., Garrett, C.B., and Bearce, D.N., 1988, New paleontologic evidence constraining the age and paleotectonic setting of the Talladega slate belt, southern Appalachians: Geological Society of America Bulletin, v. 100, p. 1291-1299.

Tull, J.F., Barineau, C.I., and Holm-Denoma, C.S., 2012, Characteristics, Extent, and Tectonic Significance of the Middle Ordovician Back-Arc Basin in the Southern Appalachian Blue Ridge, *in* Barineau, C.I., and Tull, J.F., The Talladega Slate Belt and the eastern Blue Ridge: Laurentian plate passive margin to back-arc basin tectonics in the southern Appalachian orogen: Field Trip Guidebook for the Alabama Geological Society, p. 12-26.

Tull., J.F., Holm-Denoma, C.S., and Barineau, C.I., 2014, Early to Middle Ordovician back-arc basin in the southern Appalachian Blue Ridge: Characteristics, extent, and tectonic significance: Geological Society of America Bulletin, v. 126, n. 7/8, p. 990-1015.

Tuomey, M., 1858, Second biennial report on the geology of Alabama: Alabama Geological Survey Biennial report 2, p. 292.

VanDervoort, D.S., Steltenpohl, M.G., and Schwartz, J.J., 2015, U-Pb ages from the Dadeville Complex, southernmost Appalachians, eastern Alabama: an accreted Taconic arc: Geological Society of America Abstracts with Programs, v. 47, n. 7, p. 159.

White, T.W., 2007, Geology of the 1:24,000 Tallassee, Alabama, Quadrangle, and its implications for southern Appalachian tectonics: Unpublished M.S. thesis, Auburn University, Auburn, Alabama, 74 p.

Wiedenbeck, M., et al., 2004, Further Characterization of the 91500 Zircon Crystal: Geostandards and Geoanalytical Research, v. 28, n. 1, p. 9-39.

Wielchowsky, C.C., 1983, The geology of the Brevard zone and adjacent terranes in Alabama [Ph.D. dissertation]: Rice University, Houston, Texas, 237 p.

Willard, R.A., and Adams, M.G., 1994, Newly discovered eclogite in the southern Appalachian orogen, northwestern North Carolina: Earth and Planetary Science Letters, v. 123, p. 61-70.

APPENDIX

SAMPLE LIST

Sample Name	Location (WGS 84)	Zircon Source	Sample Description
AG-1-14	32.81720°N, 85.75421°W	detrital zircons	Agricola Schist: biotite ± garnet ± sillimanite-feldspar-quartz schist, interlayered with thin-bedded dark-brown hornblende amphibolite
WS-1-14	33.19923°N, 85.29494°W	magmatic zircons	Waresville Formation: chlorite-actinolite ± magnetite schist interlayered with banded amphibolite and actinolite quartzite
WA-1-14	32.73950°N, 85.58510°W	magmatic zircons	Waverly Gneiss: feldspathic biotite-hornblende gneiss with interlayered with thin bands of amphibolite
RCA-FL6	32.62476°N, 85.68619°W	magmatic zircons	Tonalitic layer from the Ropes Creek Amphibolite: fine- to medium-grained biotite-hornblende-quartz-plagioclase gneiss
CH-1-14	32.82655°N, 85.62026°W	magmatic zircons	Camp Hill Granite Gneiss: coarse to medium-grained foliated granite to quartz diorite (tonalite) gneiss, locally biotite-rich
RM-1-14	33.15844°N, 85.28951°W	magmatic zircons	Rock Mills Granite Gneiss: coarse to medium-grained biotite granite gneiss interlayered with thin bands of epidote and amphibolite

Appendix II. LA-SF-ICP-MS U-Pb analyses of magmatic zircons

Sample				Radiogenic Ratios[1]				Ages (Ma)			
					2 σ		2 σ		2 σ		1 σ
(n=32)	U (ppm)	Th (ppm)	$^{232}Th/^{238}U$	$^{238}U/^{206}Pb$	(%) err	$^{207}Pb/^{206}Pb$	(%) err	$^{207}Pb/^{206}Pb$	abs err	$^{206}Pb/^{238}U$	abs err
CH-1-14_1	634	669	1.055	13.889	0.01	0.056	0.12	**400**	**250**	***448.03***	***6.39***
CH-1-14_2	375	492	1.312	13.889	0.02	0.054	0.12	**340**	**260**	***449.34***	***7.56***
CH-1-14_3	74	171	2.310	12.547	0.02	0.059	0.17	**260**	**290**	***493.41***	***11.01***
CH-1-14_4	93	199	2.141	13.550	0.02	0.049	0.18	**-10**	**280**	***463.18***	***11.32***
CH-1-14_5	64	123	1.915	11.641	0.03	0.053	0.26	**-60**	**330**	***534.50***	***14.40***
CH-1-14_6	103	175	1.699	13.550	0.02	0.059	0.19	**260**	**300**	***457.20***	***10.76***
CH-1-14_7	80	180	2.250	11.876	0.03	0.061	0.21	**150**	**320**	***519.10***	***15.03***
CH-1-14_8	83	167	2.010	11.820	0.03	0.054	0.21	**10**	**310**	***526.28***	***15.29***
CH-1-14_9	59	133	2.240	12.151	0.03	0.041	0.27	**-350**	**350**	***520.06***	***14.60***
CH-1-14_10	90	194	2.150	12.270	0.03	0.056	0.20	**160**	**340**	***505.90***	***14.65***
CH-1-14_11	74	167	2.250	12.658	0.03	0.057	0.19	**160**	**340**	***490.37***	***13.75***
CH-1-14_12	83	256	3.080	13.477	0.03	0.055	0.18	**140**	**310**	***462.38***	***13.71***
CH-1-14_13	57	-510	-9.000	11.723	0.04	0.039	0.28	**-410**	**350**	***539.85***	***18.57***
CH-1-14_14	47	125	2.660	12.903	0.02	0.043	0.22	**-380**	**280**	***489.11***	***11.75***
CH-1-14_15	99	156	1.574	12.987	0.03	0.056	0.22	**130**	**320**	***478.86***	***12.37***
CH-1-14_16	93	197	2.113	12.920	0.03	0.046	0.24	**-100**	**310**	***486.74***	***13.61***
CH-1-14_17	73	176	2.430	12.361	0.03	0.051	0.19	**30**	**310**	***505.13***	***13.17***
CH-1-14_18	101	259	2.560	11.710	0.03	0.064	0.19	**490**	**330**	***524.26***	***16.64***
CH-1-14_19	55	196	3.570	12.376	0.03	0.052	0.23	**70**	**350**	***504.09***	***15.38***
CH-1-14_20	34	93	2.700	13.021	0.04	0.049	0.35	**-380**	**380**	***481.42***	***18.16***
CH-1-14_21	29	102	3.580	12.903	0.04	0.037	0.46	**-630**	**430**	***492.74***	***19.31***
CH-1-14_22	32	81	2.500	12.755	0.04	0.044	0.39	**-170**	**440**	***494.19***	***19.76***
CH-1-14_23	57	140	2.460	12.180	0.03	0.052	0.19	**40**	**330**	***512.33***	***17.35***
CH-1-14_24	45	95	2.100	11.442	0.04	0.048	0.25	**-230**	**350**	***546.90***	***21.13***
CH-1-14_25	59	113	1.900	13.228	0.04	0.045	0.24	**-80**	**330**	***476.12***	***18.75***
CH-1-14_26	55	171	3.140	13.021	0.04	0.061	0.28	**10**	**370**	***474.45***	***17.92***
CH-1-14_27	74	192	2.600	12.706	0.04	0.055	0.24	**-20**	**320**	***489.50***	***17.76***
CH-1-14_28	52	114	2.210	13.889	0.04	0.054	0.30	**40**	**380**	***449.23***	***16.18***
CH-1-14_29	131	267	2.040	12.658	0.03	0.060	0.17	**300**	**290**	***488.46***	***13.34***
CH-1-14_30	88	214	2.430	12.516	0.03	0.052	0.19	**70**	**300**	***498.79***	***14.64***
CH-1-14_31	132	268	2.032	12.516	0.02	0.056	0.15	**320**	**290**	***496.01***	***9.18***
CH-1-14_32	171	320	1.870	13.850	0.02	0.057	0.14	**360**	**270**	***448.70***	***8.22***

Appendix II. LA-SF-ICP-MS U-Pb analyses of magmatic zircons

Sample				Radiogenic Ratios[1]				Ages (Ma)			
(n=32)	U (ppm)	Th (ppm)	$^{232}Th/^{238}U$	$^{238}U/^{206}Pb$	2 σ (%) err	$^{207}Pb/^{206}Pb$	2 σ (%) err	$^{207}Pb/^{206}Pb$	2 σ abs err	$^{206}Pb/^{238}U$	1 σ abs err
RCA-FL6_1	355	418	1.177	14.065	0.02	0.055	0.13	**290**	**250**	***443.40***	***9.37***
RCA-FL6_2	202	261	1.294	13.038	0.02	0.056	0.14	**330**	**250**	***476.52***	***7.92***
RCA-FL6_3	213	314	1.473	14.006	0.02	0.055	0.14	**300**	**270**	***445.13***	***7.91***
RCA-FL6_4	230	261	1.135	13.263	0.02	0.051	0.14	**200**	**250**	***471.47***	***7.91***
RCA-FL6_5	163	226	1.388	13.605	0.02	0.056	0.15	**270**	**250**	***457.22***	***9.71***
RCA-FL6_6	180	257	1.426	13.072	0.03	0.055	0.15	**250**	**280**	***476.00***	***12.72***
RCA-FL6_7	87	141	1.624	12.755	0.03	0.058	0.19	**280**	**320**	***485.78***	***13.72***
RCA-FL6_8	93	141	1.521	12.920	0.03	0.052	0.19	**70**	**300**	***483.35***	***14.03***
RCA-FL6_9	70	129	1.830	13.550	0.03	0.051	0.21	**130**	**340**	***461.67***	***12.92***
RCA-FL6_10	49	90	1.828	13.405	0.03	0.051	0.25	**-170**	**360**	***466.80***	***15.45***
RCA-FL6_11	32	94	2.940	13.263	0.04	0.058	0.47	**-880**	**470**	***467.70***	***21.18***
RCA-FL6_12	45	169	3.720	14.706	0.04	0.050	0.42	**-500**	**390**	***426.83***	***18.06***
RCA-FL6_13	45	96	2.150	11.976	0.05	0.044	0.34	**-370**	**410**	***525.58***	***23.53***
RCA-FL6_14	43	156	3.600	14.144	0.05	0.067	0.39	**-510**	**420**	***434.31***	***20.20***
RCA-FL6_15	39	122	3.100	11.891	0.04	0.046	0.33	**-330**	**430**	***528.00***	***21.38***
RCA-FL6_16	38	123	3.210	14.006	0.04	0.064	0.36	**-340**	**420**	***440.15***	***17.74***
RCA-FL6_17	45	79	1.760	11.249	0.04	0.057	0.28	**-160**	**380**	***550.04***	***19.17***
RCA-FL6_18	38	76	2.030	12.920	0.04	0.066	0.42	**-380**	**420**	***475.15***	***20.07***
RCA-FL6_19	38	77	2.060	12.092	0.04	0.058	0.34	**-230**	**430**	***511.93***	***20.05***
RCA-FL6_20	50	103	2.050	13.966	0.03	0.066	0.24	**100**	**380**	***440.27***	***14.52***
RCA-FL6_21	81	198	2.450	14.430	0.03	0.048	0.25	**-150**	**370**	***435.88***	***13.32***
RCA-FL6_22	98	208	2.120	13.038	0.03	0.061	0.18	**280**	**300**	***473.96***	***13.68***
RCA-FL6_23	105	161	1.530	12.870	0.03	0.059	0.20	**250**	**350**	***481.07***	***12.90***
RCA-FL6_24	102	309	3.030	14.881	0.03	0.050	0.22	**-70**	**310**	***421.80***	***12.02***
RCA-FL6_25	120	187	1.558	13.055	0.03	0.060	0.18	**280**	**300**	***473.77***	***12.51***
RCA-FL6_26	144	166	1.150	13.966	0.03	0.062	0.19	**310**	**310**	***442.49***	***11.37***
RCA-FL6_27	135	246	1.824	13.228	0.02	0.060	0.16	**330**	**280**	***467.71***	***10.67***
RCA-FL6_28	290	490	1.688	14.728	0.02	0.055	0.14	**330**	**270**	***423.48***	***7.00***
RCA-FL6_29	314	398	1.266	13.889	0.01	0.056	0.13	**320**	**250**	***448.35***	***6.42***
RCA-FL6_30	548	784	1.430	15.432	0.01	0.057	0.13	**380**	**250**	***403.82***	***4.92***
RCA-FL6_31	536	634	1.182	14.265	0.01	0.055	0.12	**350**	**250**	***437.08***	***5.20***
RCA-FL6_32	510	799	1.566	14.556	0.01	0.058	0.13	**430**	**250**	***426.86***	***5.52***

Appendix II. LA-SF-ICP-MS U-Pb analyses of magmatic zircons

Sample				Radiogenic Ratios[1]				Ages (Ma)			
					2 σ		2 σ		2 σ		1 σ
(n=30)	U (ppm)	Th (ppm)	$^{232}Th/^{238}U$	$^{238}U/^{206}Pb$	(%) err	$^{207}Pb/^{206}Pb$	(%) err	$^{207}Pb/^{206}Pb$	abs err	$^{206}Pb/^{238}U$	abs err
WA-1-14_1	200	510	2.550	14.045	0.02	0.057	0.15	**360**	**270**	***442.67***	***10.30***
WA-1-14_2	149	608	4.080	14.368	0.03	0.054	0.18	**150**	**290**	***434.77***	***12.80***
WA-1-14_3	136	464	3.410	15.291	0.03	0.054	0.18	**120**	**310**	***408.78***	***12.81***
WA-1-14_4	167	401	2.400	12.903	0.03	0.059	0.19	**200**	**310**	***480.03***	***12.54***
WA-1-14_5	134	574	4.280	13.850	0.03	0.053	0.18	**140**	**290**	***451.16***	***11.92***
WA-1-14_6	113	353	3.120	13.870	0.04	0.048	0.20	**-90**	**300**	***453.06***	***15.91***
WA-1-14_7	96	475	4.950	14.286	0.04	0.061	0.21	**250**	**330**	***433.28***	***15.85***
WA-1-14_8	119	585	4.920	12.516	0.03	0.059	0.19	**240**	**300**	***494.50***	***16.08***
WA-1-14_9	80	333	4.160	12.658	0.04	0.050	0.22	**-100**	**330**	***494.31***	***18.04***
WA-1-14_10	114	390	3.420	13.812	0.03	0.065	0.20	**320**	**300**	***445.63***	***15.20***
WA-1-14_11	96	376	3.920	12.937	0.03	0.050	0.24	**0**	**340**	***483.90***	***15.40***
WA-1-14_12	97	313	3.230	12.240	0.03	0.052	0.19	**30**	**330**	***509.83***	***16.45***
WA-1-14_13	112	254	2.270	12.690	0.03	0.053	0.19	**110**	**330**	***491.36***	***13.14***
WA-1-14_14	149	371	2.490	13.774	0.03	0.052	0.18	**130**	**290**	***453.94***	***11.61***
WA-1-14_15	182	493	2.710	14.245	0.03	0.060	0.17	**300**	**300**	***434.98***	***13.02***
WA-1-14_16	144	518	3.600	14.514	0.03	0.061	0.20	**310**	**290**	***426.40***	***12.83***
WA-1-14_17	577	1229	2.130	13.193	0.02	0.062	0.13	**590**	**260**	***467.89***	***10.22***
WA-1-14_18	1243	5800	4.666	13.333	0.01	0.055	0.11	**382**	**250**	***467.09***	***4.07***
WA-1-14_19	1392	10343	7.430	14.535	0.01	0.058	0.12	**465**	**240**	***427.78***	***4.33***
WA-1-14_20	1051	6043	5.750	14.205	0.01	0.057	0.12	**421**	**240**	***438.11***	***5.19***
WA-1-14_21	1017	5441	5.350	14.599	0.01	0.059	0.12	**480**	**250**	***425.38***	***5.49***
WA-1-14_22	1095	3144	2.871	14.164	0.01	0.060	0.12	**555**	**240**	***437.24***	***5.22***
WA-1-14_23	875	3981	4.550	13.908	0.02	0.058	0.12	**461**	**250**	***446.71***	***7.53***
WA-1-14_24	764	3194	4.180	13.569	0.01	0.056	0.12	**390**	**250**	***458.55***	***6.67***
WA-1-14_25	499	1091	2.187	13.089	0.01	0.057	0.13	**430**	**240**	***474.46***	***7.00***
WA-1-14_26	628	1915	3.050	12.970	0.02	0.058	0.13	**440**	**250**	***478.31***	***7.87***
WA-1-14_27	677	2891	4.270	14.881	0.02	0.057	0.12	**453**	**250**	***418.13***	***7.53***
WA-1-14_28	475	1140	2.399	12.422	0.02	0.056	0.13	**390**	**260**	***500.02***	***8.48***
WA-1-14_29	407	1079	2.650	13.106	0.02	0.053	0.13	**260**	**250**	***476.05***	***7.30***
WA-1-14_30	348	838	2.409	11.820	0.02	0.062	0.14	**550**	**280**	***520.99***	***8.29***

Appendix II. LA-SF-ICP-MS U-Pb analyses of magmatic zircons

Sample				Radiogenic Ratios(1)				Ages (Ma)			
					2 σ		2 σ		2 σ		1 σ
(n=29)	U (ppm)	Th (ppm)	$^{232}Th/^{238}U$	$^{238}U/^{206}Pb$	(%) err	$^{207}Pb/^{206}Pb$	(%) err	$^{207}Pb/^{206}Pb$	abs err	$^{206}Pb/^{238}U$	abs err
WS-1-14_1	204	439	2.151	12.610	0.01	0.056	0.14	**330**	**270**	***492.37***	***6.82***
WS-1-14_2	126	150	1.188	13.717	0.02	0.046	0.18	**-50**	**280**	***459.42***	***9.22***
WS-1-14_3	18	16	0.889	6.803	0.03	0.668	0.15	**4590**	**280**	***220.95***	***61.98***
WS-1-14_4	108	108	1.003	11.223	0.03	0.109	0.15	**1420**	**330**	***516.37***	***13.63***
WS-1-14_5	91	102	1.124	12.563	0.02	0.058	0.21	**160**	**320**	***493.17***	***11.48***
WS-1-14_6	85	95	1.120	11.834	0.02	0.073	0.16	**630**	**330**	***513.00***	***10.79***
WS-1-14_7	161	196	1.215	12.903	0.02	0.056	0.17	**220**	**290**	***481.79***	***10.69***
WS-1-14_8	80	97	1.215	12.547	0.03	0.047	0.24	**-160**	**320**	***500.57***	***13.31***
WS-1-14_9	53	72	1.355	12.392	0.04	0.094	0.31	**280**	**480**	***477.88***	***20.30***
WS-1-14_10	66	89	1.346	12.563	0.03	0.092	0.20	**780**	**400**	***472.71***	***15.25***
WS-1-14_11	47	37	0.780	12.422	0.04	0.131	0.25	**1060**	**510**	***454.17***	***20.41***
WS-1-14_12	68	136	2.000	11.947	0.04	0.062	0.29	**100**	**480**	***515.45***	***19.50***
WS-1-14_13	84	96	1.143	12.092	0.03	0.057	0.39	**-200**	**410**	***512.55***	***17.73***
WS-1-14_14	32	46	1.448	11.547	0.05	0.054	0.43	**-170**	**510**	***538.10***	***25.39***
WS-1-14_15	33	49	1.510	12.821	0.05	0.077	0.44	**-760**	**580**	***472.27***	***23.30***
WS-1-14_16	28	85	3.080	9.009	0.05	0.170	0.26	**1050**	**670**	***589.10***	***31.87***
WS-1-14_17	93	130	1.396	12.048	0.03	0.058	0.28	**70**	**340**	***513.74***	***16.79***
WS-1-14_18	29	72	2.470	11.976	0.04	0.017	1.18	**-1480**	**600**	***542.55***	***23.70***
WS-1-14_19	58	75	1.281	11.236	0.03	0.100	0.25	**740**	**470**	***521.84***	***19.40***
WS-1-14_20	28	53	1.890	11.976	0.05	0.051	0.63	**-1150**	**720**	***521.17***	***28.94***
WS-1-14_21	35	68	1.920	14.085	0.05	0.063	0.57	**-930**	**700**	***438.27***	***23.28***
WS-1-14_22	38	55	1.459	12.392	0.05	0.106	0.42	**-380**	**770**	***470.55***	***26.26***
WS-1-14_23	33	55	1.650	12.579	0.05	0.057	0.56	**-920**	**730**	***493.16***	***24.13***
WS-1-14_24	30	46	1.520	13.021	0.04	0.058	0.48	**-800**	**610**	***476.20***	***21.89***
WS-1-14_25	28	47	1.720	10.661	0.04	0.054	0.50	**-590**	**490**	***581.70***	***24.30***
WS-1-14_26	35	37	1.055	9.970	0.04	0.104	0.30	**440**	**590**	***583.38***	***26.03***
WS-1-14_27	34	44	1.296	10.020	0.05	0.062	0.45	**-330**	**510**	***611.94***	***29.39***
WS-1-14_28	126	236	1.867	11.947	0.02	0.061	0.16	**380**	**280**	***516.40***	***9.80***
WS-1-14_29	113	321	2.840	12.903	0.03	0.057	0.26	**10**	**350**	***481.03***	***14.93***

Appendix II. LA-SF-ICP-MS U-Pb analyses of magmatic zircons

Primary Std.				Radiogenic Ratios[1]				Ages (Ma)			
					2 σ		2 σ		2 σ		1 σ
(n=18)	U (ppm)	Th (ppm)	$^{232}Th/^{238}U$	$^{238}U/^{206}Pb$	(%) err	$^{207}Pb/^{206}Pb$	(%) err	$^{207}Pb/^{206}Pb$	abs err	$^{206}Pb/^{238}U$	abs err
91500_1	80.5	209	2.600	5.504	0.02	0.071	0.14	**790**	**290**	***1082.08***	***22.84***
91500_2	79.8	217	2.720	5.708	0.02	0.073	0.14	**790**	**280**	***1042.07***	***18.13***
91500_3	84.1	230	2.730	5.559	0.02	0.075	0.15	**820**	**290**	***1066.20***	***20.24***
91500_4	65.9	199	3.020	5.456	0.02	0.073	0.15	**750**	**290**	***1088.61***	***24.12***
91500_5	97.9	238	2.436	5.559	0.02	0.084	0.13	**1080**	**280**	***1080.00***	***140.00***
91500_6	87.5	235	2.688	5.549	0.02	0.081	0.14	**1020**	**270**	***1020.00***	***135.00***
91500_7	87.8	234	2.665	5.643	0.02	0.075	0.13	**910**	**260**	***1051.37***	***21.33***
91500_8	74.1	198	2.670	5.546	0.02	0.077	0.13	**960**	**270**	***1066.25***	***20.79***
91500_9	81.2	209	2.570	5.596	0.02	0.072	0.14	**820**	**290**	***1063.10***	***20.59***
91500_10	78.2	217	2.780	5.559	0.02	0.069	0.14	**690**	**270**	***1074.73***	***23.08***
91500_11	79.5	219	2.760	5.721	0.02	0.079	0.14	**950**	**280**	***1032.11***	***23.35***
91500_12	74.7	203	2.720	5.376	0.02	0.078	0.14	**880**	**280**	***1096.79***	***22.91***
91500_13	85.7	226	2.640	5.627	0.02	0.073	0.15	**760**	**300**	***1056.05***	***23.52***
91500_14	80.4	214	2.660	5.682	0.02	0.069	0.14	**730**	**280**	***1051.81***	***22.49***
91500_15	80	210	2.620	5.485	0.02	0.078	0.14	**920**	**280**	***1075.82***	***23.15***
91500_16	79.3	216	2.730	5.587	0.02	0.078	0.14	**820**	**300**	***1057.38***	***22.59***
91500_17	83	221	2.660	5.593	0.02	0.071	0.14	**730**	**280**	***1065.24***	***21.17***
91500_18	77.6	205	2.640	5.653	0.02	0.078	0.14	**940**	**290**	***1045.64***	***21.50***

Second. Std.				Radiogenic Ratios[1]				Ages (Ma)			
					2 σ		2 σ		2 σ		1 σ
(n=23)	U (ppm)	Th (ppm)	$^{232}Th/^{238}U$	$^{238}U/^{206}Pb$	(%) err	$^{207}Pb/^{206}Pb$	(%) err	$^{207}Pb/^{206}Pb$	abs err	$^{206}Pb/^{238}U$	abs err
Plesovice_1	1064	8023	7.54	18.182	0.02	0.054	0.13	**300**	**250**	***344.93***	***5.44***
Plesovice_2	975	7517	7.71	17.762	0.02	0.053	0.12	**315**	**250**	***353.20***	***6.32***
Plesovice_3	950	6432	6.77	17.212	0.02	0.049	0.12	**140**	**240**	***366.25***	***7.55***
Plesovice_4	829	6143	7.41	17.153	0.02	0.054	0.13	**260**	**240**	***365.35***	***8.47***
Plesovice_5	3220	21735	6.75	17.825	0.02	0.051	0.11	**209**	**230**	***353.13***	***6.31***
Plesovice_6	1470	12730	8.66	16.807	0.02	0.050	0.12	**200**	**240**	***374.24***	***6.64***
Plesovice_7	797	7962	9.99	18.315	0.02	0.054	0.13	**320**	**250**	***342.38***	***7.23***
Plesovice_8	1840	13984	7.6	18.484	0.02	0.056	0.12	**418**	**250**	***338.55***	***6.60***
Plesovice_9	1370	12741	9.3	17.794	0.02	0.054	0.12	**318**	**240**	***352.46***	***5.41***
Plesovice_10	875	7744	8.85	19.048	0.02	0.053	0.12	**292**	**250**	***330.06***	***6.01***
Plesovice_11	678	6882	10.15	18.692	0.02	0.051	0.13	**230**	**240**	***336.70***	***5.73***
Plesovice_12	694	7148	10.3	18.382	0.02	0.053	0.13	**250**	**240**	***341.81***	***7.85***
Plesovice_13	632	6788	10.74	18.416	0.02	0.051	0.13	**200**	**240**	***341.86***	***6.94***
Plesovice_14	521	5731	11	18.282	0.02	0.062	0.13	**540**	**250**	***339.90***	***6.62***
Plesovice_15	572	6343	11.09	18.587	0.02	0.063	0.13	**620**	**270**	***333.74***	***6.61***
Plesovice_16	1001	8529	8.52	18.349	0.02	0.055	0.12	**350**	**240**	***341.59***	***6.32***
Plesovice_17	1030	7169	6.96	18.182	0.02	0.057	0.12	**440**	**250**	***343.50***	***7.52***
Plesovice_18	1130	6656	5.89	18.182	0.02	0.053	0.12	**310**	**250**	***345.14***	***7.53***
Plesovice_19	903	5599	6.2	18.248	0.02	0.055	0.12	**330**	**240**	***343.44***	***6.93***
Plesovice_20	652	6618	10.15	18.182	0.03	0.054	0.13	**280**	**240**	***345.01***	***8.45***
Plesovice_21	679	7326	10.79	18.083	0.03	0.056	0.13	**360**	**250**	***346.02***	***10.57***
Plesovice_22	706	7357	10.42	18.519	0.02	0.056	0.13	**370**	**250**	***337.93***	***6.62***
Plesovice_23	733	7660	10.45	18.416	0.02	0.053	0.12	**280**	**240**	***340.98***	***6.93***

[1] 204-corrected

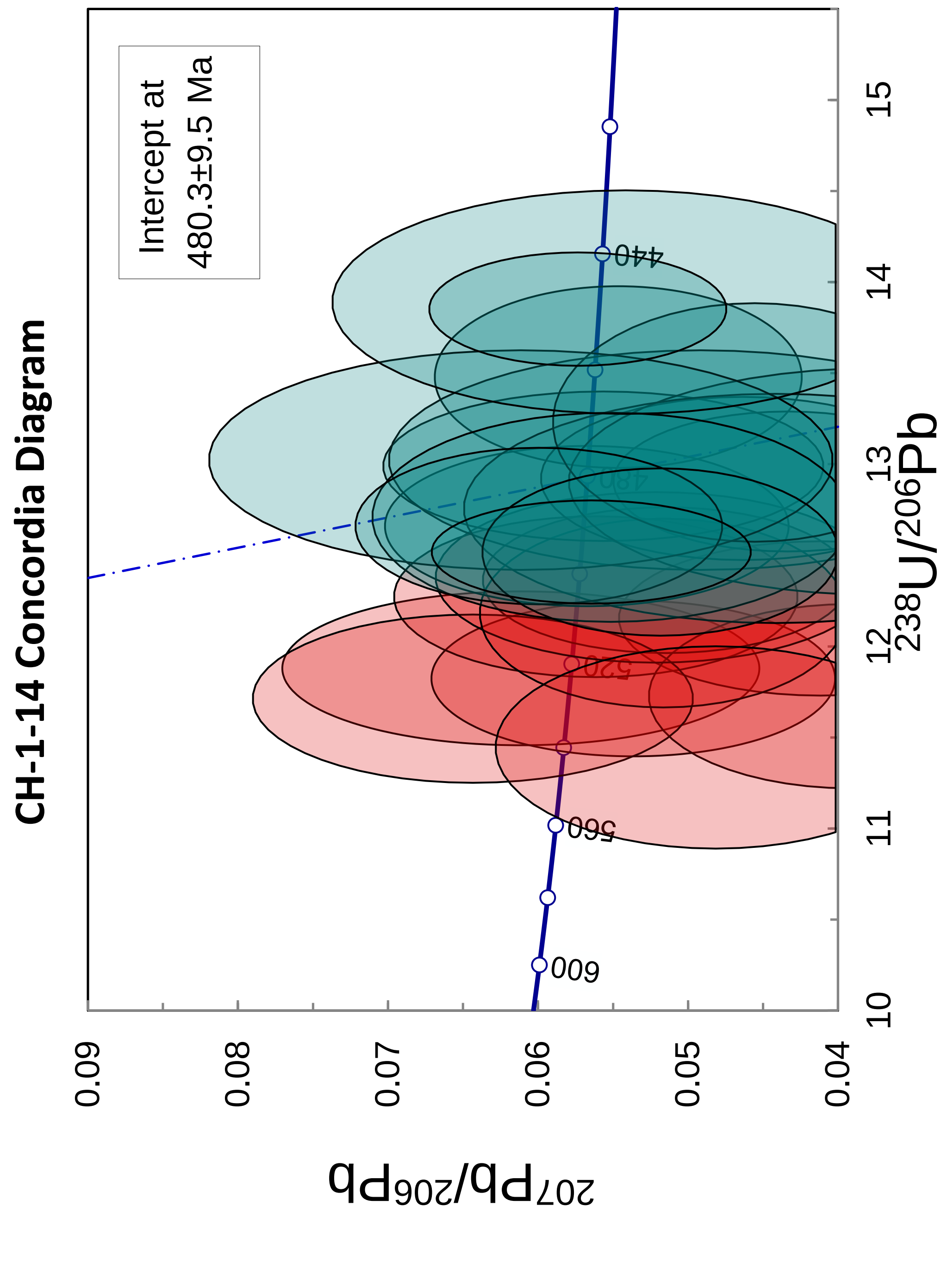
CH-1-14 Concordia Diagram
Intercept at
480.3±9.5 Ma
600
560
520
480
440
10
11
12
13
14
15
0.09
0.08
0.07
0.06
0.05
0.04
$^{238}U/^{206}Pb$
$^{207}Pb/^{206}Pb$

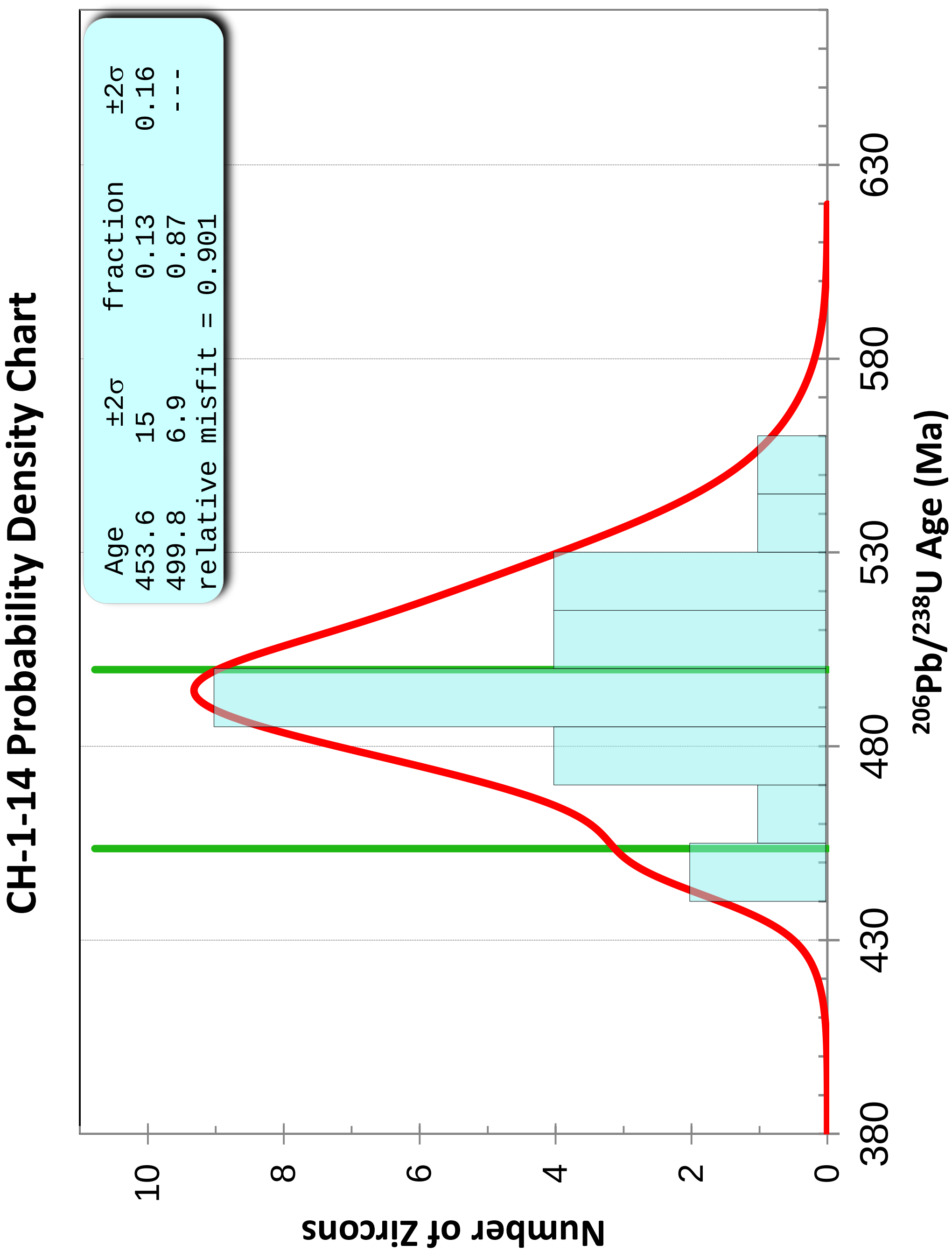
CH-1-14 Probability Density Chart
Age ±2σ fraction ±2σ
453.6 15 0.13 0.16
499.8 6.9 0.87 ---
relative misfit = 0.901
Number of Zircons
0 2 4 6 8 10
380 430 480 530 580 630
^{206}Pb/^{238}U Age (Ma)

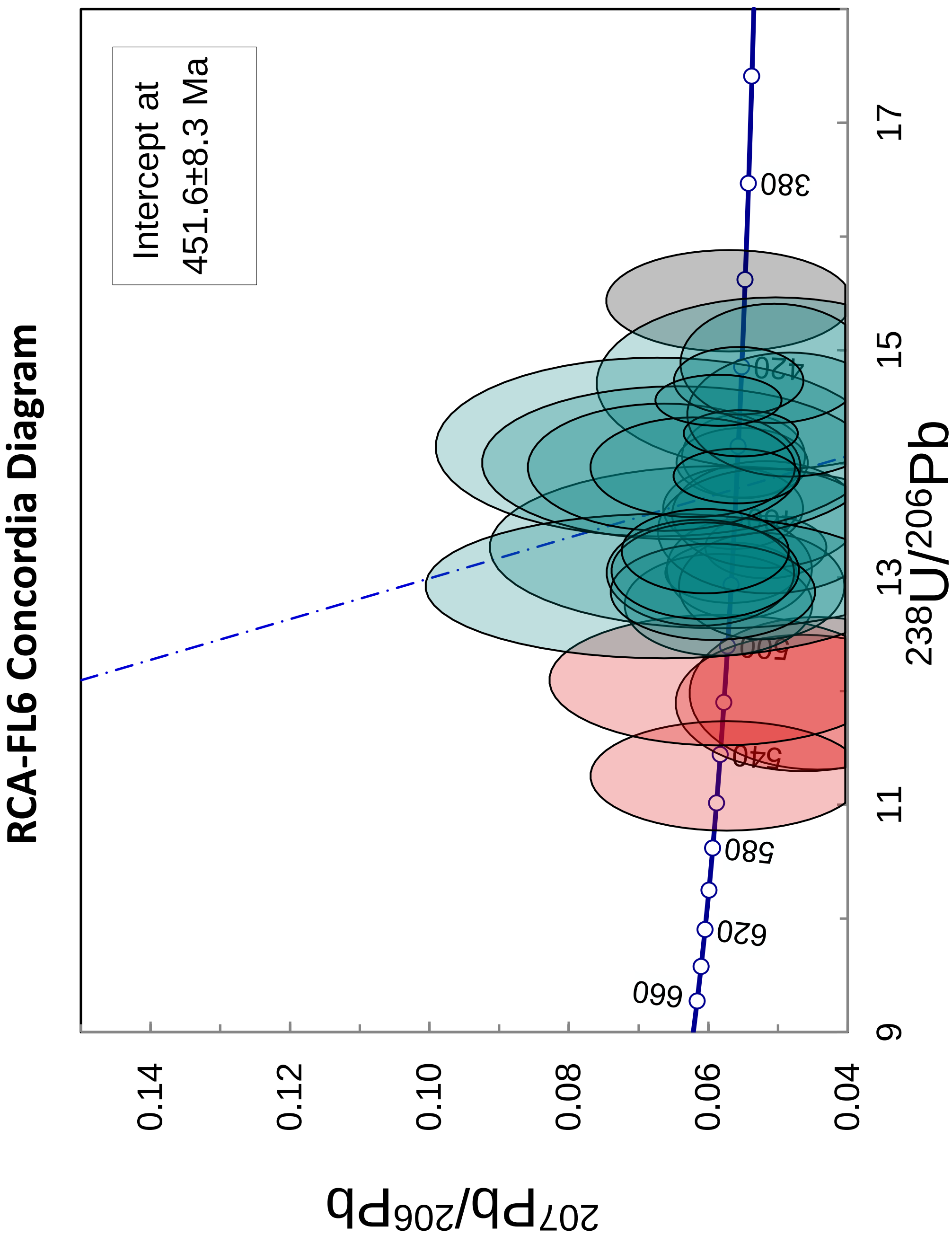
RCA-FL6 Concordia Diagram
Intercept at
451.6±8.3 Ma
$^{238}U/^{206}Pb$
$^{207}Pb/^{206}Pb$
0.14
0.12
0.10
0.08
0.06
0.04
9
11
13
15
17
660
620
580
540
500
420
380

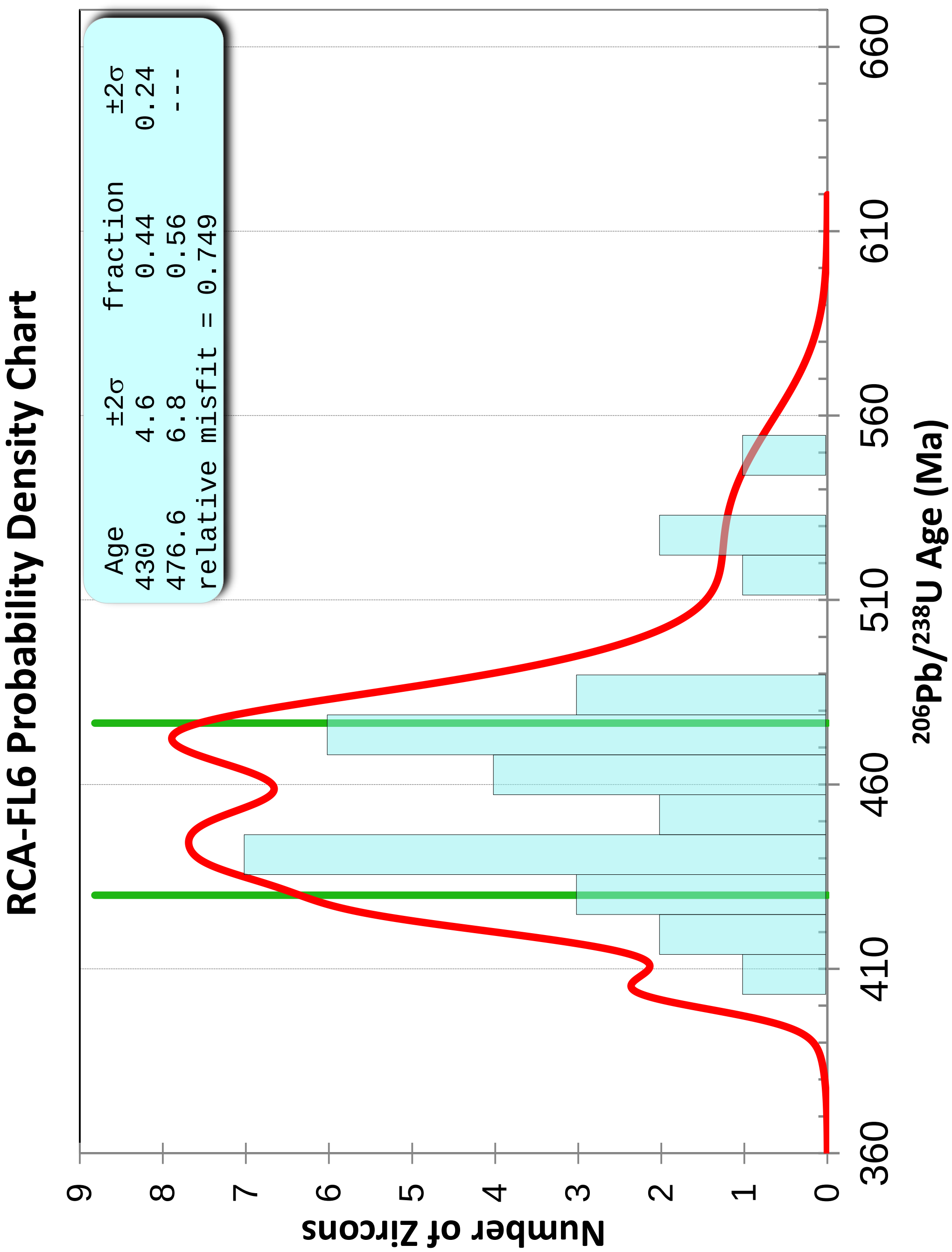
RCA-FL6 Probability Density Chart
Age ±2σ fraction ±2σ
430 4.6 0.44 0.24
476.6 6.8 0.56 ---
relative misfit = 0.749
Number of Zircons
0
1
2
3
4
5
6
7
8
9
360
410
460
510
560
610
660
206Pb/238U Age (Ma)

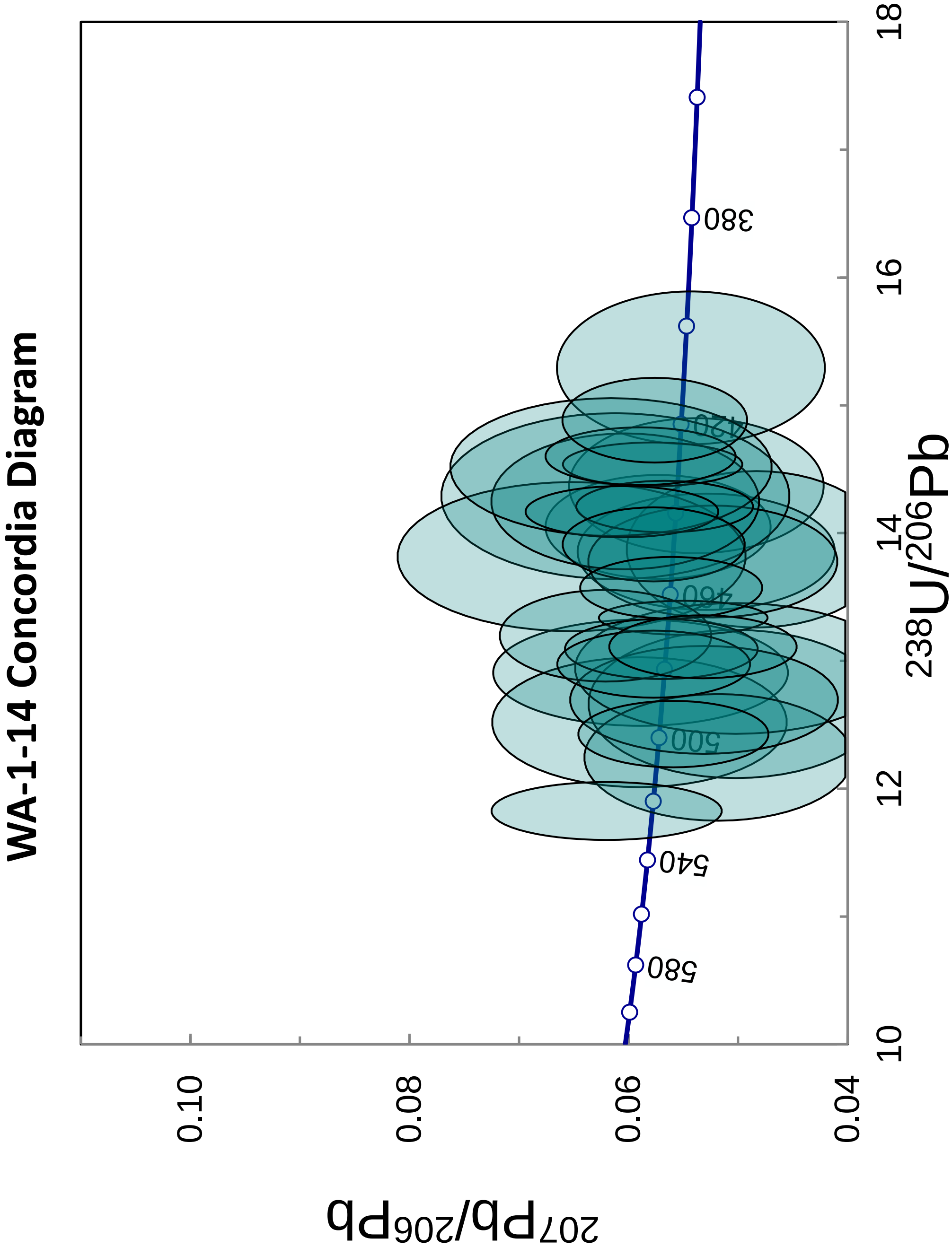
WA-1-14 Concordia Diagram
$^{238}U/^{206}Pb$
$^{207}Pb/^{206}Pb$
0.10
0.08
0.06
0.04
10
12
14
16
18
380
420
460
500
540
580

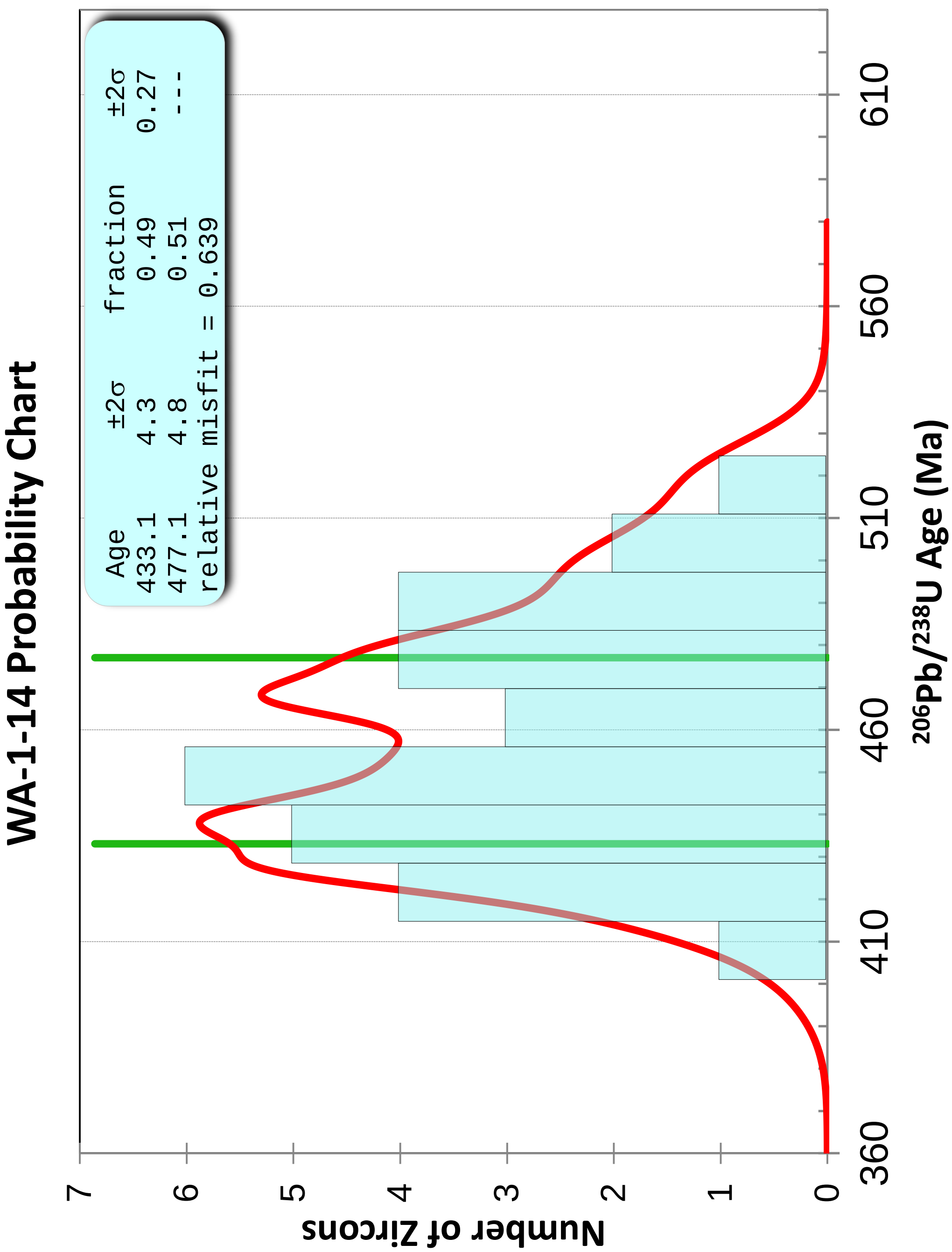
WA-1-14 Probability Chart
Age ±2σ fraction ±2σ
433.1 4.3 0.49 0.27
477.1 4.8 0.51 ---
relative misfit = 0.639
Number of Zircons
0 1 2 3 4 5 6 7
360 410 460 510 560 610
$^{206}Pb/^{238}U$ Age (Ma)

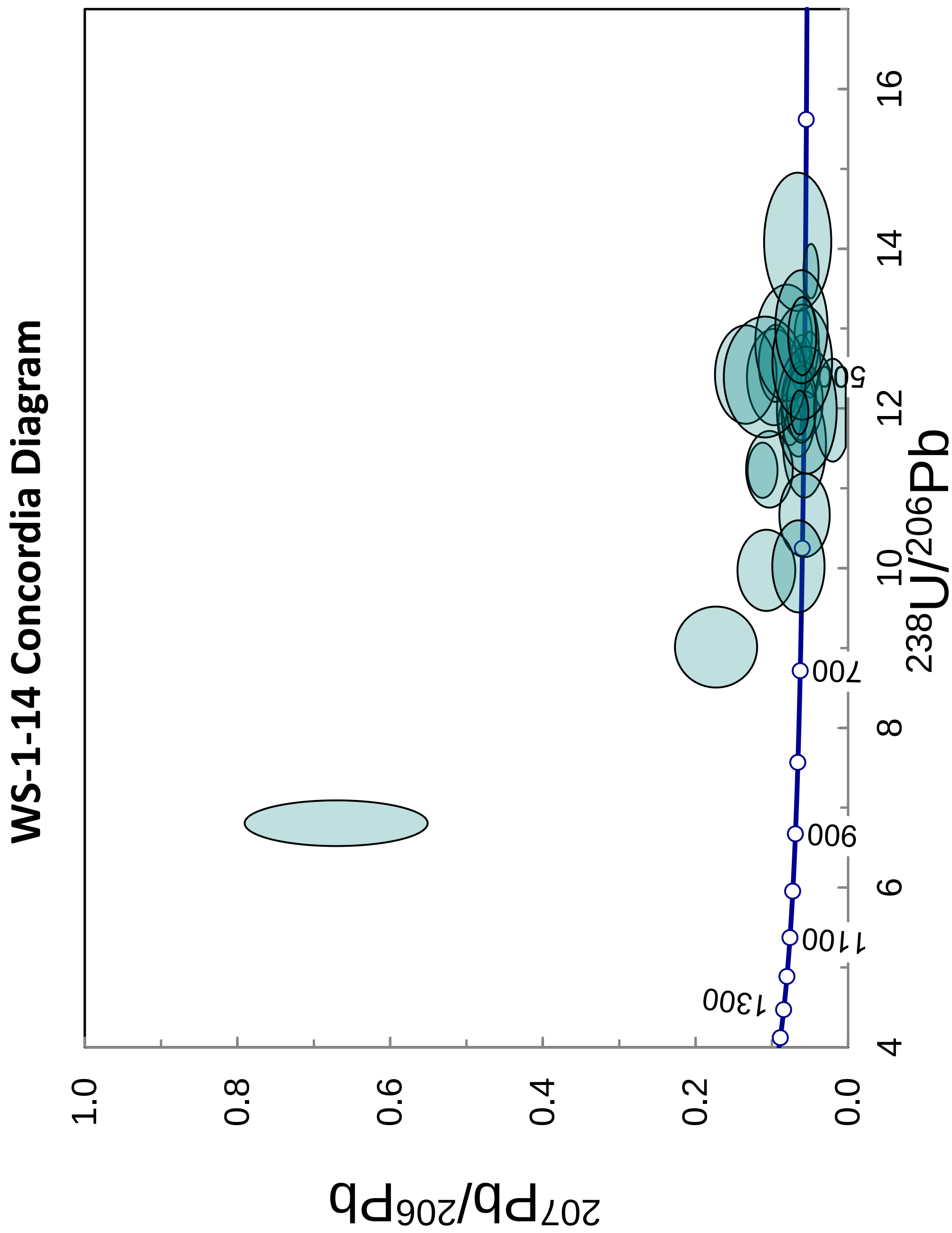
WS-1-14 Concordia Diagram
$^{207}Pb/^{206}Pb$
$^{238}U/^{206}Pb$
1.0
0.8
0.6
0.4
0.2
0.0
4
6
8
10
12
14
16
1300
1100
900
700
500

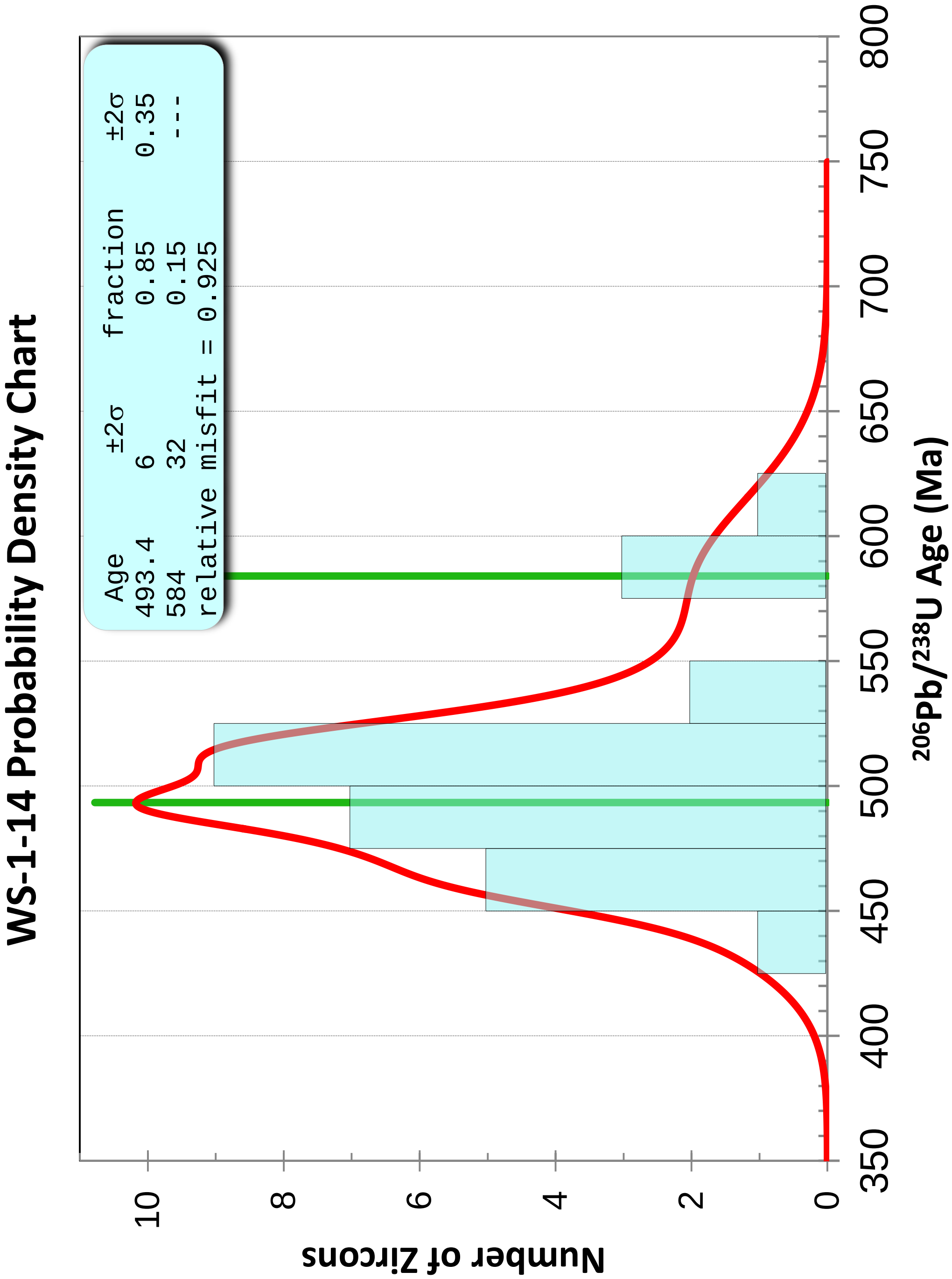
WS-1-14 Probability Density Chart
Age ±2σ fraction ±2σ
493.4 6 0.85 0.35
584 32 0.15 ---
relative misfit = 0.925
Number of Zircons
0
2
4
6
8
10
350
400
450
500
550
600
650
700
750
800
206Pb/238U Age (Ma)

Appendix III. LA-SF-ICP-MS U-Pb analyses of detrital zircons

Sample				Radiogenic Ratios[1]				Ages (Ma)			
					2 σ		2 σ		2 σ		1 σ
(n=82)	U (ppm)	Th (ppm)	^{232}Th/^{238}U	^{238}U/^{206}Pb	(%) err	^{207}Pb/^{206}Pb	(%) err	^{207}Pb/^{206}Pb	abs err	^{206}Pb/^{238}U	abs err
AG-1-14_1	321	74	0.231	6.382	0.02	0.069	0.16	**840**	**340**	***940.07***	***20.86***
AG-1-14_2	288	20	0.071	9.124	0.01	0.063	0.16	**700**	**290**	***669.44***	***8.64***
AG-1-14_3	906	5	0.005	15.576	0.03	0.055	0.15	**362**	**310**	***400.94***	***12.37***
AG-1-14_4	571	182	0.319	7.241	0.02	0.069	0.16	**850**	**320**	***831.64***	***13.48***
AG-1-14_5	740	78	0.105	10.384	0.03	0.067	0.15	**777**	**310**	***587.64***	***16.50***
AG-1-14_6	1646	276	0.168	16.000	0.03	0.052	0.15	**260**	**300**	***391.80***	***10.54***
AG-1-14_7	470	53	0.114	8.905	0.02	0.064	0.16	**653**	**310**	***684.88***	***11.39***
AG-1-14_8	1148	552	0.481	7.899	0.02	0.078	0.15	**1121**	**310**	***756.36***	***14.77***
AG-1-14_9	376	61	0.161	9.737	0.02	0.070	0.16	**886**	**320**	***623.26***	***15.68***
AG-1-14_10	843	35	0.042	11.123	0.02	0.059	0.16	**528**	**320**	***554.52***	***10.32***
AG-1-14_11	118	39	0.331	5.942	0.03	0.074	0.16	**920**	**330**	***1001.26***	***27.47***
AG-1-14_12	253	98	0.389	5.666	0.02	0.078	0.15	**1070**	**330**	***1070.00***	***168.37***
AG-1-14_13	320	119	0.370	6.897	0.02	0.076	0.16	**1031**	**320**	***864.91***	***20.24***
AG-1-14_14	230	30	0.132	9.124	0.03	0.072	0.15	**870**	**330**	***662.25***	***18.57***
AG-1-14_15	1522	350	0.230	6.536	0.04	0.079	0.15	**1120**	**320**	***907.80***	***38.70***
AG-1-14_16	1046	59	0.057	14.144	0.02	0.065	0.15	**719**	**330**	***435.44***	***9.03***
AG-1-14_17	708	51	0.072	6.949	0.02	0.079	0.15	**1142**	**300**	***854.74***	***15.78***
AG-1-14_18	1118	237	0.212	9.302	0.01	0.069	0.16	**863**	**320**	***651.99***	***9.82***
AG-1-14_19	3220	161	0.050	14.993	0.01	0.060	0.15	**566**	**270**	***413.66***	***6.06***
AG-1-14_20	1622	238	0.147	12.706	0.01	0.073	0.15	**964**	**290**	***479.03***	***7.75***
AG-1-14_21	210	45	0.216	13.605	0.02	0.057	0.17	**350**	**310**	***457.00***	***9.11***
AG-1-14_22	333	0	0.001	10.081	0.02	0.059	0.17	**560**	**280**	***610.29***	***13.09***
AG-1-14_23	138	36	0.262	6.720	0.02	0.071	0.16	**840**	**340**	***892.21***	***14.67***
AG-1-14_24	200	28	0.138	9.259	0.02	0.066	0.15	**700**	**320**	***657.84***	***10.79***
AG-1-14_25	121	48	0.398	7.252	0.02	0.071	0.16	**810**	**330**	***829.05***	***16.47***
AG-1-14_26	635	18	0.029	13.441	0.01	0.057	0.15	**458**	**330**	***462.25***	***6.98***
AG-1-14_27	383	96	0.251	7.057	0.02	0.069	0.15	**840**	**320**	***853.05***	***14.13***
AG-1-14_28	675	77	0.114	6.978	0.01	0.068	0.15	**845**	**320**	***863.33***	***11.46***
AG-1-14_29	148.7	26	0.178	6.390	0.02	0.067	0.15	**760**	**330**	***940.98***	***15.68***
AG-1-14_30	151	39	0.258	7.485	0.02	0.068	0.16	**750**	**340**	***806.46***	***15.92***
AG-1-14_31	1560	492	0.315	14.749	0.01	0.052	0.15	**262**	**330**	***424.83***	***5.41***
AG-1-14_32	641	25	0.039	12.531	0.02	0.062	0.16	**600**	**320**	***491.91***	***8.82***
AG-1-14_33	308	78	0.253	6.345	0.02	0.082	0.16	**1160**	**330**	***930.26***	***16.47***
AG-1-14_34	933	157	0.168	6.165	0.02	0.078	0.15	**1121**	**290**	***961.03***	***19.26***
AG-1-14_35	772	268	0.347	6.321	0.02	0.077	0.16	**1081**	**300**	***939.84***	***21.72***
AG-1-14_36	869	121	0.139	8.475	0.02	0.071	0.15	**898**	**320**	***711.96***	***17.17***
AG-1-14_37	885	119	0.134	8.496	0.02	0.088	0.15	**1346**	**300**	***696.03***	***17.71***
AG-1-14_38	1290	189	0.146	7.087	0.02	0.080	0.15	**1162**	**310**	***837.70***	***14.14***

				Radiogenic Ratios[1]				Ages (Ma)			
Sample (n=82)	**U (ppm)**	**Th (ppm)**	**$^{232}Th/^{238}U$**	**$^{238}U/^{206}Pb$**	**2 σ (%) err**	**$^{207}Pb/^{206}Pb$**	**2 σ (%) err**	**$^{207}Pb/^{206}Pb$**	**2 σ abs err**	**$^{206}Pb/^{238}U$**	**1 σ abs err**
AG-1-14_39	346	52	0.150	2.674	0.02	0.190	0.15	**2723**	**240**	***2723.00***	***122.45***
AG-1-14_40	2420	48	0.020	7.003	0.01	0.077	0.14	**1112**	**280**	***851.05***	***10.39***
AG-1-14_41	2290	152	0.066	8.013	0.01	0.073	0.15	**986**	**310**	***750.55***	***9.82***
AG-1-14_42	5660	422	0.075	13.280	0.01	0.077	0.14	**1101**	**300**	***456.49***	***5.82***
AG-1-14_43	2280	399	0.175	9.107	0.01	0.081	0.15	**1209**	**310**	***655.97***	***10.23***
AG-1-14_44	582	266	0.457	5.949	0.02	0.080	0.15	**1153**	**310**	***993.09***	***17.71***
AG-1-14_45	1030	212	0.206	6.729	0.01	0.077	0.16	**1106**	**310**	***884.27***	***12.03***
AG-1-14_46	314	151	0.481	5.163	0.02	0.092	0.15	**1420**	**300**	***1420.00***	***153.06***
AG-1-14_47	549	153	0.279	5.956	0.02	0.077	0.16	**1105**	**320**	***994.66***	***19.08***
AG-1-14_48	327	46	0.139	12.837	0.02	0.065	0.17	**700**	**320**	***478.86***	***7.79***
AG-1-14_49	1570	252	0.161	6.013	0.01	0.082	0.15	**1232**	**280**	***980.01***	***12.39***
AG-1-14_50	1408	219	0.155	6.549	0.01	0.076	0.14	**1084**	**290**	***908.66***	***11.81***
AG-1-14_51	610	93	0.153	10.638	0.02	0.068	0.15	**804**	**320**	***572.82***	***9.78***
AG-1-14_52	557	143	0.256	8.403	0.02	0.071	0.16	**890**	**330**	***718.35***	***13.23***
AG-1-14_53	511	103	0.202	9.158	0.02	0.069	0.16	**845**	**330**	***662.02***	***11.20***
AG-1-14_54	1000	86	0.086	11.682	0.02	0.062	0.15	**624**	**320**	***526.69***	***8.85***
AG-1-14_55	1630	91	0.056	8.019	0.01	0.084	0.16	**1273**	**280**	***739.80***	***11.74***
AG-1-14_56	2280	340	0.149	6.689	0.01	0.068	0.15	**849**	**310**	***899.46***	***11.55***
AG-1-14_57	1596	764	0.478	4.697	0.01	0.079	0.15	**1150**	**310**	***1150.00***	***158.16***
AG-1-14_58	646	137	0.212	6.882	0.02	0.069	0.16	**839**	**310**	***873.49***	***14.92***
AG-1-14_59	930	121	0.130	9.285	0.02	0.062	0.15	**608**	**330**	***658.95***	***10.47***
AG-1-14_60	7600	298	0.039	10.627	0.01	0.062	0.15	**642**	**320**	***578.22***	***8.31***
AG-1-14_61	1718	247	0.144	7.968	0.01	0.071	0.16	**950**	**290**	***756.49***	***8.62***
AG-1-14_62	2610	499	0.191	7.740	0.02	0.083	0.16	**1242**	**300**	***766.64***	***15.20***
AG-1-14_63	2700	662	0.245	5.949	0.01	0.073	0.15	**1006**	**310**	***1006.00***	***158.16***
AG-1-14_64	2960	676	0.228	6.793	0.01	0.069	0.14	**878**	**300**	***884.44***	***11.50***
AG-1-14_65	1447	494	0.341	8.467	0.02	0.067	0.15	**778**	**310**	***716.06***	***11.98***
AG-1-14_66	4000	108	0.027	13.793	0.01	0.053	0.15	**325**	**320**	***452.61***	***5.76***
AG-1-14_67	14520	1036	0.071	13.089	0.01	0.061	0.15	**622**	**320**	***472.04***	***5.88***
AG-1-14_68	7400	1545	0.209	6.798	0.01	0.071	0.16	**940**	**300**	***882.12***	***11.01***
AG-1-14_69	6040	1382	0.229	8.032	0.01	0.070	0.14	**892**	**300**	***751.75***	***9.34***
AG-1-14_70	2510	971	0.387	7.692	0.01	0.079	0.15	**1144**	**320**	***775.09***	***10.64***
AG-1-14_71	2550	155	0.061	7.220	0.02	0.067	0.15	**815**	**340**	***836.22***	***14.40***
AG-1-14_72	766	47	0.062	7.062	0.01	0.069	0.14	**862**	**310**	***852.15***	***13.03***
AG-1-14_73	383	68	0.177	7.246	0.02	0.082	0.15	**1193**	**300**	***818.43***	***16.21***
AG-1-14_74	1228	268	0.218	8.032	0.01	0.074	0.15	**1010**	**310**	***747.97***	***11.37***
AG-1-14_75	1644	302	0.184	7.413	0.01	0.068	0.15	**857**	**320**	***814.06***	***10.55***
AG-1-14_76	1159	238	0.205	7.893	0.01	0.067	0.15	**818**	**320**	***767.08***	***11.53***

Appendix III. LA-SF-ICP-MS U-Pb analyses of detrital zircons

Sample				Radiogenic Ratios[1]				Ages (Ma)			
(n=82)	U (ppm)	Th (ppm)	$^{232}Th/^{238}U$	$^{238}U/^{206}Pb$	2 σ (%) err	$^{207}Pb/^{206}Pb$	2 σ (%) err	$^{207}Pb/^{206}Pb$	2 σ abs err	$^{206}Pb/^{238}U$	1 σ abs err
AG-1-14_77	2940	244	0.083	8.058	0.01	0.070	0.14	**924**	**300**	***748.77***	***10.92***
AG-1-14_78	345	68	0.197	8.382	0.01	0.068	0.15	**819**	**330**	***722.68***	***10.34***
AG-1-14_79	654	45	0.069	10.764	0.01	0.102	0.15	**1625**	**290**	***542.90***	***9.10***
AG-1-14_80	584	106	0.181	6.993	0.01	0.072	0.15	**944**	**310**	***857.57***	***12.72***
AG-1-14_81	336	58	0.174	7.231	0.02	0.067	0.15	**815**	**310**	***835.05***	***14.12***
AG-1-14_82	244	22	0.090	12.453	0.02	0.059	0.15	**541**	**310**	***496.74***	***8.20***

Primary Std.				Radiogenic Ratios[1]				Ages (Ma)			
(n=12)	U (ppm)	Th (ppm)	$^{232}Th/^{238}U$	$^{238}U/^{206}Pb$	2 σ (%) err	$^{207}Pb/^{206}Pb$	2 σ (%) err	$^{207}Pb/^{206}Pb$	2 σ abs err	$^{206}Pb/^{238}U$	1 σ abs err
91500_1	79.7	31	0.394	5.593	0.03	0.076	0.16	**930**	**340**	***1059.24***	***27.77***
91500_2	81	31	0.385	5.721	0.03	0.074	0.16	**890**	**340**	***1038.49***	***29.20***
91500_3	79.2	31	0.388	5.525	0.03	0.076	0.17	**850**	**340**	***1071.57***	***29.09***
91500_4	78.9	28	0.358	5.376	0.03	0.074	0.18	**860**	**370**	***1102.48***	***33.40***
91500_5	1550	266	0.172	5.734	0.02	0.075	0.15	**1044**	**320**	***1044.00***	***163.27***
91500_6	61.1	24	0.398	5.435	0.03	0.074	0.16	**840**	**350**	***1091.42***	***30.39***
91500_7	199	35	0.174	5.602	0.02	0.076	0.16	**1010**	**340**	***1010.00***	***173.47***
91500_8	66.6	26	0.383	5.464	0.03	0.074	0.18	**770**	**360**	***1085.55***	***30.57***
91500_9	83	31	0.368	5.485	0.03	0.075	0.17	**810**	**370**	***1080.61***	***28.03***
91500_10	95	35	0.364	5.559	0.03	0.075	0.17	**820**	**360**	***1065.93***	***29.66***
91500_11	64.6	22	0.342	5.556	0.03	0.075	0.17	**780**	**350**	***1067.43***	***33.33***
91500_12	110.4	57	0.515	5.666	0.02	0.075	0.16	**1030**	**330**	***1030.00***	***168.37***

Second. Std.				Radiogenic Ratios[1]				Ages (Ma)			
(n=9)	U (ppm)	Th (ppm)	$^{232}Th/^{238}U$	$^{238}U/^{206}Pb$	2 σ (%) err	$^{207}Pb/^{206}Pb$	2 σ (%) err	$^{207}Pb/^{206}Pb$	2 σ abs err	$^{206}Pb/^{238}U$	1 σ abs err
Plesovice_1	731	69	0.095	19.011	0.02	0.052	0.16	**210**	**290**	***331.00***	***7.77***
Plesovice_2	426	40	0.093	17.153	0.03	0.048	0.17	**60**	**310**	***368.11***	***10.92***
Plesovice_3	260	20	0.078	17.953	0.03	0.050	0.18	**120**	**310**	***351.08***	***10.30***
Plesovice_4	302	28	0.094	18.349	0.02	0.056	0.17	**320**	**320**	***341.18***	***8.40***
Plesovice_5	148	11	0.072	18.797	0.03	0.050	0.19	**20**	**300**	***335.37***	***9.39***
Plesovice_6	349	26	0.076	19.455	0.03	0.050	0.19	**60**	**310**	***324.16***	***9.70***
Plesovice_7	249	22	0.088	19.305	0.03	0.051	0.19	**170**	**320**	***326.21***	***9.06***
Plesovice_8	3920	505	0.129	19.048	0.02	0.051	0.16	**190**	**290**	***330.79***	***7.77***
Plesovice_9	243	32	0.130	18.315	0.02	0.049	0.16	**140**	**290**	***344.59***	***7.78***

[1] 204-corrected

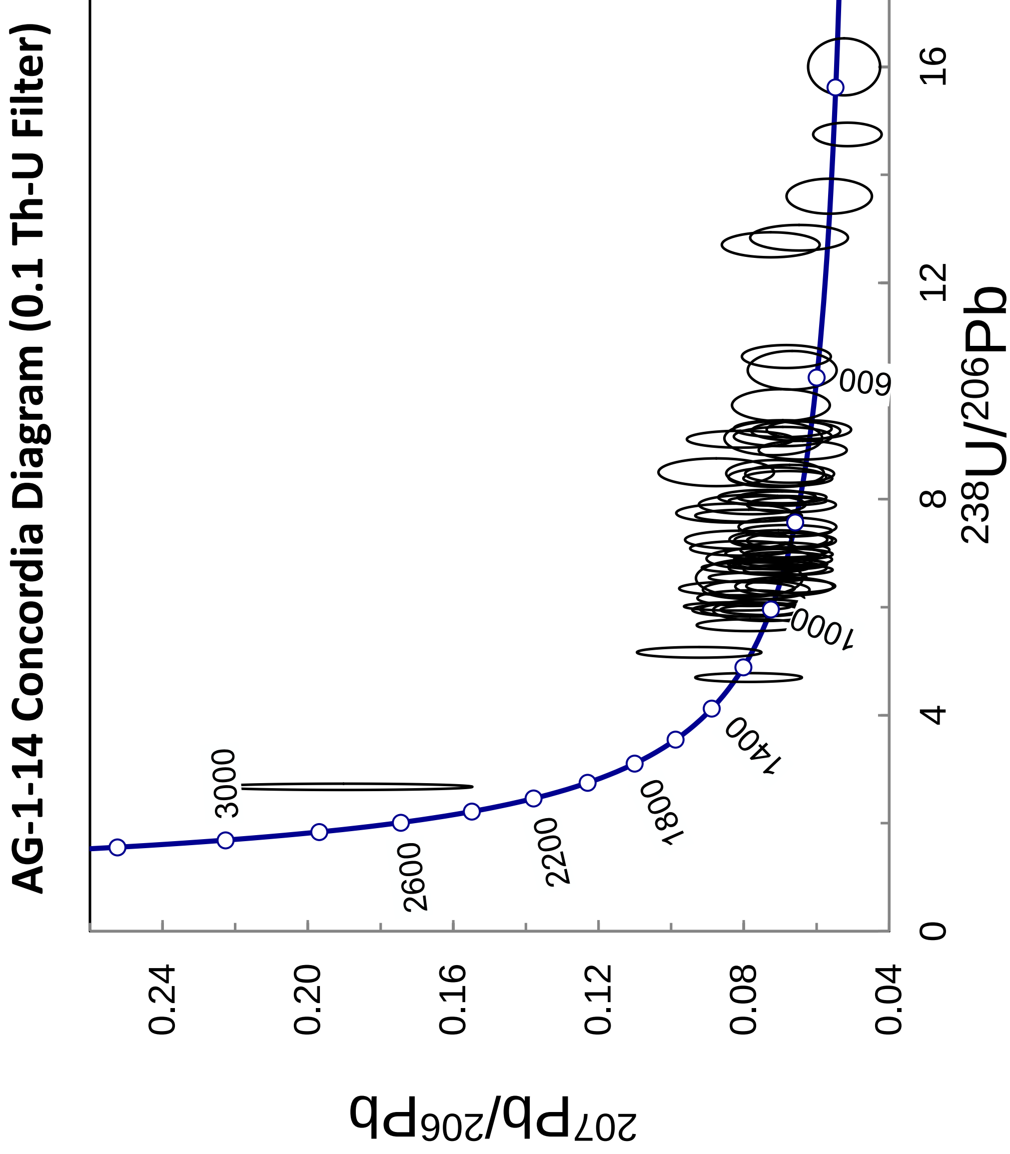
AG-1-14 Concordia Diagram (0.1 Th-U Filter)
3000
2600
2200
1800
1400
1000
600
0.24
0.20
0.16
0.12
0.08
0.04
0
4
8
12
16
20
207Pb/206Pb
238U/206Pb

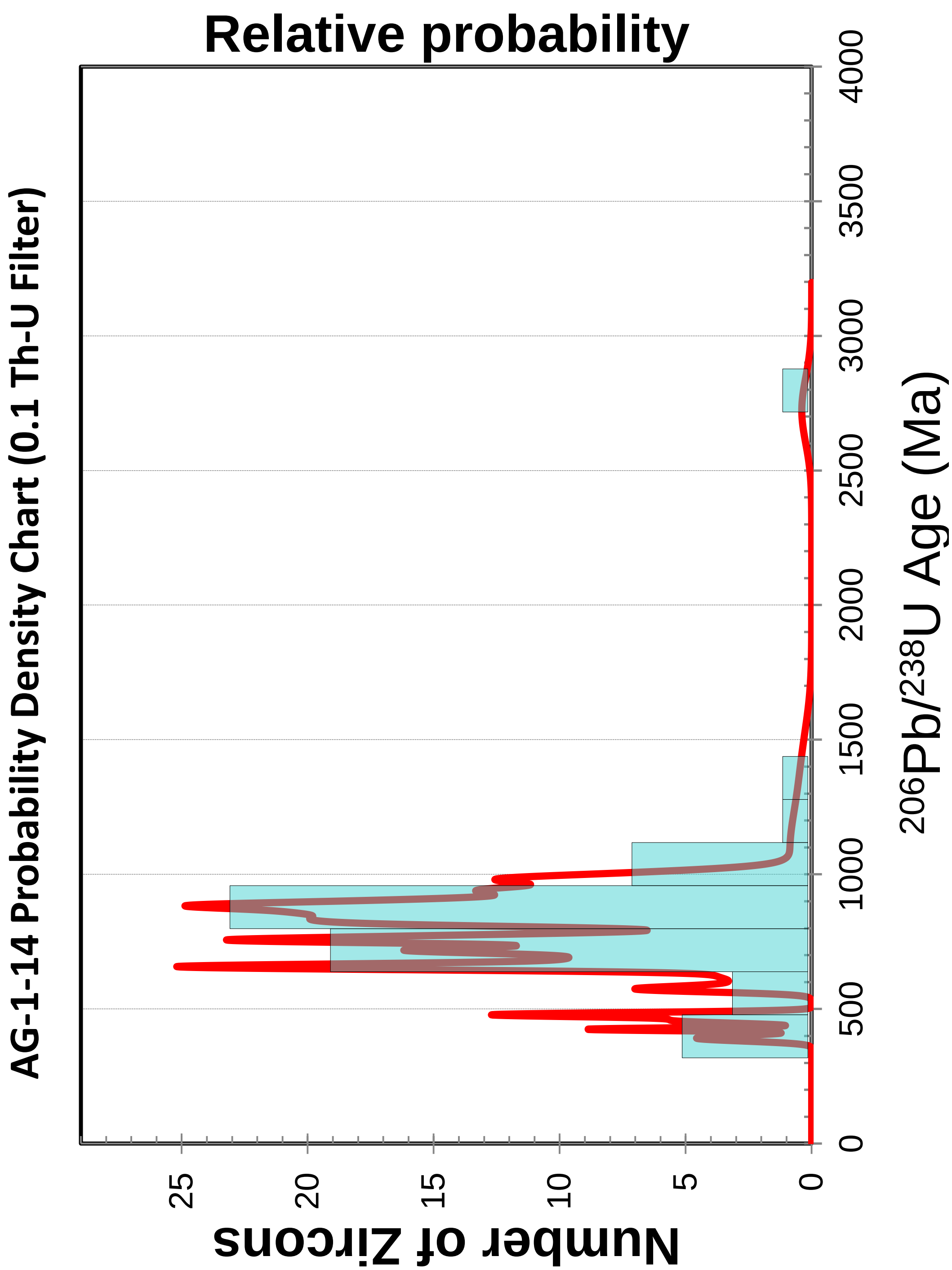
AG-1-14 Probability Density Chart (0.1 Th-U Filter)
Relative probability
206Pb/238U Age (Ma)
Number of Zircons
0
500
1000
1500
2000
2500
3000
3500
4000
0
5
10
15
20
25

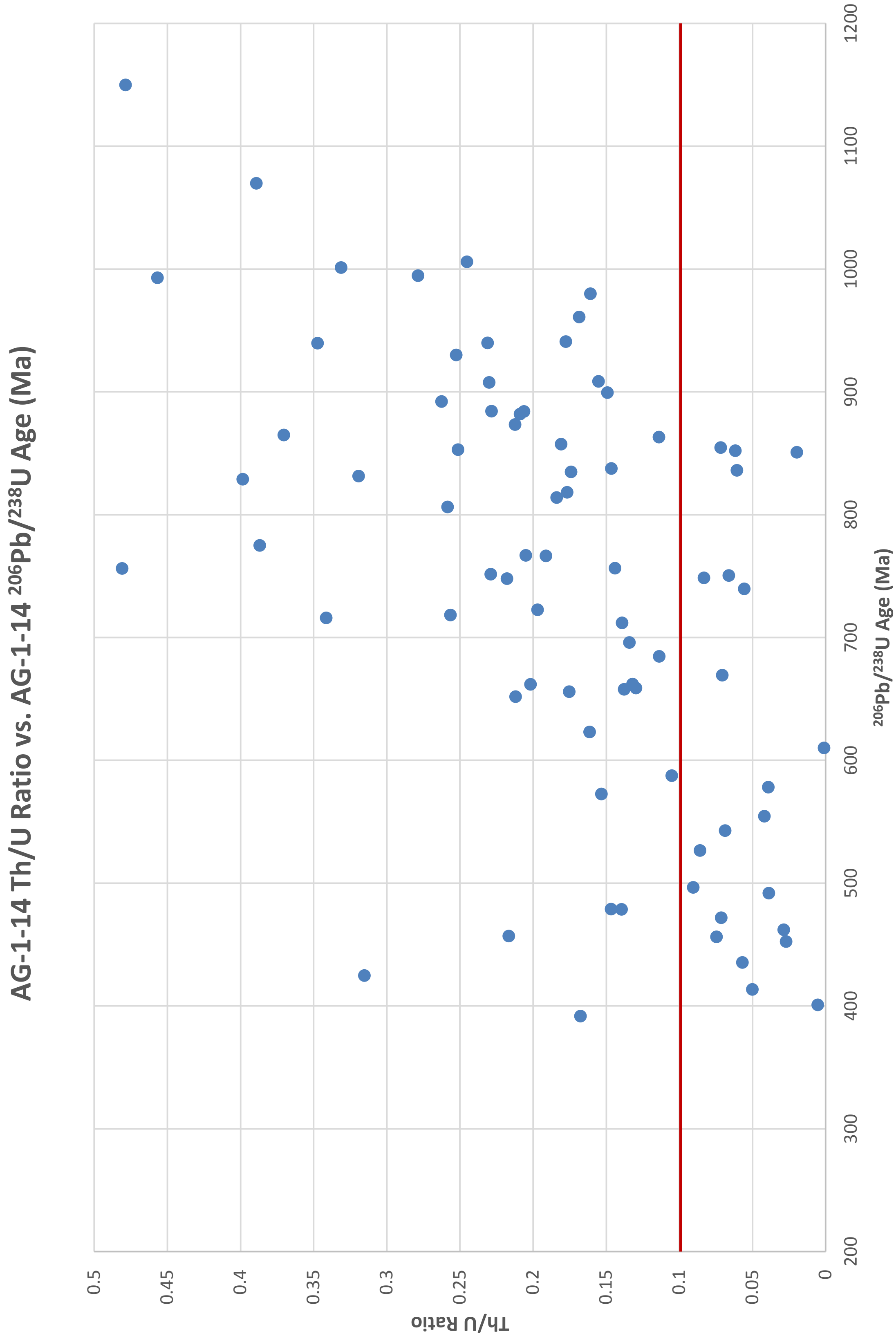
AG-1-14 Th/U Ratio vs. AG-1-14 ^{206}Pb/^{238}U Age (Ma)
Th/U Ratio
^{206}Pb/^{238}U Age (Ma)
0
0.05
0.1
0.15
0.2
0.25
0.3
0.35
0.4
0.45
0.5
200
300
400
500
600
700
800
900
1000
1100
1200